RESEARCH ARTICLE

A buried late MIS 3 shoreline in northern Norway — implications for ice extent and volume

Lars Olsen

Geological Survey of Norway, 7491 Trondheim, Norway.
lars.olsen@ngu.no

Buried beach gravel in northern Norway represents a late Middle Weichselian/Marine Isotope Stage (MIS) 3 shoreline and indicates a significant late MIS 3 ice retreat. An age of c. 50–31 cal ka BP, or most likely c. 35–33 cal ka BP, obtained on shells, stratigraphical evidence and comparisons between local and global sea-level data, indicate a local/regional glacioisostatic depression which was about 50–70% of that of the Younger Dryas interval. This suggests a late MIS 3 ice thickness/volume similar to or less than during the last part of the Preboreal, during which only minor or isolated remnants of the inland ice remained.

Keywords: northern Norway, MIS 3, Scandinavian ice sheet, glacioisostacy

Introduction

The extension of the glaciers in the western part of the Scandinavian Ice Sheet during the Marine Isotope Stage (MIS) 3 ice advance at c. 45 cal ka BP reached beyond the coastline in SW Norway (e.g., Larsen et al. 1987). The subsequent ice retreat, prior to the Last Glacial Maximum (LGM), has been discussed based on the distribution of sites which indicate ice-free conditions of this age. For example, the sites representing the Ålesund Interstadial (Mangerud et al. 1981), with an age now redated to 34–28 ^{14}C ka BP (Mangerud et al., in print), indicate an ice-free coast in SW Norway and retreat of the ice margin almost to the position of the late-glacial, Younger Dryas, maximum ice margin (Figure 1). Additional data, including sedimentary stratigraphy and dates from both coastal and inland locations, indicate a much more extensive late MIS 3 ice retreat in most parts of Norway (e.g., Olsen et al. 2001a, b). However, the stratigraphic correlations between sites and between regions are often hampered by dates of low precision and accuracy, which imply an uncertain location of the ice margin at each step in time and therefore also an uncertain minimum ice extension.

In this paper I try to reach beyond this problem by using data with implications particularly for ice volume, which generally changes at a slower rate and also has a wider regional effect than ice extension. To do this I have used traces of late MIS 3 raised shorelines and other sea-level data from two previously

Olsen, L. (2010) A buried late MIS 3 shoreline in northern Norway—implications for ice extent and volume. *Norges geologiske undersøkelse Bulletin*, **450**, 1–14.

Figure 1. Key map of Scandinavia showing the study areas (grey squares), the position of the major ice margins during the late-glacial Younger Dryas interval (grey lines; dotted line = tentatively), and maximum extension of ice remnants during the last part of the Preboreal (stippled red). Ages are given in cal ka BP.

described localities, Leirhola on Arnøya (Andreassen et al. 1985) and Ytresjøen (Olsen 2002) (Figure 1). These localities have been revisited and are described here, with new field data included as reference sites for discussing the glacioisostatic conditions and implications for the size, and particularly the volume, of the ice sheet.

Methods

Standard methods for regional Quaternary geological mapping used by the Geological Survey of Norway (Bergstrøm et al. 2001) have been used also during the studies referred to here. These methods include, e.g., site observations with description

of lithology and stratigraphy of sediments. The registrations include striations on bedrock and boulders (under tills) and various sediment data, e.g., grain-size distribution, colour, compactness, clast roundness, clast fabric and structures. Clast-fabric measurements have been carried out with similar but fewer measurements (n=20) than the standard method (n=33–50) used during regional Quaternary mapping (e.g., Olsen and Hamborg 1983). The reduced number of measured clast long axes, however, was considered high enough in view of the relatively strong, preferred orientation of the clasts (70% or more showing a main trend ±20° with n=20), and the fact that the settings are distinct fjord landscapes with high relief and with all known ice movements directed along the fjords.

Age estimations in this paper are mainly based on ^{14}C dating of marine shells (Tables 1 and 2). This was carried out at the dating laboratories at the Universities of Trondheim and Uppsala, and most of the dates have been published before (Andreassen et al. 1985, Olsen 2002). ^{14}C ages were calibrated to calendar years BP according to the calibration programme version 'Fairbanks0107' which is available on the Internet (Fairbanks et al. 2005). A reservoir age of 440 years, subtracted from each ^{14}C age, was used here. For high ages outside calculation range (>45 ka), I have simply added 4000 years to the ^{14}C age to obtain ages in calendar years (Olsen et al. 2001a, p. 75), and standard deviation is unchanged.

Leirhola

The stratigraphic sections at Leirhola are located c. 4–20 m a.s.l. (Figure 2a, b) (70°2.5' N, 20°30' E). Bedrock on Arnøya is dominated by mica schist, gneiss, metasandstone, dolomite,

Table 1. ^{14}C dates of shells from Arnøya and Ytresjøen, northern Norway. No. 1, 4–6: after Andreassen et al. (1985), no. 2–3: this paper; and no. 7–8: after Olsen (2002).

No	Site	Lab. Ref.	Unit	Material	Age ^{14}C yr BP	± 1 st.d.	Age cal yr BP	± 1 st.d.
1	Lauksundet	T-3507	Till "T1"	*Astarte sp. / Mya truncata*	27400	±1500 / 1200	32697	±1623 / 1277
2	Leirhola, site II	TUa-3624	Till T3	*Arctica isl. / Mya truncata*	44755	±1745 / 1435	48755*	±1745 / 1435*
3	Leirhola, site I	TUa-3626	Till T3	*Arctica isl. / Mya truncata*	48635	±2595 / 1960	52635*	±2595 / 1960*
4	Leirhola site I	T-4020	I	*Chlamys* and *Portl. arctica / lenticula*	29000	±4200 / 2700	34190	±4442 / 2705
5	Leirhola site I	T-4021	I	Div. shells	30200	±4100 / 2700	35448	±4229 / 2657
6	Leirhola site I	T-3509	I	*Mya/Astarte / Arctica isl.*	c. 40500 (>37500)	±3000**	c. 44500**	±3000**
7	Ytresjøen	UtC-8315	B/C	*Balanus bal.* (one fragm.)	28280	±240	33659	±292
8	Ytresjøen	UtC-8316	C/D	*Mya truncata* (one fragm.)	35060	±600	40395	±591

**) See description under* Methods *in the main text. **) Standard deviation for dating no. 6 is not reported, but is here simply set to 3000 yr, which also gives a fair calibrated age.*

Table 2. Sea-level data from Nordland (Olsen 2002) in northern Norway compared to sea-level data from coral terraces in New Guinea** (Shackleton 1987). A and B in the columns to the right refer to the m-values in columns A (Glacioisostacy, Younger Dryas) and B (Glacioisostacy, late Middle Weichselian (MW)).*

Sea-level data from*:	Y Dryas 11.5–12.7 ka m a.s.l.	Late Middle Weichselian m a.s.l.	Eustacy** YD m a.s.l.	Eustacy** late MW m a.s.l.	A. Glacio-isostacy, YD	B. Glacio-isostacy, late MW	B/A-ratio	% B of A
Åsmoen 1 age c. 34 ka	90	> 62	-45	-45	135 m	> 107 m	> 0.792	> 79.2
Åsmoen 2 age c. 33 ka	90	> 71	-45	-45	135 m	> 116 m	> 0.859	> 85.9
Ytresjøen age c. 33 ka	88	c. 23	-45	-45	133 m	c. 68 m	0.511	51.1
Oldra age c. 37 ka	90	> 23	-45	-55	135 m	> 78 m	> 0.578	> 57.8
Kjeldal age c. 38 ka	93	> 40	-45	-60	138 m	> 100 m	> 0.753	> 75.3

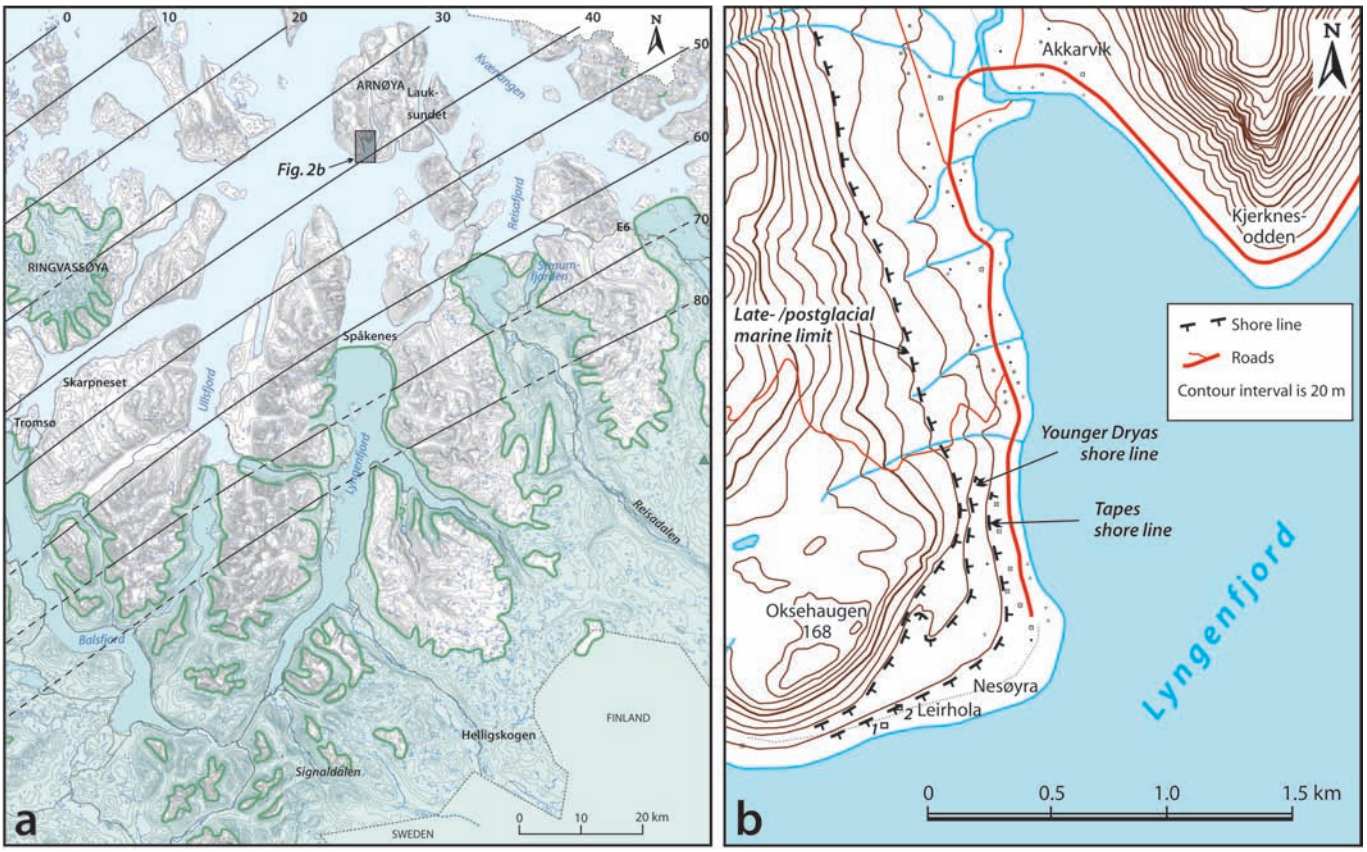

Figure 2. (a) Map of Troms and location of Arnøya. The Younger Dryas isobases (black lines, stippled on ice) and glacier extension (bluish transparent colour) are shown. (b) Close-up map showing the location of the Leirhola sites I (1) and II (2). Shorelines representing the late-/post-glacial marine limit, the YD and the Tapes intervals are also indicated.

greenstone and greenschist (Roberts 1974), and Quaternary sediments, which cover about 83% of the surface, are dominated by till, weathered material, scree and talus material, and marine shore deposits (Sveian et al. 2005). There are numerous cirque moraines on the island, most of which are supposedly of Younger Dryas (YD) age (Sveian and Bergstrøm 2004). The marine limit and the YD shoreline close to the Leirhola sites are located at c. 60 m a.s.l. and 38 m a.s.l., respectively (Figure 2b). The last deglaciation at Leirhola may have occurred as early as 15 cal ka BP (c. 13 ka ^{14}C BP), i.e. shortly after the D-event described from the outer fjord/inner shelf area farther south in Troms county (Vorren and Plassen 2002).

Leirhola site I

Three sections in the slope of a strand terrace at c. 10 m a.s.l. have earlier been described by Andreassen et al. (1985). These sections are here named Leirhola I (L I) (Figure 3) and include deformed glacimarine/marine sediments which are overlain by a diamicton interpreted as till. Another diamicton, also inferred to be a till, is resting on top.

Both upper tills include deformed and probably partly dislocated glacimarine/marine sediments as well as diamict material with subangular to subrounded clasts, some of which show glacial striations. Marine shells from the lower till and from the subtill sediments date to 26.3–51.3 ^{14}C ka BP (within ±1 std and n=5) (Table 1). An age of c. 27.4 ^{14}C ka BP has been obtained from the dating of a shell in a surficial till at Lauksundet on the eastern side of the island (Andreassen et al. 1985). The till at Lauksundet is considered to be equivalent to the uppermost till at L II, based on a similarity of lithology and texture. Furthermore, regional mapping has shown that it is most likely that the uppermost tills at these sites and elsewhere on the island are of LGM and early late-glacial age (Sveian et al. 2005).

Leirhola site II

The new excavation (L II; a combination of L II–1 and L II–2; Figure 3) is located about 40 m from L I at the boundary between the Tapes shore terrace and the slope up to the YD shore terrace.

In the deepest part of the excavation (L II–2), till T3 from the upper part of L I is easily recognised by its fine-grained and compact character and its bluish-grey colour, under a thin cover of brownish-grey sandy and gravelly material. The pebbles in the sandy and gravelly top cover of till T3 are mainly subangular, and quite similar to the clasts in the till. The position at the top of the till with the overlying massive clay G (Figure 4), together with the subangular nature of the pebbles, suggest that this sub-

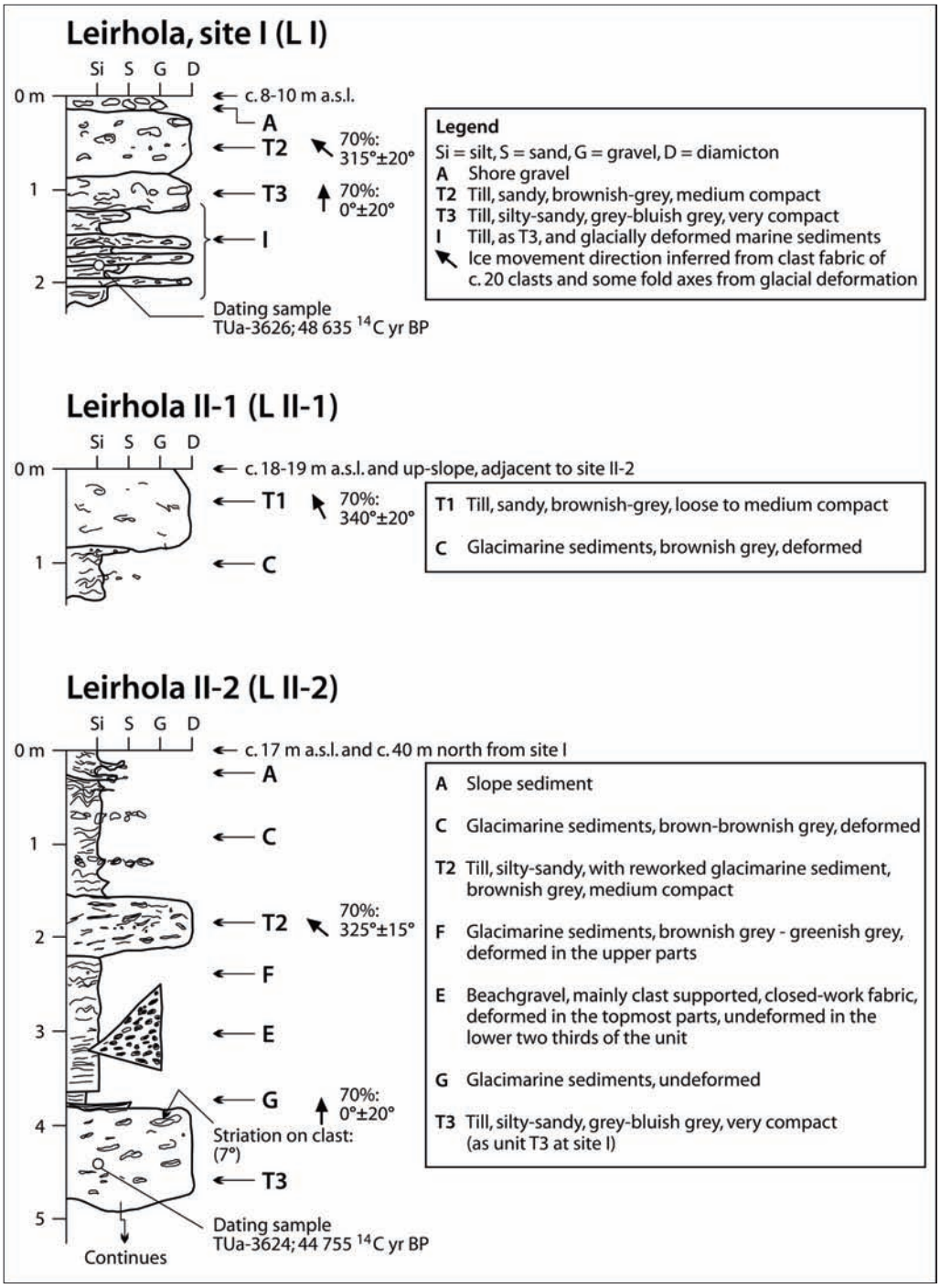

Figure 3. Stratigraphic logs from Leirhola sites I, II–1 and II–2. The log from Leirhola I is simplified and combines several sections described by Andreassen et al. (1985). The term Leirhola site II is used in the main text for a combination of sites II–1 and II–2. For details of dates, see Table 1. A suggested correlation between these sections is shown in Figure 5.

unit is a product of ice-rafting or possibly glacifluvial outwash rather than having originated by wave washing in shallow water (e.g., a shore deposit). Small fragments of marine shells are found in the till. Above till T3 follows an undisturbed, bluish-grey, massive clay that changes upwards into laminated clayey silt and sand (G), which are inferred to be glacimarine. Sediment unit F then follows (Figure 3). It is a faintly laminated, almost massive bedded, pale brownish-grey to greenish-grey sandy silt, which is undisturbed in its lower part, but deformed by slumping and subsequent glacial deformation in its upper part. These sediments are also interpreted as being of glacimarine origin. Gravel unit E, inferred to be a shore gravel, cuts into glacimarine units F and G (Figures 3 and 4) and wedges out in F. The excavation also revealed a cross-section through a beach ridge developed in shore gravel unit E. The buried erosional top of the ridge reached up to c. 1.5 m above the surrounding, subhorizontal, shore gravel horizon (E). The upper one-third of unit E (in the ridge cross section) shows deformational structures which indicate glacial thrusting and folding. This process may have resulted in the increased height of the ridge as compared to the

Figure 4. Photograph of the sandy gravelly top cover of till unit T3 (H on the photo) overlain by undeformed glacimarine sediments (unit G) and the lower part of shore gravel unit E.

original beach ridge. The lower two-thirds of unit E (i.e., about 1 m in thickness) show normal beach ridge structures, including pebble imbrication (Figure 4), and no signs of deformation. This would indicate that the original height of the beach ridge may have been around 1 m. Glacimarine unit F contains structures in its upper parts that point to slumping and sliding towards the upper part of the beach ridge, followed by glacial thrusting and overriding. These structures, however, were not observed in the sediments of unit F below the shore gravel E.

Till T2 overlies glacimarine unit F and is moderately compact, greenish-grey to brownish-grey and relatively fine grained with a silty and sandy matrix. The glacimarine sediments (unit C), which overlie till T2, are deformed, silty and sandy, faintly laminated and have a brownish-grey colour and are again overlain by till T1. This till is apparently more coarse grained, lithologically and texturally more variable, and generally has a less compact character than the underlying tills. The colour of till T1 varies between greenish-grey and brownish-grey, and this till, partly combined or intermixed with till T2, is considered to be the dominant surficial till on Arnøya. Till T1 is capped by sandy, slope-gravitational sediments (A). The youngest unit A also includes wave-washed material (sand, gravel, and some stones and boulders) on the Tapes and younger postglacial shore terraces.

The ice movement direction during the deposition of tills T3 and T2 is inferred from measurements of moderate precision (±10°) of deformation structures (fold axes, thrust planes) in unit I (at L I) and unit F, respectively, and from some clast fabric measurements from each till. From these data, it seems that tills T3 and T2 were deposited during ice flow towards the N and NW, respectively (Figure 3), which is also supported by striations on the tops of clasts under each till. Deformation structures (mainly fold axes) in unit C, striations on exposed bedrock and clast fabrics in the surficial till at L II–1 and elsewhere on Arnøya suggest that the uppermost till T1 was deposited during ice movement towards the N–NW. The observations of ice-flow directions are in full agreement with ice growth in the south and ice flow into the Lyngenfjord system (Figure 2), which probably occurred in this region during all major glaciations of the Quaternary, including the LGM. The records from L I and L II (L II–1 and L II–2) are combined in a schematic figure (Figure 5), which also includes inferred (eroded) parts of units T2 and E (stippled).

Ytresjøen

Ytresjøen is also located distally to the YD ice margin. It is located in a road cut at c. 21–27 m a.s.l. (Figure 6) (66°48.24' N, 13°34.8' E). Bedrock is dominated by mica schist, mica gneiss and granites (Gjelle et al. 1995). Quaternary sediments and the occurrences of YD cirque moraines are similar to those on Arnøya (Olsen 2002, Olsen and Bergstrøm 2003). The marine limit and the YD shoreline close to the site are located at c. 100 m a.s.l. and 90 m a.s.l., respectively. The last deglaciation at Ytresjøen is dated to c. 13.8 cal ka BP (c. 12 ^{14}C ka BP; Olsen 2002).

A sediment succession (Figure 6) from Ytresjøen has been described briefly by Olsen (2002). It includes from bottom to top: a sublittoral, gravelly sand with shells, mainly of *Mya truncata* (unit D); a lower till (unit C) containing a large boulder (1.5x3x>3 m) in the uppermost zone, with a horizontal belt of *Balanus sp*. on the exposed seaward side and glacial striae on top. The belt with *Balanus* shells may indicate the mean sea level of a former ice-free interval, in this case c. 23 m above the present sea level. Overlying the lower till is an upper till (unit B), with a shore deposit on top (unit A). Clast fabrics in the upper till show features similar to the striations on the large boulder and on exposed bedrock in the area, indicating ice movement towards the W–NW (Olsen 2002, Olsen and Bergstrøm 2003). ^{14}C dates from this site have given ages of c. 28.3 ^{14}C ka BP for a shell from the *Balanus* belt on the boulder, and c. 35 ^{14}C ka BP from a shell in the contact zone between the lower till and the subjacent sediments (unit D) (Table 1).

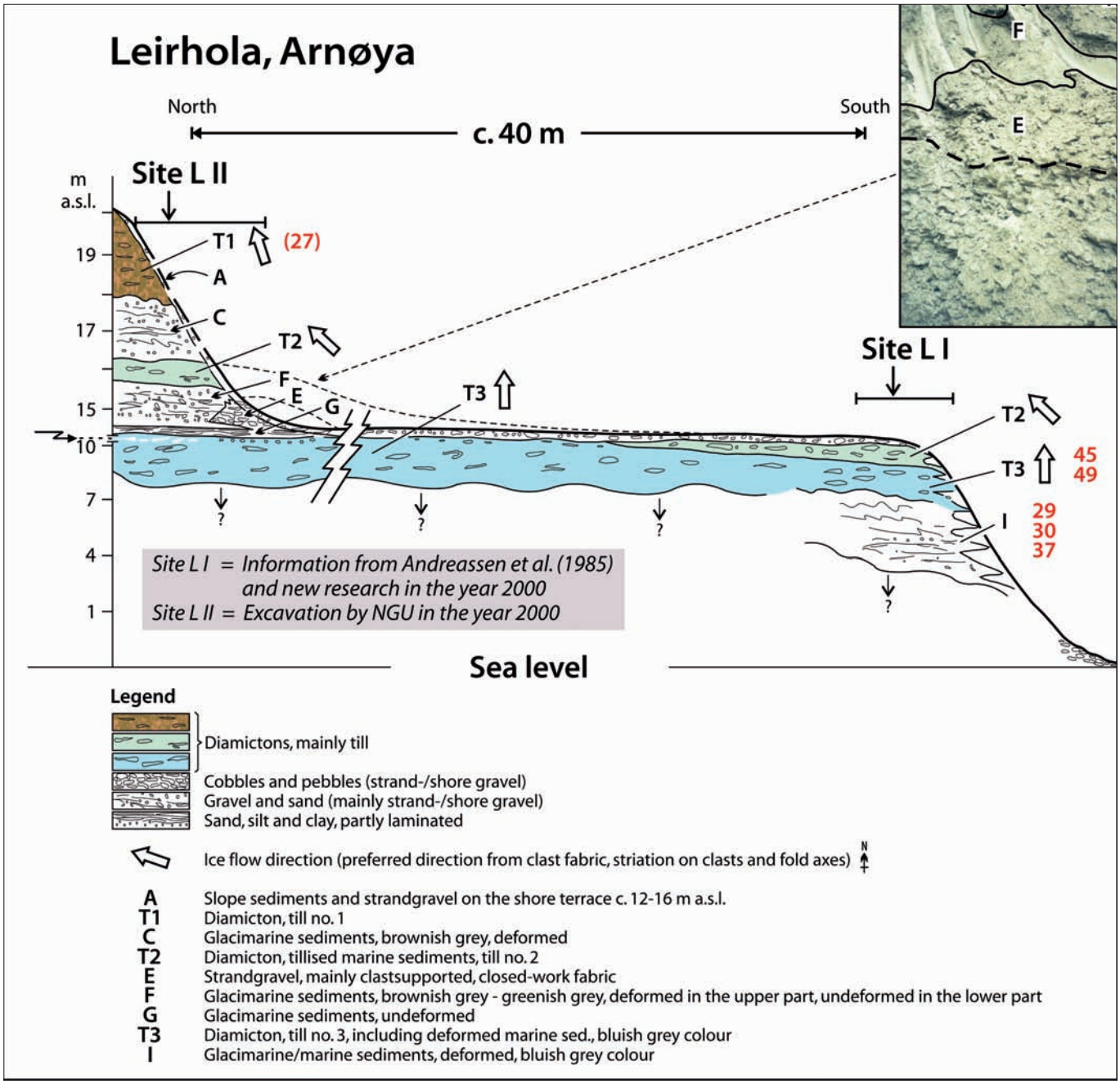

Figure 5. Simplified sketch of a N–S profile through Leirhola II and I. NGU=Geological Survey of Norway. Note the change in scale just above 10 m (a.s.l.) and the compression of the horizontal scale indicated by parallel 'zigzag' lines through units A and T3. The inset photograph represents a c. 2 m vertical section in L II and includes the basal part of till unit T2, the deformed upper part of glacimarine unit F, the topmost eroded and deformed part of the shore gravel unit E, and the lower undeformed part (below stippled line) of the shore gravel in the cross section through the inferred beach ridge. Dates in ^{14}C ka BP (red numbers) are indicated stratigraphically, except those from unit I, which are plotted in chronological order with respect to age. The ^{14}C date indicated as (27) from till T1 is from the adjacent site Lauksundet (after Andreassen et al. 1985).

Reliability of the ^{14}C dates

Radiocarbon dates of 30–40 ka-old shell samples are very sensitive to contamination with young C, and small samples are more sensitive than larger samples. All the shell dates from Leirhola and from a neighbouring area on Arnøya (Lauksundet; Figure 2) were performed on small samples taken mainly from fragments of shells and from shallow depths, and only a minor outer part was removed in each case before dating (Andreassen et al. 1985, and this paper). Resedimentation of shells from older units occurs frequently in coastal settings (e.g., Olsen 2002), and is a complicating factor for sediment age estimations. Together, these factors indicate that the dates from Arnøya, which all have high standard deviations (Table 1), should be considered with great caution. However, the fine-grained bluish-grey sediment in the oldest unit I (glacimarine deposit) at site L I, where the present groundwater level is well below the recorded sections, indicates anoxic conditions with only a very small amount of percolation

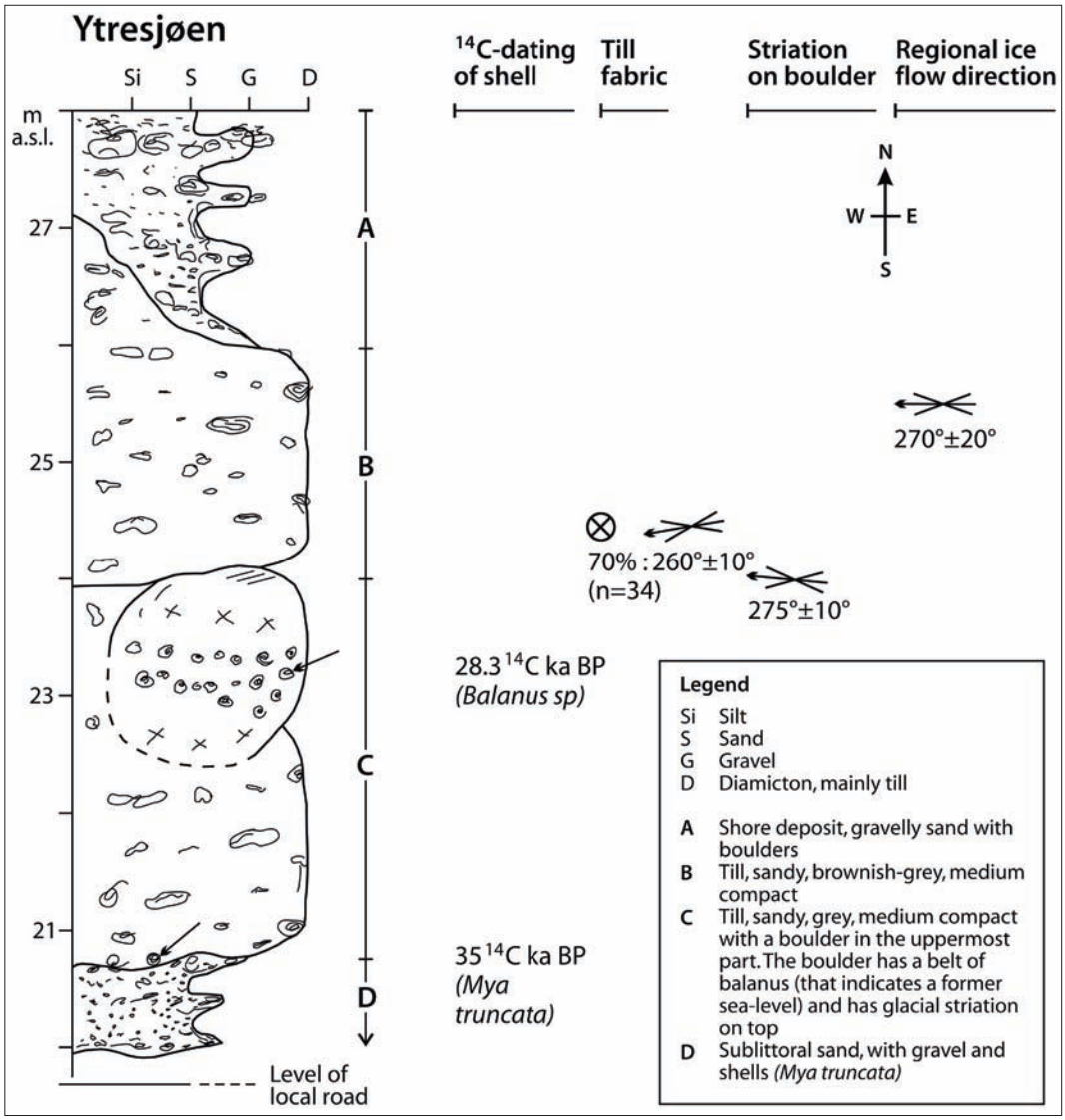

Figure 6. Stratigraphic log from Ytresjøen, Nordland, modified from Olsen (2002). The positions of the dated samples (shells) are shown with arrows on the log. See Table 1 for details of the dates.

of fresh groundwater. The input of young C may therefore have been low, and since there is no positive indication of contamination, but signs of resedimentation of older shells in overlying units, I conclude that the age range of 31–55 cal ka BP, including ±1 std for dates from this unit (Table 1), is reliable and that the age of unit I is around 35–50 cal ka BP.

The two dates from Ytresjøen (Table 1) are both ^{14}C-AMS dates of single fragments of well preserved shells. Both samples were taken from newly exposed sections at a sediment depth of more than 2–4 m. The dates at c. 33.6 cal ka BP (c. 28.3 ^{14}C ka BP) and c. 40 cal ka BP (c. 35 ^{14}C ka BP), which have low standard deviations, are both considered reliable.

Sea-level history inferred from Leirhola I and II

Eight relative sea levels of different age have been recorded at and around Leirhola (L I and L II) on Arnøya (Figure 7). The oldest of these is the 35–50 cal ka BP sea level at more than 10 m a.s.l., possibly 15 m a.s.l. or more, represented by glacimarine sediment unit I (site L I; Figure 3). The subsequent recorded sea-level phase, after an intervening glacial advance and retreat (represented by till unit T3 and its sandy and gravelly top cover), is represented by the glacimarine sediments of units G and F with a sea level reaching at least to 18–19 m a.s.l. The latter was followed by a regression phase reaching a minimum sea level at least as low as 14 m a.s.l. as represented by strand gravel of unit E. After another glacial advance (represented by till unit T2), the sea level rose to at least 20–21 m a.s.l. as indicated by the glacimarine sediments in unit C. The last glacial advance (till T1) was followed by two late-glacial phases with maximum sea levels of 60 m a.s.l. (marine limit) and 38 m a.s.l. (YD), an early postglacial phase with a weakly developed shoreline (step in the slope) at c. 25–27 m a.s.l. (Preboreal), and another postglacial phase with a maximum transgressional sea level at c. 16–18 m a.s.l. (Tapes).

Figure 7 compares the sea-level history from Leirhola (upper panel) to the global eustatic history inferred from coral terrace levels in New Guinea and the age model proposed by Shackleton (1987) (lower panel). These data sets are based on different

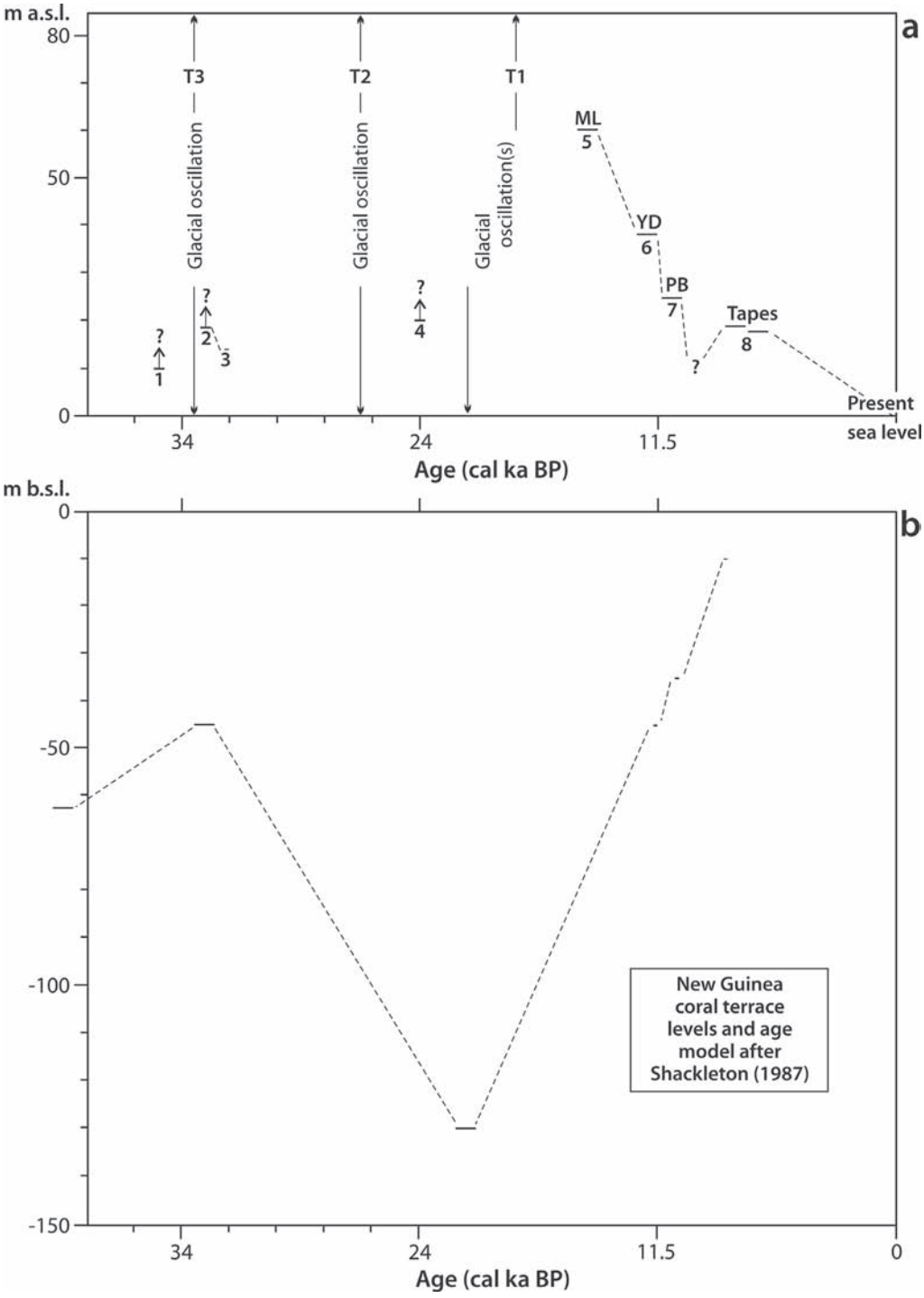

Figure 7. (a) Sea levels numbered 1–8 derived from Leirhola I and II are shown. T1, T2 and T3 refer to till units, and ML, YD, PB and Tapes refer to shorelines at the late-/post-glacial marine limit, during Younger Dryas, Preboreal and the Tapes intervals, respectively. Note that the ages for till T1, sea level 4 and till T2 are tentative. Note also that all pre-T1 sea levels are minimum estimates only, except for no. 3, which represents a more accurately estimated sea level (14 m a.s.l.). (b) Global eustatic data shown in the lower panel are modified from Shackleton (1987).

dating materials, different age models and derive from different regions, and the ages are therefore expected to be slightly out of phase. However, even with a possible small discrepancy in ages, it seems that the Arnøya sea-level history matches fairly well with the eustatic history at around c. 33–35 cal ka BP, which is considered to be the most likely minimum age of shore gravel unit E (discussed below).

Discussion

The shore gravel of unit E (Figures 3, 4 and 5) may represent a regression minimum to 14 m a.s.l. after a phase with a relative sea level that was several metres higher (Figure 7). The position of the Leirhola sites on the southern shore of the island indicates that the ice sheet did not reach Arnøya during the time of formation of the 14 m shore deposit. Therefore, the extension of the glacier towards the north must have been no more than during

the late-glacial Skarpnes Substage (c. 13.9 cal ka BP) (Andersen 1968, Vorren and Plassen 2002) or slightly less (e.g., as that during the Tromsø-Lyngen (Spåkenes)/YD Substage, Figure 2a). A further discussion of the size of the ice sheet during the 14 m sea-level phase is difficult without consideration of the glacioisostatic conditions. I surmise that the New Guinea coral terrace levels may be a fairly good direct indicator of global sea levels during MIS 3 (Chappell 1983, 2002, Ota et al. 1993), and I therefore use these data here with the age model of Shackleton (1987) as the eustatic data source (e.g., Figure 7).

The 14 m sea level (Figure 5) predates the tills T1 and T2, which are considered to be of LGM and early late-glacial age. The best age estimate for the 14 m sea level is, therefore, that it is younger than unit I (35–50 cal ka BP) and the subsequent intervals represented by till T3 and glacimarine units G and F (Figures 3 and 5), and older than the LGM. Considering the global eustacy for this age interval (Shackleton 1987), the location of the Leirhola sites compared to the YD ice margin (Figure 2a), and the associated glacioisostatic conditions, any age between 50 and 33 cal ka BP for this sea level seems possible (Table 3). However, the age intervals with ice cover (further discussed below), e.g., shortly after 45 and 34 cal ka BP, may be excluded. An age older than 45 cal ka BP is possible, but only if the ^{14}C dates (from unit I) are severely contaminated with young C (see above). Even a slightly younger age is possible, but perhaps less likely since it is closer in time to the ice growth leading to the first LGM advance, prior to 25–26 cal ka BP (e.g., Vorren et al. 1988, Møller et al. 1992, Alm 1993, Olsen et al. 2001b).

I have estimated the relative glacioisostatic conditions of Arnøya (Table 3). The pre-LGM 14 m (a.s.l.) sea level on Arnøya is combined with the global eustacy at different ages and compared with the relative glacioisostatic conditions during the YD. For example, given an age of 33 cal ka BP for the 14 m sea level on Arnøya, the relative glacioisostatic depression would be c. 70% of that during the YD. However, it is not straightforward to use this as a direct estimate of the size of the 33 cal ka BP ice sheet as 70% of the YD ice sheet, because the glacioisostatic conditions depend on the memory of ice load in the crust. The following question should therefore be addressed. Was the crust loaded by a large ice sheet or a smaller one a short time before the 14 m sea-level event on Arnøya? I will consider this problem later.

Glacioisostacy, i.e., the response of the Earth's crust to loading and unloading of an ice body, can be described geophysically (e.g., Lambeck et al. 1998) or in a much more simple manner by using only empirical data. In this paper I use a simple 'model' where only the vertical movement of the Earth's crust is considered.

Based on a comparison with shoreline displacement and eustatic sea-level data, it seems that most of the recovery of the Earth's crust after the last glaciation in Scandinavia occurred within a few thousand years. Therefore, I use tentatively the 'half-life' of rebound, which I set at, e.g., 3000 yr, to represent the average postglacial rebound rate after release of the ice load. This

Table 3. Sea-level data from Arnøya, northern Norway (various sources), and from coral terraces in New Guinea (after Shackleton 1987). Ages are in cal ka BP. The Andøya-Trofors interstadials (A.-T. interst.) have a proposed age of 17–21 ^{14}C ka BP (20–25 cal ka BP), after Olsen et al. (2001b).

Sea-level data from:	Post-Tapes c. 5 ka m a.s.l.	Tapes 6.5–8 ka m a.s.l.	Preboreal 10.1–10.2 ka m a.s.l.	YD 11.5–12.7 ka m a.s.l.	A.-T. interst. m a.s.l.	Pre-LGM c. 33 ka m a.s.l.	MIS 3 c. 35 ka m a.s.l.	MIS 3 c. 40 ka m a.s.l.	MIS 3 c. 52 ka m a.s.l.	Comments
Buried shore deposit, Arnøya					14	14	14	14	14	Data from site L II
Eustacy; New Guinea terraces	0	-10	-35	-45	-130	-45	-50	-63	-30	Data from Shackleton (1987)
Y Dryas shore (11.5–12.7 ka)				38						Various sources (from NGU, and others)
Preboreal (10.1–10.2 ka)			27							
Tapes shore (6.5–8 ka)		16								
Post-Tapes, max. (c. 5 ka)	14									
Isostatic depression in metres	14	26	62	83	144	59	64	77	44	*) Ages > 45 ka BP less likely, based on C14-dates of subjacent unit I
Isostatic depr. vs YD isostatic depression	17 %	31 %	75 %	100 %	173 %	71 %	77 %	93 %	53 %	
Favourable (+)/unfavourable (–) result of isostatic conditions and age versus (vs) location of site vs YD ice margin					–	+	+	+	*	

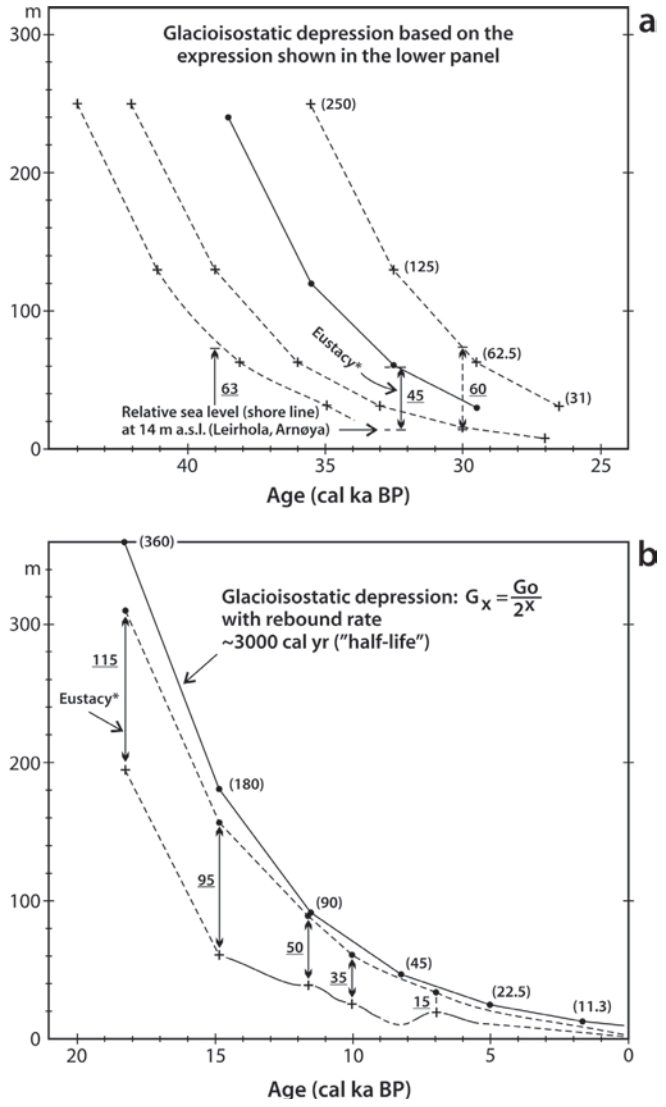

*Figure 8. Comparison between glacioisostatic depression after the equation $G_x=G_o/2^x$, assuming an initial depression (G_o) of the crust of 250 m (a, upper panel) and 360 m (b, lower panel) at selected start times for the rebound, and from relative sea level + absolute value of 'global' eustatic sea level in metres. The relative/eustatic sea-level curve between 18 and 15 cal ka BP in the lower panel is tentative (estimated from the glacioisostacy equation for comparison). The middle curve (full line) in the upper panel is based on the observed late Middle Weichselian 14 m (a.s.l.) shoreline with its possible age at 33 cal ka BP at Leirhola + global eustacy data, and rebound corresponding to these data and the given equation. *) Eustatic data are after Shackleton (1987) (upper panel) and Bard et al. (1990) and Fairbanks (1989) (lower panel).*

may be valid for the marginal zones of the former ice sheet, such as at the outer coastal parts of northern Norway where Arnøya is located. The rebound rate in the inner fjord regions has been much higher, as indicated by steep, postglacial, shoreline displacement curves, e.g., from the Oslofjord, the Trondheimsfjord and the Varangerfjord areas (Figure 1) (Hafsten 1956, Kjemperud 1986, Fletcher et al. 1993). The half-life of rebound is therefore a value that is specific for each area. The postglacial rebound in this model can be calculated from the equation: $G_x=G_o/2^x$, where G_o is the glacioisostatic depression at a given time and G_x is the glacioisostatic depression at x half-lives after this time. This gives a theoretical rebound as an exponentially declining curve during the entire postglacial period, which may be a fair and useful approximation to the real glacial rebound, at least for the marginal zones of the ice sheet.

Precise data, e.g., for the position of and distance to the central ice dome, and the age of initial ice growth are needed for advanced modelling of ice thickness and ice-sheet rebound (e.g., Lambeck et al. 2006). These data are not known in detail for the MIS 3 Scandinavian ice sheet. Therefore, I use here a simple 'model' where an ice load is considered to depress the Earth's crust by approximately one-third of the ice thickness (Paterson 1994). By assuming a very small *average* lowering of the bedrock surface due to erosion over the last 50 ka and with an assumed G_o=360 m, which therefore implies an ice-load effect of at least a 1000 m-thick ice sheet at 18 cal ka BP, I have shown in Figure 8 that there is a fairly good match between the calculated and the empirical data (relative sea-level/shoreline displacement and global eustacy) in the interval 15 cal ka BP to the present. The hypothetical Gx curve is supposed to reflect the recovery of the crust due to additional loading from ice, i.e., the total loading from ice minus eustatic water lowering (Figure 8, lower panel).

It is also shown that the glacioisostacy equation used together with the 14 m sea level from Leirhola at its possible age of 33 cal ka BP and the eustacy of that time is compatible with rebound after deglaciation of a c. 720 m-thick ice sheet (=240 m glacioisostatic depression) at c. 39 cal ka BP (Figure 8, upper panel).

From the published record it is known that there was a major ice advance in different parts of Norway at c. 45 cal ka BP which reached even beyond the coastline in SW Norway (Larsen et al. 1987, Mangerud et al. 2003) and northern Norway (Vorren et al. 1981, Olsen et al. 2001b, Olsen 2002). It is also known that significant ice growth, also reaching beyond the coastline, occurred at around 33–34 cal ka BP, i.e., after the Ålesund interstadial (Mangerud et al. 1981, Andreassen et al. 1985, Larsen et al. 1987, Olsen et al. 2001b). The redefined age range of the Ålesund interstadial is now 34–28 ^{14}C ka BP (c. 39–33 cal ka BP) (Mangerud et al. 1981, 2003, in print, Larsen et al. 1987). Different scenarios for the ice thickness (based on glacioisostatic depression) and age of the 14 m shoreline can be considered from Figure 8 (upper panel) and the regional record. If the duration of the deglaciation of the 45 ka ice sheet was short and most of the ice had melted before 41–42 cal ka BP, then a considerable ice growth just before or during (preferably towards the end of) the 39–33 ka interval would appear to be required to fit with the Leirhola shore line at 14 m a.s.l. and 33–35 cal ka BP (Figure 8). If, on the other hand, this deglaciation took a long time, then no ice growth or only a moderate ice growth towards the end of the 39–33 ka BP age interval would seem to be required to match the Leirhola data. Furthermore, an age closer to 40 cal ka BP for the shore line would require either a very rapid deglaciation after the 45 cal ka BP ice sheet or, alternatively, an ice sheet that was considerably thinner (<750 m) than I have postulated based on the regional data (e.g., Olsen et al. 2001b).

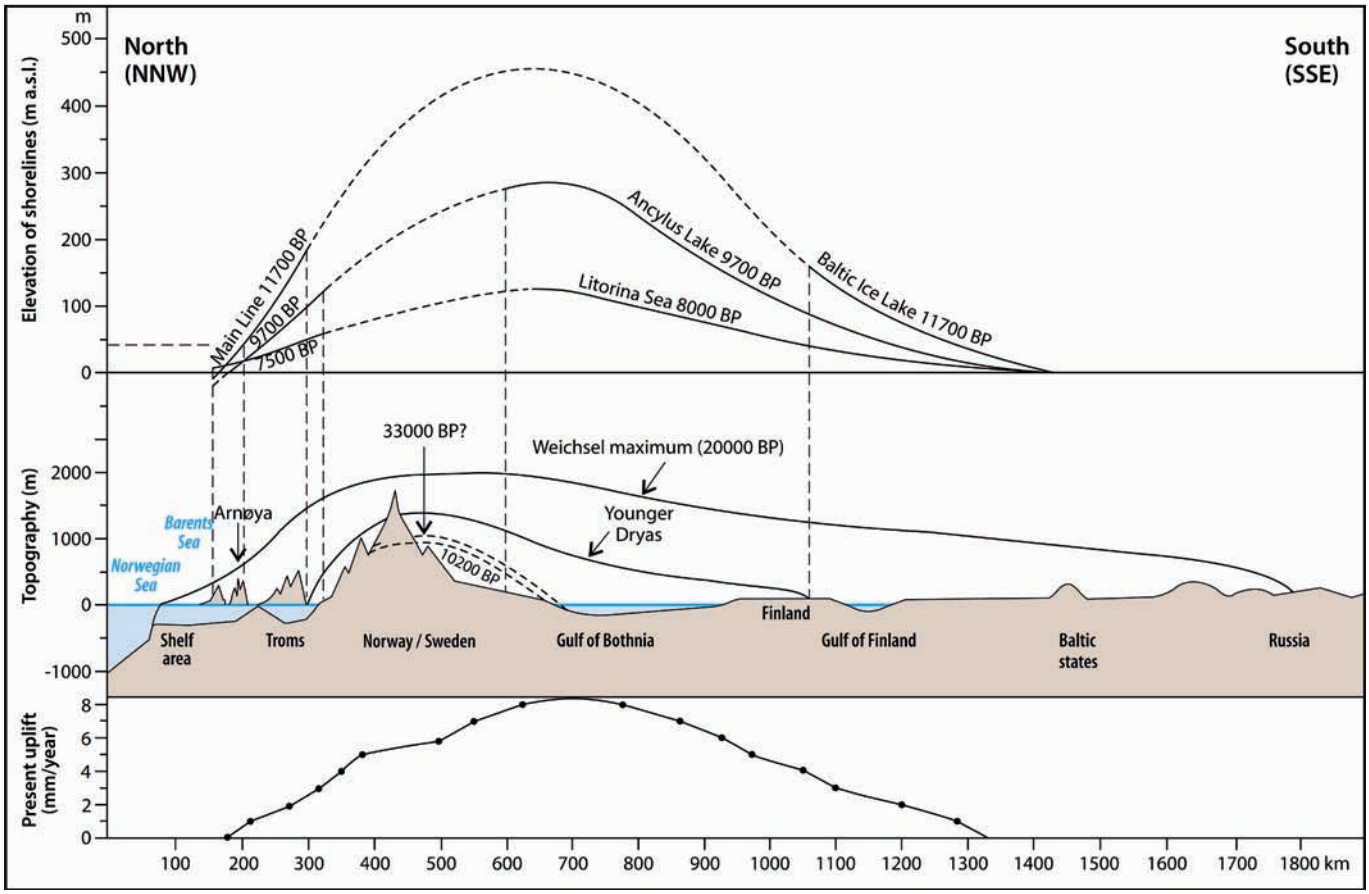

Figure 9. Sea levels, ice surfaces and present uplift data plotted in profiles along a NNW–SSE transect (location indicated in Figure 1). The conceptual idea, the sea levels (upper panel) and the ice surfaces (middle panel) are modified from Svendsen and Mangerud (1987). The sea levels *are adjusted in the northernmost part based on regional Quaternary mapping during the 1990s. The* ice surfaces *are based on a model with reduced ice thickness and a profile levelling out in the lowland and basin areas as well as on the shelves. The ice-surface profile at c. 35–33 cal ka BP (33000 BP) is based on the estimates in Tables 2 and 3 with a 50–70% isostatic depression as compared to that of the YD interval.* The recent uplift data *(lower panel) are from Dehls et al. (2000).*

There are few indications for accurate estimates of late Middle Weichselian relative sea levels in Norway. Most of the sea-level indicators are based on reworked marine shells, many of which are resedimented in tills and other sediments (e.g., Mangerud et al. 1981) and are therefore of limited value as sea-level indicators. However, some of the finds represent marine shells in sedimentary units in subtill positions and are therefore conceivably more accurate indicators of sea level. Five of these, all from Nordland, northern Norway, are listed in Table 2, and their glacioisostatic conditions indicate a 51–>85% depression of the crust as compared with that of the YD. I consider the most precise and accurate of these sea-level data to be those from the Ytresjøen locality (Table 2). The ^{14}C dating of one of these *Balanus* shells at c. 33.6 cal ka BP suggests an age close to that for the proposed most likely age of the shore deposit at 14 m a.s.l. at Leirhola, Arnøya. The similarity between the Ytresjøen and Leirhola data is even more intriguing if considered that, also at Ytresjøen, the preceding considerable ice advance, as represented by a till, occurred just before the discussed sea-level event. At Ytresjøen, this ice advance is constrained between c. 40 and 33.6 cal ka BP (Table 1) (Olsen 2002).

The glacioisostatic conditions during the Ytresjøen sea-level event indicate a 51% depression of the crust compared to that of the YD. With the preceding large ice load in mind, this signifies an even smaller ice remnant during the discussed sea-level event than is implied from the Leirhola data.

Conclusions

From the record of a late Middle Weichselian sub-till shore deposit at 14 m a.s.l. at Leirhola, Arnøya, northern Norway, it may be concluded that:

1) The ice extension during the formation of the shore deposit may have reached a maximum extent slightly greater than during the late-glacial Younger Dryas interval.
2) An age at c. 33 cal ka BP for the 14 m shoreline is in accord with the published record, with a large ice sheet at c. 45 cal ka BP that retreated rapidly (e.g., Olsen et al. 2001b), and with new ice growth at c. 34–33 cal ka BP (Larsen et al. 1987), which was followed by a rapid and significant ice retreat shortly after that time (Olsen et al. 2001b). An age

for the shoreline at 35–34 cal ka BP may also match with the regional record if the ice retreat after the 45 cal ka BP glaciation was slower, and if the 34–33 cal ka BP ice growth occurred mainly after the 14 m sea-level phase. Even older age alternatives may be possible, but these suggest a very rapid deglaciation after the 45 cal ka BP glaciation and/or a much thinner (<750 m) ice sheet than expected.

3) The relative glacioisostatic depression during formation of the shore deposit at 14 m a.s.l. on Arnøya was only c. 70–80% of that of the YD interval (Table 3). This result, combined with the published record of large ice growths/advances in Norway at c. 45 and 33–34 cal ka BP, implies that the volume (thickness) of the ice sheet during the shore deposit formation was *much less* than during the YD, and was probably more like the size attained during a late part of the Preboreal (Figure 1).
4) Corresponding sea-level data from Ytresjøen and other sites in northern Norway indicate a lesser relative glacioisostatic depression, almost as low as 50% of that of YD (Table 2), and therefore also imply a much smaller ice remnant during the discussed sea-level event.

Acknowledgements

The excavation and fieldwork carried out on Arnøya in the year 2000 were financed by the Geological Survey of Norway (NGU), whilst the University of Tromsø provided financial support for the initial work almost two decades earlier presented by Andreassen et al. (1985). The work at Ytresjøen was mainly carried out in 1998 and financed by NGU. This paper has benefited from constructive comments of an earlier version by Jan Mangerud, by an anonymous reviewer and by Barbara Wohlfarth; the English has been improved by David Roberts. Irene Lundquist has drawn the figures. I am grateful to all these persons and institutes for their support.

References

Alm, T. (1993) Øvre Æråsvatn - palynostratigraphy of a 22,000 to 10,000 BP lacustrine record on Andøya, northern Norway. *Boreas*, **22**, 171–188.

Andersen, B.G. (1968) Glacial geology of Western Troms, North Norway. *Norges geologiske undersøkelse*, **256**, 1–160.

Andreassen, K., Vorren, T.O. and Johansen, K.B. (1985) Pre-Late Weichselian glacimarine sediments at Arnøy, North Norway. *Geologiska Föreningens i Stockholm Förhandlingar*, **107**, 63–70.

Bard, E., Hamelin, B. and Fairbanks, R.G. (1990) U-Th ages obtained by mass spectrometry in corals from Barbados: sea level during the past 130,000 years. *Nature*, **346**, 456–458.

Bergstrøm, B., Reite, A., Sveian, H. and Olsen, L. (2001) Feltrutiner, kartleggings-prinsipper og standarder for kvartærgeologisk kartlegging ved NGU. *Norges geologiske undersøkelse Rapport 2001.018*, 23 pp.

Chappell, J. (1983) A revised sea-level record for the last 300,000 years from Papua New Guinea. *Search*, **14**, 99–101.

Chappell, J. (2002) Sea level changes forced ice breakouts in the Last Glacial cycle: new results from coral terraces. *Quaternary Science Reviews*, **21**, 1229–1240.

Dehls, J.F., Olesen, O., Olsen, L. and Blikra, L.H. (2000) Neotectonic faulting in northern Norway; the Stuoragurra and Nordmannvikdalen postglacial faults. *Quaternary Science Reviews*, **19**, 1447–1460.

Fairbanks, R.G. (1989) A 17,000-year glacio-eustatic sea level record: influence of glacial melting rates on the Younger Dryas event and deep-ocean circulation. *Nature*, **342**, 637–642.

Fairbanks, R.G., Mortlock, R.A., Chiu, T.-C., Cao, L., Kaplan, A., Guilderson, T.P., Fairbanks, T.W., Bloom, A.L., Grootes, P.M. and Nadeau, M.-J. (2005) Radiocarbon calibration curve spanning 0 to 50,000 years BP based on paired $^{230}Th/^{234}U/^{238}U$ and ^{14}C dates on pristine corals. *Quaternary Science Reviews*, **24**, 1781–1796.

Fletcher III, C.H., Fairbridge, R.W, Møller, J.J. and Long, A.J. (1993) Emergence of the Varanger Peninsula, Arctic Norway, and climate changes since deglaciation. *The Holocene*, **3**, 116–127.

Gjelle, S., Bergstrøm, B., Gustavson, M., Olsen, L. and Sveian, H. (1995) Geology and landscape around the Arctic Circle in Norway. *Norges geologiske undersøkelse*. ISBN 82–7385–164–8, pp. 1–128.

Hafsten, U. (1956) Pollen-analytic investigations on the late Quaternary development in the inner Oslofjord area. *Universitetet i Bergen. Årbok 1956, Naturvitenskapelig rekke*, **8**, 1–161.

Kjemperud, A. (1986) Late Weichselian and Holocene shoreline displacement in the Trondheimsfjord area, central Norway. *Boreas*, **15**, 61–82.

Lambeck, K., Smither, C. and Johnston, P. (1998) Sea-level change, glacial rebound and mantle viscosity for northern Europe. *Geophysical Journal International*, **134**, 102–144.

Lambeck, K., Purcell, A., Funder, S., Kjær, K.H., Larsen, E. and Möller, P. (2006) Constraints on the Late Saalian to early Middle Weichselian ice sheet of Eurasia from field data and rebound modelling. *Boreas*, **35**, 539–575.

Larsen, E., Gulliksen, S., Lauritzen, S.-E., Lie, R., Løvlie, R. and Mangerud, J. (1987) Cave stratigraphy in western Norway; multiple Weichselian glaciations and interstadial vertebrate fauna. *Boreas*, **16**, 267–292.

Mangerud, J., Gulliksen, S., Larsen, E., Longva, O., Miller, G.H., Sejrup, H.-P. and Sønstegaard, E. (1981) A Middle Weichselian ice-free period in Western Norway: the Ålesund Interstadial. *Boreas*, **10**, 447–462.

Mangerud, J., Løvlie, R., Gulliksen, S., Hufthammer, A. K., Larsen, E. and Valen, V. (2003) Paleomagnetic correlations between Scandinavian Ice-Sheet fluctuations and Greenland Dansgaard-Oeschger events, 45,000–25,000 yr B.P. *Quaternary Research*, **59**, 213–222.

Mangerud, J, Gulliksen, S. and Larsen, E. (in print) ^{14}C-dated fluctuations of the western flank of the Scandinavian Ice Sheet 45–25 kyr BP compared with Bølling-Younger Dryas fluctuations

and Dansgaard-Oeschger events in Greenland. *Boreas*, 10.1111/j.1592–3885.2009.00127.x.ISSN 0300–9483.

Møller, J.J., Danielsen, T.K. and Fjalstad, A. (1992) Late Weichselian glacial maximum on Andøya, North Norway. *Boreas*, **21**, 1–13.

Olsen, L. (2002) Mid and Late Weichselian, ice-sheet fluctuations northwest of the Svartisen glacier, Nordland, northern Norway. *Norges geologiske undersøkelse Bulletin*, **440**, 39–52.

Olsen, L. and Bergstrøm, B. (2003) Meløy 1928 IV—Quaternary geological map in scale 1:50 000. *Geological Survey of Norway*.

Olsen, L. and Hamborg, M. (1983) Morenestratigrafi og isbevegelser fra Weichsel, sørvestre Finnmarksvidda, Nord-Norge. *Norges geologiske undersøkelse Bulletin*, **378**, 93–113.

Olsen, L., van der Borg, K., Bergstrøm, B., Sveian, H., Lauritzen, S.-E. and Hansen, G. (2001a) AMS radiocarbon dating of glacigenic sediments with low organic content—an important tool for reconstructing the history of glacial variations in Norway. *Norsk Geologisk Tidsskrift*, **81**, 59–92.

Olsen, L., Sveian, H. and Bergstrøm, B. (2001b) Rapid adjustments of the western part of the Scandinavian ice sheet during the Mid- and Late Weichselian—a new model. *Norsk Geologisk Tidsskrift*, **81**, 93–118.

Ota, Y., Chappell, J., Kelley, R., Yonekura, N., Matsumoto, E., Nishimura, T. and Head, J. (1993) Holocene coral reef terraces and coseismic uplift of Huon Peninsula, Papua New Guinea. *Quaternary Research*, **40**, 177–188.

Paterson, W.S.B. (1994) *The physics of glaciers*. Third edition, Elsevier, Oxford, 480 pp.

Roberts, D. (1974) Hammerfest. Description of the 1:250 000 geological map. *Norges geologiske undersøkelse*, **301**, 1–66.

Shackleton, N. (1987) Oxygen isotope, ice volume and sea level. *Quaternary Science Reviews*, **6**, 183–190.

Sveian, H. and Bergstrøm, B. (2004) Isens fotefar i Nord-Troms. *In* Dahl, R. and Sveian, H. (eds.) *Ka dokker mein førr stein! Geologi, landskap og ressurser i Troms*. Norges geologiske undersøkelse, pp. 100–109.

Sveian, H., Riiber, K., Bergstrøm, B. and Reite, A.J. (2005) Troms fylke, løsmassekart M 1:310 000. *Norges geologiske undersøkelse*.

Svendsen, J.I. and Mangerud, J. (1987) Late Weichselian and Holocene sea-level history for a cross-section of western Norway. *Journal of Quaternary Science*, **2**, 113–132.

Vorren, T.O. and Plassen, L. (2002) Deglaciation and palaeoclimate of the Andfjord-Vågsfjord area, North Norway. *Boreas*, **31**, 97–125.

Vorren, T.O., Corner, G.D. and Nagy, J. (1981) Weichselian sediments containing redeposited interstadial/interglacial fossils at Slettaelva, North Norway. *Boreas*, **19**, 477–484.

Vorren, T.O., Vorren, K.-D., Alm, T., Gulliksen, S. and Løvlie, R. (1988) The last deglaciation (20,000 to 11,000 B.P.) on Andøya, northern Norway. *Boreas*, **17**, 41–77.

RESEARCH ARTICLE

Mesozoic sediments and structures onshore Norway and in the coastal zone

Reidulv Bøe[1], Håkon Fossen[2], Morten Smelror[1]

[1]*Geological Survey of Norway (NGU), P.O. Box 6315 Sluppen, 7491 Trondheim, Norway.*
[2]*University of Bergen, Department of Earth Science, P.O. Box 7800, 5020 Bergen, Norway.*
reidulv.boe@ngu.no

In mainland Norway, Mesozoic sedimentary rocks (Jurassic and Cretaceous) outcrop only on Andøya. These are the youngest rocks on land anywhere in Norway. Triassic dykes occur in West Norway, while Mesozoic structures and fault products are common at major and minor fault zones in various parts of coastal Norway. Sedimentary rocks occur in half-grabens in many fjords, especially in Mid Norway and northern Nordland. Most of these are of Middle-Late Jurassic age, and are interpreted to represent the remains of a much more extensive Jurassic-Cretaceous sedimentary succession that covered large parts of coastal Norway. These sedimentary rocks were downfaulted during tectonic activity in Late Jurassic-Early Cretaceous times thus escaping late Tertiary-Pleistocene erosion.

Introduction

The aim of this contribution is to summarise results from studies of Mesozoic sediments and structures onshore Norway and in the coastal zone over the past 150–160 years. A comprehensive summary of this kind has previously not been published, although Ørvig (1960) presented a small chapter, mainly on the Mesozoic rocks on Andøya, in *'Geology of Norway'*.

Erratic blocks of Mesozoic rocks were found in Norway for the first time in 1845, on the northwest shore of Beitstadfjorden (Figure 1). In 1867, T. Dahl investigated an outcrop of coal utilised by local farmers on Andøya. Subsequent mapping on Andøya and new finds of erratic blocks along the coast of Norway indicated that Mesozoic rocks could be present in several fjords and offshore the present coastline (Ørvig 1960 and references therein). Geophysical and geological mapping of the Norwegian continental margin started in the 1960s. The mapping of the shelf was intensified after discovery of the Ekofisk oil field in the North Sea in 1969. However, Oftedahl (1975) was the first to map Mesozoic rocks in the coastal zone. This activity was intensified in the 1980s with publication of several studies (Holtedahl 1988,1993, Bøe and Bjerkli 1989, Bøe 1991, Bøe et al. 1992, 2005, 2008, Thorsnes 1995, Fossen et al. 1997, Bøe and Skilbrei 1998, Davidsen et al. 2001a, b, Sommaruga and Bøe 2002). In addition, shallow sampling and stratigraphic drilling was performed by IKU (now Sintef Petroleum Research) in many subcropping sedimentary units along the coast (Mørk et al. 1983, Bugge et al. 1984, 1989, 1993, 2002, Sættem et al. 1985, Fjerdingstad et al. 1985, Aarhus et al. 1987, Skarbø et al. 1988, Rokoengen et al. 1989, Smelror et al. 1989, 1994,

Bøe, R., Fossen, H. and Smelror, M. (2010) Mesozoic sediments and structures onshore Norway and in the coastal zone. *Norges geologiske undersøkelse Bulletin,* **450**, 15-32.

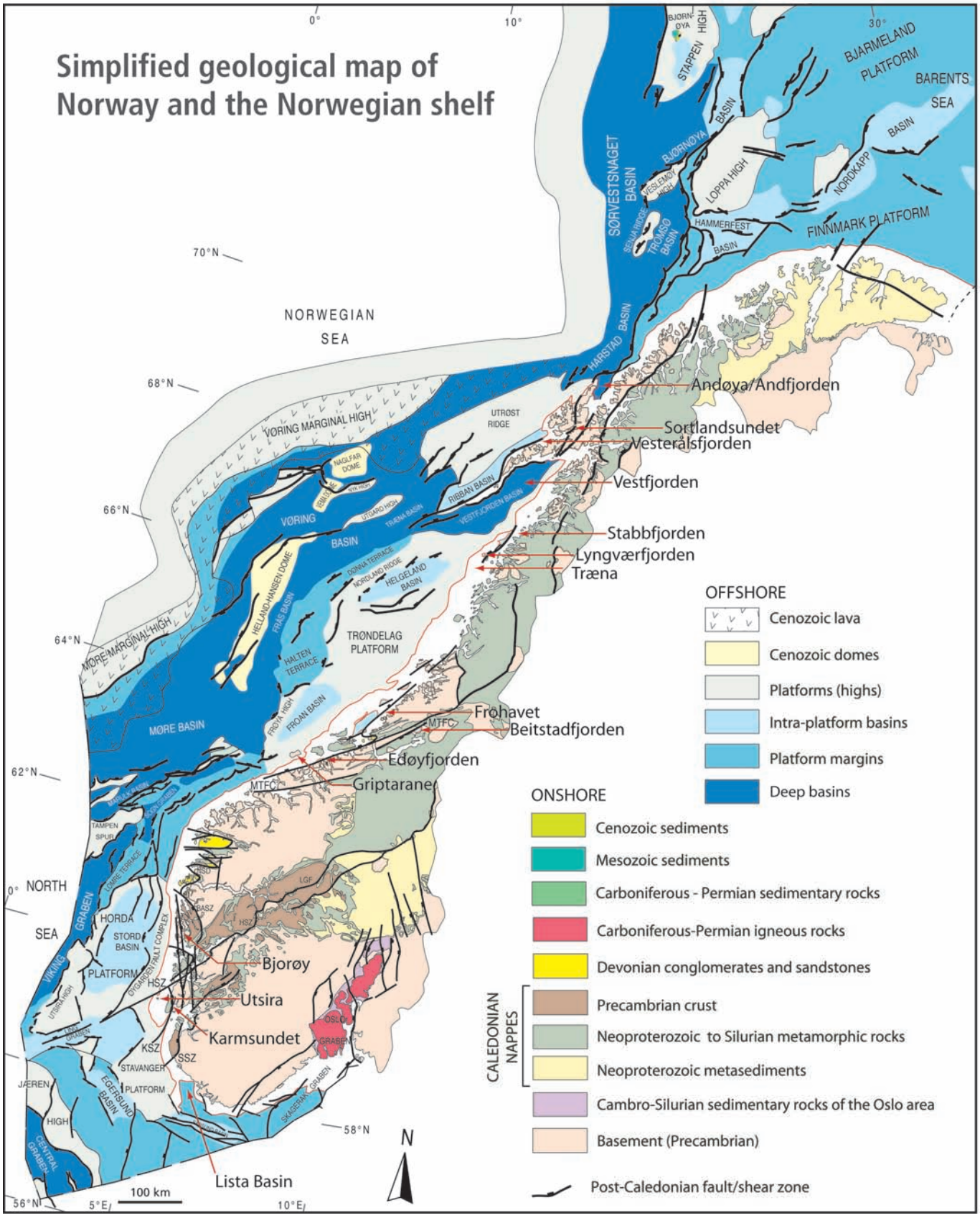

Figure 1. Overview map showing geological structures on the Norwegian continental shelf south of Bjørnøya and simplified geology of mainland Norway. The locations of Mesozoic basins, successions and structures discussed in the text are shown. The compilation is based on maps from the Norwegian Petroleum Directorate, the Geological Survey of Norway, and various published and unpublished data.

Hansen et al. 1992, Løseth and Tveten 1996).

The offshore Mesozoic sedimentary stratigraphy and structures are well documented in numerous contributions by academia and the petroleum industry (e.g., Evans et al. 2003, Martinsen and Dreyer 2001, Wandås et al. (2005), Ramberg et al. 2006, Smelror et al. 2009). The focus of this chapter is thus on Mesozoic rocks and structures in the coastal zone of mainland Norway, with only a short overview of the continental shelf.

Mesozoic sediments and structures on the continental shelf

Barents Sea

The Barents Sea (Figure 1) is located in an intracratonic setting between the Norwegian-Russian mainland, the Arctic Ocean margin and the Norwegian-Greenland Sea (Figure 1). The region has been affected by several phases of tectonism since the termination of Caledonian movements in the Early Devonian. The dominant structural trends are ENE–WSW to NE–SW and NNE–SSW to NNW–SSE, with a local influence of WNW–ESE-striking elements (Gabrielsen et al. 1990). Major faults with similar trends are known from the mainland of Finnmark, Norway, and Northwest Russia, where Mesozoic ages of movement have been inferred (Lippard and Roberts 1987, Karputz et al. 1993, Roberts and Lippard 2005). The post-Devonian succession of the Barents Shelf shows a close resemblance to the Upper Palaeozoic to Tertiary successions on Svalbard, which represent an uplifted part of the northern Barents Shelf.

In the latest Permian and Early Triassic, the western Barents Shelf experienced uplift and erosion, followed by a tectonically relatively quiet period in the Triassic to Early Jurassic. During the Mesozoic, the shelf experienced repeated cycles of coastal and deltaic progradations into the wide shelf basin from the north and northwest. The Triassic and Early Jurassic succession consists of a series of thick, upward-coarsening sequences assigned to the Sassendalen and Kapp Toscana groups. The coastal sediments of the Sassendalen Group grade eastwards and southwards into shelf mudstones, and in the southwestern Barents Shelf, shallow to deep shelf sediments were deposited. The overlying Kapp Toscana Group contains a number of upward-coarsening sequences, with an increasing content of sandstones towards the top. On Svalbard, the uppermost part is condensed. The group consists of nearshore, deltaic deposits.

A period of crustal stretching and associated block faulting started in the Middle Jurassic and increased during the Late Jurassic, terminating with the formation of the major basins and highs on the Barents Shelf (Gabrielsen et al. 1990). During this period of crustal extension, some areas experienced rapid and extreme subsidence (Tromsø Basin, western Bjørnøya Basin), while other areas show signs of local inversion (i.e., along the Ringvassøya-Loppa Fault Complex). The Middle Jurassic to Lower Cretaceous succession is dominated by dark, commonly organic-rich mudstones, but includes also deltaic and shelf sandstones (Nøttvedt et al. 1993, Dallmann et al. 1999, Smelror et al. 2001). Condensed units of shelf carbonates were developed on local highs during the Valanginian-Barremian (Smelror et al. 1998). In the Aptian-Albian, a thick series of stacked, transgressive shelf sandstones, siltstones and shales accumulated over larger parts of the Barents Shelf.

The opening of the Arctic Basin in Late Cretaceous time resulted in uplift of the northern Barents Sea region. On Svalbard, Upper Cretaceous and lowermost Tertiary strata are missing. On the shelf, reverse faulting and folding occurred in several areas, even though extension may have continued on the regional scale (Gabrielsen et al. 1990).

Norwegian Sea

In the Permian and Early Triassic, rift basins continued to develop between Norway and Greenland as a result of crustal extension that had started already in Devonian and Carboniferous time. An embayment of the ocean gradually developed towards the south (Blystad et al. 1995, Brekke 2000). A warm climate persisted throughout the Triassic, and in the Late Triassic, global plate motions gradually led to a more humid climate (Müller et al. 2005). This caused strong chemical weathering and oxidation of land areas, and deposition of red-coloured sediments both on land and along the coasts. Deposition of mudstones and some evaporites predominated between Norway and Greenland in the Early Triassic. In the Middle Triassic, the area of rifting in the Norwegian Sea (Figure 1) became less active and there was a change to deposition on fluvial plains. In the Late Triassic, there was renewed stretching of the crust (Müller et al. 2005). This resulted in marine transgressions with deposition of more than 1000 m of salt and mudstone, followed by continental sedimentation, first lake and finally fluvial deposits. The Triassic succession in the Norwegian Sea is locally several thousand metres thick (Müller et al. 2005, Nystuen et al. 2006).

In the latest Triassic, crustal movements caused uplift of mainland Norway, precipitation increased, and coarse-grained sediments were deposited along the coast and on the continental shelf (Müller et al. 2005). This deposition (Åre Formation) continued into the Early Jurassic, when extensive bogs, resulting in thick coal beds, developed on coastal plains. A shallow seaway with strong tidal currents gradually developed between the ocean in the north and Tethys. The sandstones of the Tilje Formation show evidence of this tidal environment (Martinius et al. 2001). Due to a wet climate, pronounced erosion and denudation of mainland Norway occurred. Sediments were deposited in estuaries and deltas along a strongly fluctuating coastline, with sandstone units covering large parts of the shelf (Dalland et al. 1988, Brekke et al. 2001). Several of the most important hydrocarbon reservoirs in the Norwegian Sea are of Early and Middle Jurassic age.

In the latest Middle Jurassic-Late Jurassic, NW–SE extension was renewed along the rift axis in the Norwegian Sea (Blystad et

al. 1995). This caused subsidence and development of large rift structures with numerous horsts and grabens on the Mid-Norwegian shelf (Gabrielsen et al. 1999, Osmundsen et al. 2002). The eastern flank of the rift in the Norwegian Sea is represented by the Halten and Dønna Terraces and the Nordland Ridge, while the Trøndelag Platform represents the rift shoulder to the east. At the same time, there was extensive deposition of organic-rich mud in isolated fault basins, and coastal areas were transgressed due to a global sea-level high stand. The Spekk Formation, deposited in the Late Jurassic, is the major source rock for hydrocarbons on the Mid-Norwegian shelf.

In the Cretaceous, a transition from extension and rifting to seafloor spreading in the Norwegian Sea occurred. Campanian-Palaeocene rifting was followed by seafloor spreading in the Early Eocene (Brekke et al. 2001, Færseth and Lien 2002, Lien 2005). Due to crustal thinning and thermal subsidence, deep, regional basins formed along the main axis of the rift movements, e.g., the Møre, Vøring and Vestfjorden basins. The main Campanian-Palaeocene rifting and seafloor spreading took place to the west of these basins (Brekke et al. 2001). The basins were filled with 8–10 km of fine-grained sediments derived mainly from the west (Greenland) (Brekke 2000). Sandstones deposited on submarine fans were derived partly from Greenland, from local highs such as the Nordland Ridge, and in some areas from the Norwegian mainland (e.g., Lien 2005).

North Sea

The North Sea basin (Figure 1) (Evans et al. 2003) probably initiated in the Permian at approximately the same time as the Oslo and Skagerrak Grabens to the southeast and related graben systems to the north (Færseth 1996). Basin subsidence accelerated into the Triassic, and continental, clastic red-beds, up to several kilometres thick, are found in many of the deep North Sea wells. The stratigraphic thickness of Triassic strata is largely controlled by Permian salt structures in the southern North Sea. In the northern North Sea, where Permian salt is thin or absent, the Triassic stratigraphy is controlled by the evolution of half-grabens (Steel and Ryseth 1990, Færseth 1996).

The Øygarden Fault Complex (Figure 1) comprises coast-parallel fault segments with up to 5 km vertical throw, and defines the eastern margin of the Permo-Triassic North Sea rift. As shown by Steel and Ryseth (1990), it includes a wedge-shaped, syntectonic, Lower Triassic succession overlain by Middle Triassic to Middle Jurassic post-rift sediments. The Permo-Triassic rift axis is interpreted to be located beneath the Horda Platform east of the Late Jurassic Viking Graben (Færseth et al. 1996, Odinsen et al. 2000).

The Permo-Triassic rift phase terminated at the end of the Early Triassic, and clastic post-rift deposits then filled into the passively subsiding rift basin until the onset of a new rift phase in the late Middle Jurassic. A general change in post-rift sedimentation, from continental Triassic to deltaic conditions in Early to Middle Jurassic time, occurred. The Jurassic sandstones, notably the Brent Group, form major reservoirs in the North Sea (Husmo et al. 2002).

A framework of faults was established throughout the North Sea during the Permo-Triassic rifting phase (Færseth 1996). Some of these were reactivated during the late Middle Jurassic to latest Jurassic rifting. Large faults defining first-order fault blocks show evidence of kilometre-scale, pre-Jurassic offsets (e.g., Færseth 1996, Gabrielsen et al. 1999, Fossen 2000, Odinsen et al. 2000). The Late Jurassic rift axis, defined by the right-stepping Viking Graben, was located west of the Horda Platform. The Øygarden Fault Complex and many other faults on the Horda Platform thus experienced only modest post-Triassic reactivation.

In the Late Jurassic, the Viking Graben and deep parts of rotated fault blocks developed into deep marine basins in which organic-rich shales of the Viking Group (Draupne Formation) were deposited. These form the main source of hydrocarbons in the North Sea. Jurassic rifting ended for the most part in Mid Volgian time although extension locally continued into the Cretaceous (Færseth et al. 1995, Færseth and Lien 2002).

In the Cretaceous, the North Sea experienced infill of deep basins created during the Late Jurassic rifting climax. Periods of significant tectonic activity occurred, and during Hauterian-Barremian times, local structural highs were uplifted and deeply eroded. The Barremian landscape was largely filled in by the end of the Early Cretaceous, and all structural highs and most of the eastern basin margin were flooded in the Santonian (Bugge et al. 2001). The Cretaceous stratigraphic column is dominated by shales and, in the southern North Sea, chalks formed by accumulation of *coccoliths* from a planktonic calc algae. Sandstones can be linked to periods of tectonic activity and/or change in relative sea level (Bugge et al. 2001).

Mesozoic sediments and structures onshore and in the coastal zone

The paragraphs beneath summarise work on Mesozoic sediments and structures onshore Norway and in the coastal zone. The summary is mainly based on published work, but several new figures are presented.

Northern Norway

Andøya and Andfjorden

Andøya (Figure 1) contains the only succession of Mesozoic sediments in mainland Norway. The field was first detected by T. Dahl in 1867 (Ørvig 1960), and a minor coal bed at the southern margin of the field led explorationists to drill for coal in the last part of the 19th century. During the 1970s, hydrocarbon drilling was undertaken by a local-based company, and detailed sedimentological investigations were carried out by Dalland (1981 and references therein).

The Jurassic-Cretaceous succession on Andøya is approximately 900 m thick, and occurs in a small, partly fault-bounded area at the eastern coast of the island (Figure 2) (Zwaan et al. 1998). A weathering zone, and thin remnants of a formerly very thick Palaeozoic sediment cover underlie sediments of Middle Jurassic age (Dalland 1981, Manum et al. 1991). The age of the weathering zone is poorly constrained and debated. Sturt et al. (1979) reported a K–Ar age of Late Devonian/Middle Carboniferous for the weathering profile, while Løseth and Tveten (1996) and Smelror et al. (2001) suggested that the extensive weathering of the basement took place in the Middle Jurassic. This latter interpretation is based on correlation to the offshore record where similar weathering profiles have been recorded (Smelror et al. 2001, Mørk et al. 2003).

The outcrop area on Andøya is located at the western margin of a narrow N–S-trending graben. The graben continues below Andfjorden to the east, where the thickness is 2–3 km, and farther northwards into the deep Harstad Basin (Figure 1). The succession consists of two major upward-fining sequences, one of Bajocian-Bathonian to Volgian age, and the other of Ryazanian/Valanginian to Aptian age (Birkelund et al. 1978, Dalland 1981, Zakharov et al. 1981, Aarhus et al. 1986) (Figure 3).

The lowermost Ramså Formation comprises braided river sands at the base (Hestberget Member), overlain by lake or lagoonal deposits with local coals (Kullgrøfta Member), and fluvial to beach and shallow-marine sands in the upper part (Bonteigen Member) (Figure 3). The overlying Dragneset Formation grades from calcareous sandstone (Breisanden Member) in the lower part to siltstone and shale in the upper part (Taumhølet and Ratjønna members). Remains of Ichtyosaurians and many other fossils have been found in this member (Ørvig 1960 and references therein).

Figure 2. Map showing the locations of Mesozoic successions on Andøya and in Andfjorden, Gavlfjorden, Vesterålsfjorden and Sortlandssundet. The map is partly based on unpublished seismic data supplied by B. Davidsen. Dark green: previously unpublished areas of Mesozoic rocks.

The overlying Nybrua Formation, separated from the Jurassic succession by an unconformity, forms a regionally extensive unit of shallow-marine marl and sandstone in the lower part of the Cretaceous (Leira and Skjærmyrbekken members). Overlying this unit are intermediate- to deep-marine mudstones and shales of the Skarstein Formation (Nordelva and Hellneset members). Parts of the Andøya succession are lithologically similar to time-equivalent sections in East Greenland, the northern North Sea, the Norwegian Sea and the Barents Sea (Dalland 1981, Smelror et al. 2001) (Figure 4).

A period of major uplift and erosion took place during the Late Triassic. Faulting occurred in Middle Jurassic and probably also during Hauterivan/Barremian and Aptian time. The northern boundary fault of the Mesozoic succession is clearly syndepositional in nature. There may also have been tectonic activity in Late Berriasian/Early Valanginian and Turonian times.

Vesterålen

The Sortlandsundet basin (Figures 1 and 2) is a half-graben (5 x 3.5 km) defined by a normal fault in the southeast and unconformable boundaries to the northeast, northwest and southwest (Davidsen et al. 2001a, b). Mesozoic sedimentary strata within the basin are more than 440 m thick and display seismic reflectors dipping a few degrees to the southeast. Glacier-transported erratic blocks, assumed to derive from the Sortlandsundet basin, are found along the shorelines 3–10 km north of the basin. These blocks, which comprise quartz-rich sediments varying in grain size from conglomerates to fine sandstones, contain numerous fossils, e.g., bivalves, belemnites, ammonites and plant remains. Dinoflagellates from the samples show that a majority of the samples are probably of Bathonian-Callovian age, while age determination based on bivalves gives a Portlandian age for some of the samples (Fürsich and Thomsen 2005). The contrasting age determination has not been explained.

Mesozoic strata also occur in Vesterålsfjorden and Gavlfjorden (Figure 2) (Davidsen et al. 2001b). In Gavlfjorden, seismic data indicate fault boundaries along the eastern and western margins of the fjord, while the southern boundary is an unconformity. The Mesozoic succession is here up to 300 m thick.

Vestfjorden

The Vestfjorden Basin (Figure 1) is essentially a Cretaceous half-graben with its main boundary fault to the northwest, along the Lofoten Ridge (Blystad et al. 1995). Important normal faults also occur to the southeast, along the mainland, where Triassic and Jurassic rocks may locally subcrop at the seabed. The basin contains 8–10 km of Cretaceous sediments, interpreted to reflect mainly passive infill of the Jurassic rift topography (e.g., Færseth and Lien 2002). However, the area has not been opened up for oil and gas exploration, and the sedimentary succession

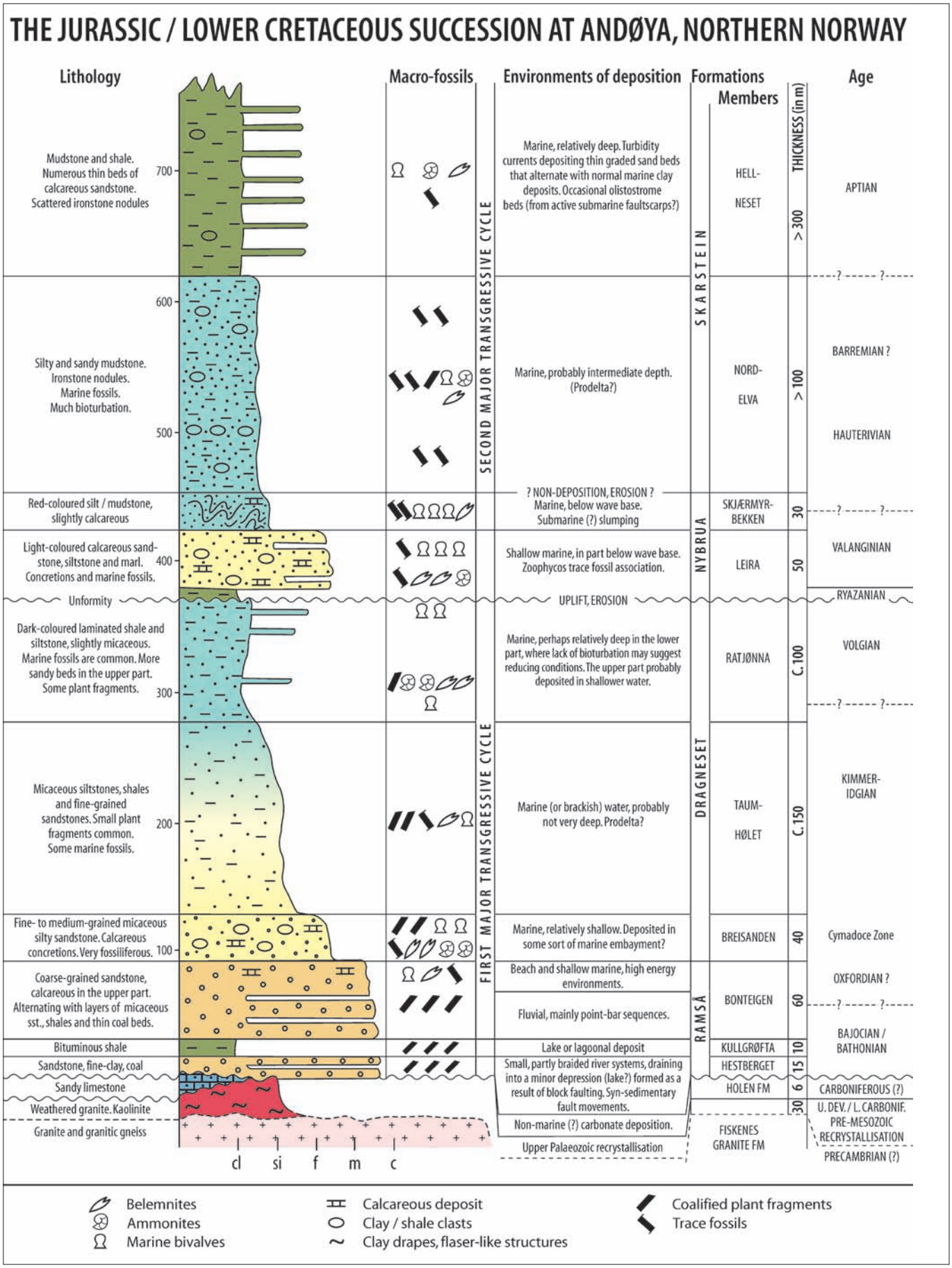

Figure 3. The Mesozoic sedimentary succession on Andøya. Only the lower part of the Lower Cretaceous Hellneset Member is shown. Redrawn from Dalland (1981).

is thus poorly known. It is assumed that there was a connection between the Andfjorden and Vestfjorden basins before the Late Tertiary-Quaternary uplift and erosion.

Stabbfjorden/Lyngværfjorden/Træna

The Stabbfjorden and Lyngværfjorden basins (Figure 1) were discovered during reconnaissance mapping in 1998 (Bøe et al. 2008). The NE–SW-trending Stabbfjorden basin, northwest of Meløya, is 28 km long and 3–10 km wide, with a sedimentary rock succession that is up to 800 m thick. The Lyngværfjorden basin, northeast of Træna, has a length of about 12 km, whereas the width is up to 3 km and the depth possibly more than 350 m. Ice-transported, erratic blocks of sedimentary rocks found on skerries near the two basins comprise conglomerates, sandstones, siltstones and mudstones (Figure 5). Palynomorphs show that they range in age from Barremian to Triassic (Bøe et al. 2008). The majority of the samples are of Middle-Late Jurassic age and reflect shallow marine deposition. The Triassic sediments were possibly deposited in a continental environment. The lithofacies reflect the well-known tectonic phases

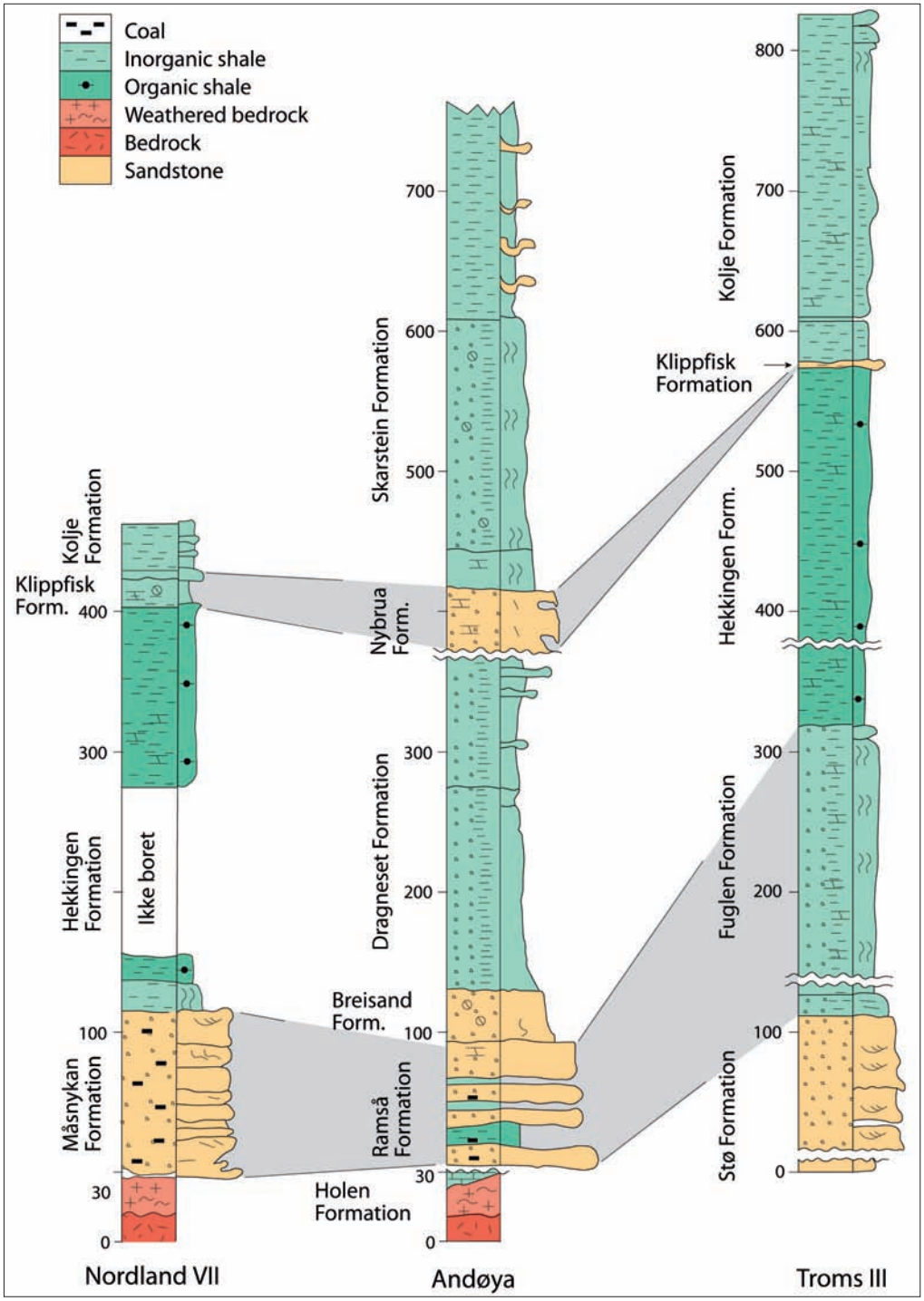

Figure 4. Lithostratigraphic and sequence stratigraphic correlation between cored successions at Andøya, Troms III and Nordland IV. Modified from Smelror et al. (2001) and Henningsen (2006).

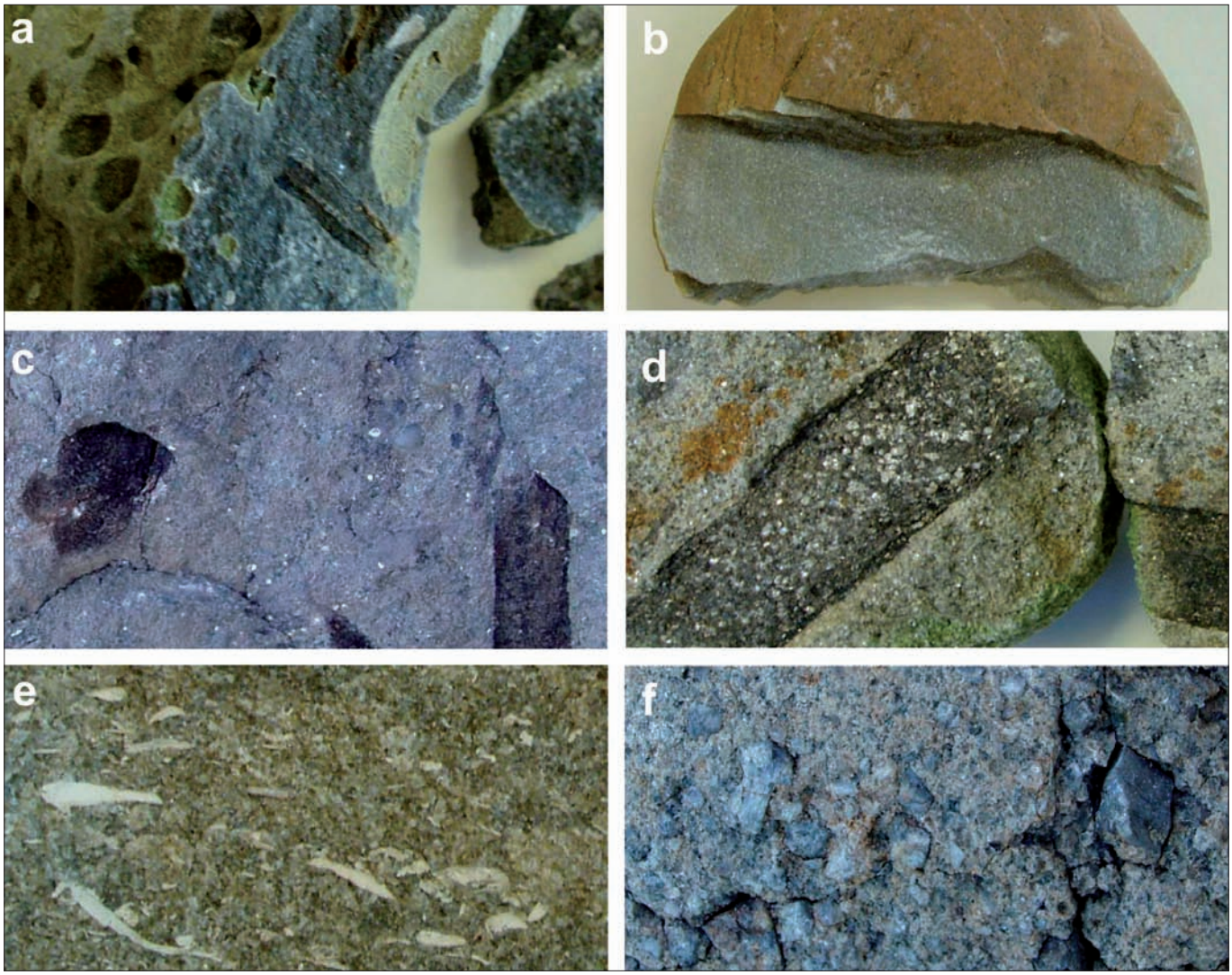

Figure 5. Photographs of erratic blocks from the Stabbfjorden basin. (a) Middle-Upper Jurassic sandstone with shells and coal fragments, (b) Middle-Upper Jurassic siltstone with shells, (c) Upper Jurassic sandstone with shells and coal fragments, (d) Middle-Upper Jurassic sandstone with shells and coal fragments, (e) Middle-Upper Jurassic bioclastic sandstone, (f) Lower Cretaceous conglomerate. The pictures are approximately 4 x 8 cm. Modified from Bøe et al. (2008).

and sea-level changes that have been reported for the Middle Jurassic-Early Cretaceous in this area. A succession of assumed Triassic age also occurs in Trænfjorden, southeast of Træna (Bøe et al. 2008). This can probably be correlated with an Upper Permian-Lower Triassic, fully marine succession of sandstones, coarse-grained turbidites, shales and reworked sabkha sediments cored 12 km southwest of the Træna islands (Bugge et al. 2002).

Mid Norway

The development of Mesozoic basins along the coast of Mid Norway is closely related to activity on the long-lived Møre-Trøndelag Fault Complex (MTFC), which can be traced from the southern Møre Basin Margin to the inner parts of Trondheimsfjorden and farther northeast into the Grong district (Grønlie and Roberts 1989, Grønlie et al. 1994, Blystad et al. 1995, Gabrielsen et al. 1999). Two of the major onshore fault systems of the MTFC are the steeply NW-dipping Hitra-Snåsa and Verran Faults, which originally developed in Devonian time in a late-Caledonian, ductile, sinistral shear regime (Grønlie and Roberts 1989, Osmundsen et al. 2006).

Mid Norway was affected by a rift episode lasting from the Bajocian to the Volgian, but with transition from an initial rifting stage to a rifting climax in the Callovian (e.g, Brekke et al. 2001, Færseth and Lien 2002). This resulted in essentially dip-slip normal faulting along the older structural lines of weakness and development of horst and graben (half-graben) structures. Subsequently, a phase of dextral strike-slip movements down-faulted and deformed the sequences, especially in the Beitstadfjorden Basin (Bøe and Bjerkli 1989).

Beitstadfjorden Basin

The Beitstadfjorden Basin (14 km long and 6 km wide) (Figures 6 and 7) is located at the northeastern extremity of Trondheimsfjorden. The basin is related to a SSE-dipping normal fault, which is a branch of the generally steeply WNW-dipping Verran Fault system. Many smaller faults within the basin are

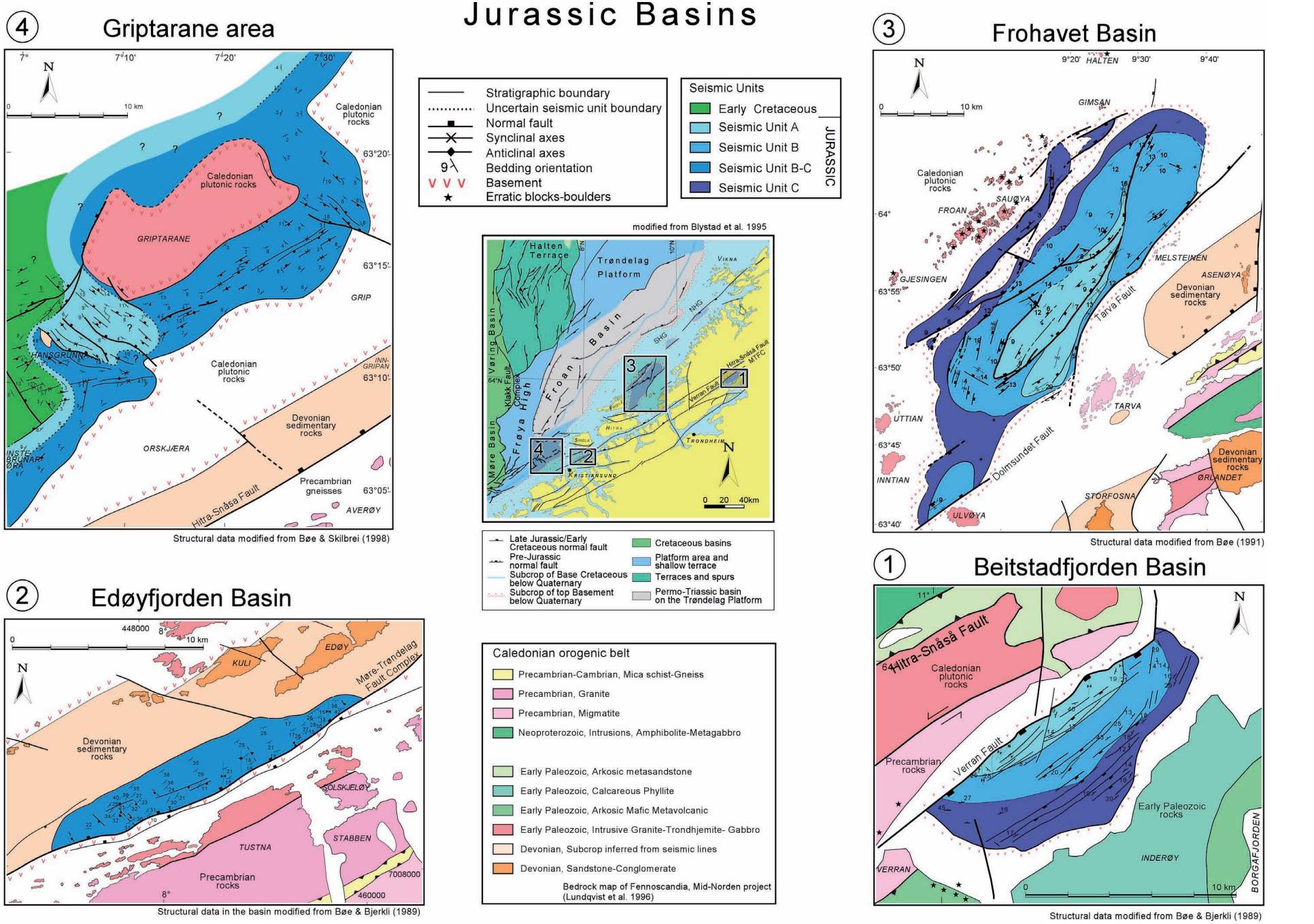

Figure 6. Subcrop maps of Jurassic basins, Mid Norway. Modified from Sommaruga and Bøe (2002).

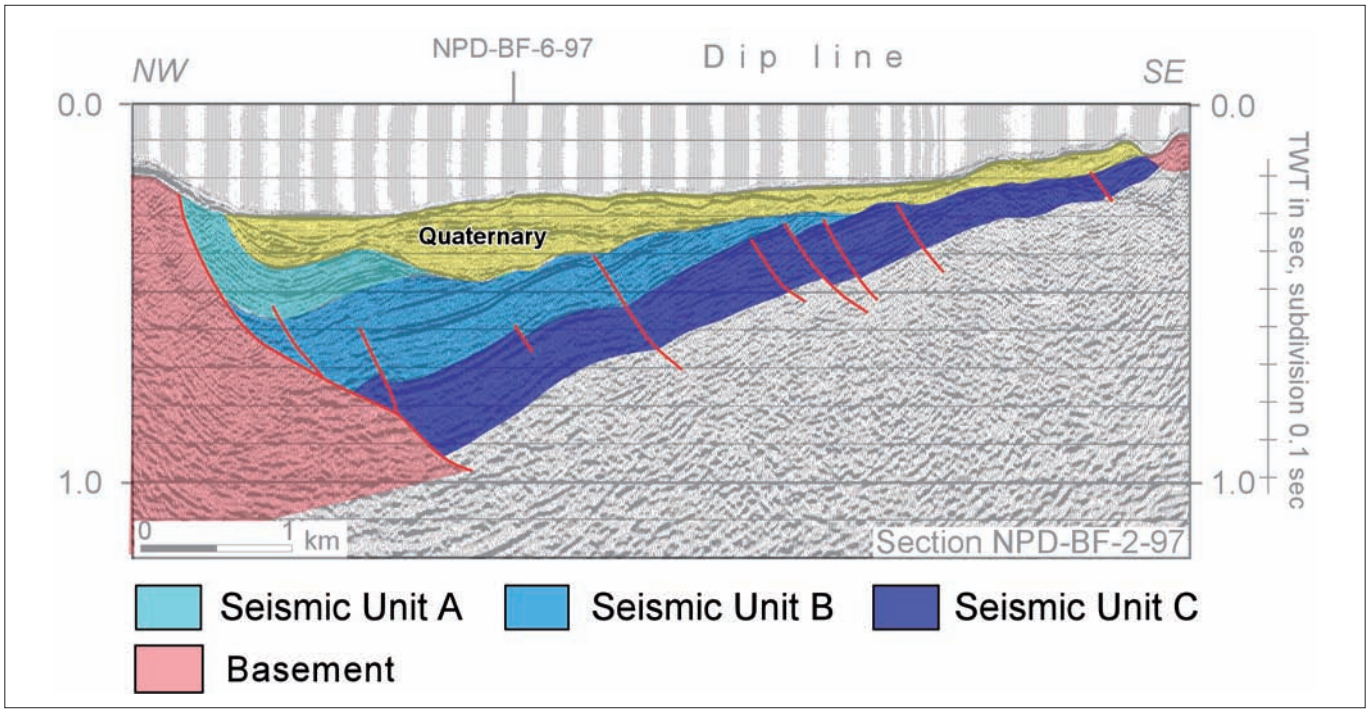

Figure 7. Seismic line, Beitstadfjord Basin. Modified from Sommaruga and Bøe (2002).

sub-parallel to the main fault of the Verran Fault system. Another set of faults, oriented NNE–SSW, crosscuts the ENE–WSW system and is therefore considered to be younger (Bøe and Bjerkli 1989). Strata dip up to 15° to the NNW, i.e., towards the deepest parts of the basin, but changes of dip occur along faults and along the strike of the basin. The thickness of the Jurassic succession (see discussion on age below) is around 1000 m.

Edøyfjorden Basin

The Edøyfjorden Basin (Figure 6) is an elongated half-graben (18 km long and 3 km wide) that is downthrown in the south-southeast by the ENE–WSW-trending Hitra-Snåsa Fault (Bøe and Bjerkli 1989). A few hundred metres farther south, another fault probably represents the southwestern prolongation of the main Verran Fault. Mesozoic strata generally dip 15–25° towards the south-southeast, but swing into an E–W strike in the northeastern wedge of the basin. The vertical slip along the Hitra-Snåsa Fault is of the order of several hundred metres to 1 km, and the thickness of the Mesozoic succession is ca. 1000 m.

Frohavet Basin and Frøyfjorden

The Frohavet Basin (almost 60 km long and up to 20 km wide) (Figure 6) is controlled by two large normal faults that downthrow to the northwest (Bøe 1991). A narrow basement ridge separates the main basin from a smaller, elongated basin close to the Froan Islands in the northwest. The Tarva Fault (oriented NE–SW and turning to a NNE–SSW-trend in the southwest) and the Dolmsundet Fault (oriented NE–SW) occur along the southeastern margin of the basin. Many small synthetic and antithetic faults occur along the major faults. A third fault trend, NW–SE, is represented by only a few structures, but these seem to offset the NE–SW faults and are, therefore, thought to be younger. Gentle synclines within the basin are mainly oriented NE-SW, subparallel to the Tarva and Dolmsundet Faults. Seismic units thicken slightly towards the Tarva Fault, indicating syn-depositional movements. The maximum thickness of Jurassic rocks, in the central part of the basin, is ca. 1200 m.

The 5.3 km-long Frøya Tunnel beneath Frøyfjorden passes through a major zone of faulting and brecciation which parallels the MTFC (Bøe et al. 2005). Faults and fractures are concentrated in deformation zones that developed during Devonian to Tertiary crustal movements (Bøe et al. 2005). Drillcores from these zones include segments comprising possible Upper Palaeozoic and Mesozoic sediments (Figure 8). These were probably deposited on a fractured peneplain, and subsequently incorporated into faults during their reactivation in Mid Jurassic and later times. Extensive weathering of the fault rocks mainly post-dates brittle deformation and brecciation. Part of the weathering may have occurred in Late Triassic-Early Jurassic time, prior to the Middle Jurassic transgression and deposition of the sedimentary succession in Frohavet (Bøe et al. 2005). Also Olesen et al. (2007), from aeromagnetic data, has suggested the presence of Mesozoic deep-weathered fracture zones in south Norway.

Griptarane area

Griptarane (Figure 6) is a basement topographic high located northwest of Kristiansund, between the Frøya High and the is-

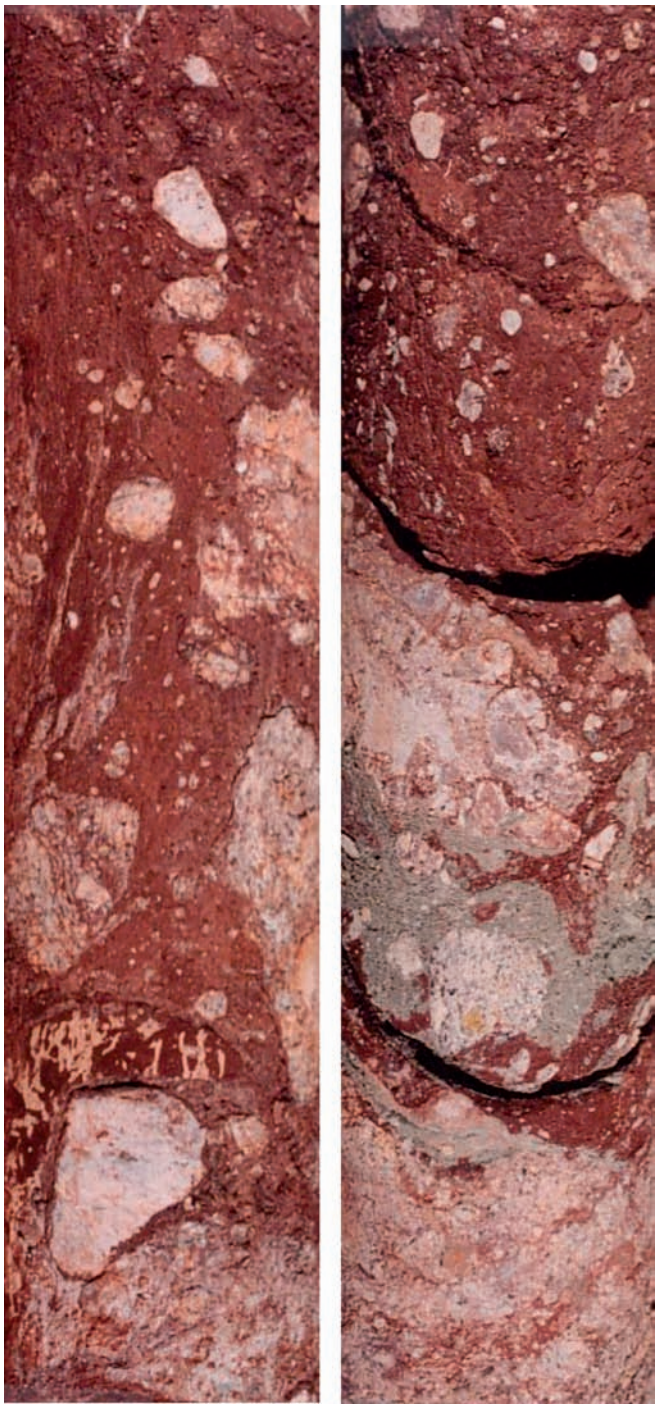

Figure 8. Matrix-rich, sediment- and gneiss-bearing fault breccias in cores from the Frøyfjorden fault zone. Core width is 7 cm. From Bøe et al. (2005).

land of Smøla (Bøe and Skilbrei 1998). Griptarane is surrounded by Jurassic strata, which are covered by thicker Cretaceous units to the west. Jurassic rocks are preserved in a synclinal flexure, oriented NE–SW to the southeast of the Griptarane high, and NW–SE to the northeast and southwest of Griptarane. Dips are rather shallow, 3–10°. Several large, WNW–ESE-trending normal faults with downthrows towards the northeast occur. The WNW–ESE structural trend is subparallel to the orientation of fjords and lineaments along the coast of Møre and Trøndelag, and also to fault trends within the Devonian basins. Two of these faults offset the Jurassic-basement boundary. There are also several large, NE–SW-trending faults. Most of these dip towards the northwest, and the one at the northwest margin of Griptarane continues as a major fault towards the Slørebotn Sub-Basin/Møre Basin Margin. The thickness of the Jurassic succession is ca. 600 m south of Griptarane.

Seismic units, depositional environment and stratigraphic correlation

On seismic sections from the Beitstadfjorden and Frohavet Basins, seismic units A (upper), B (middle) and C (lower) have been identified (Sommaruga and Bøe 2002) (Figure 7). The Edøyfjorden seismic sections show a single seismic unit, which can possibly be attributed to Units B–C in Frohavet and Beitstadfjorden. The Griptarane area presents two seismic units; the upper unit may possibly be attributed to Unit A and the second to Units B–C. In terms of facies, Unit C was interpreted to comprise predominantly continental sandstones and conglomerates, Unit B shales or mudstones, while Unit A represents alternating sandstone, shale and carbonate (Sommaruga and Bøe 2002). The succession from Unit C to Unit A may reflect a general upward change from continental to shallow-marine deposition. The most reliable information on the age of the three units is from nearby drillholes in the Slørebotn Sub-Basin, Møre Basin-Frøya High and Møre Basin Margin (Skarbø et al. 1988, Smelror et al. 1994, Jongepier et al. 1996) and fossiliferous erratic blocks left by glaciers on islands and skerries on the oceanward side of the basins (Kjerulf 1870, Nordhagen 1921, Carstens 1929, Horn 1931, Manum 1964, Vigran 1970, Bugge et al. 1984, Johansen et al. 1988). Erratic blocks from Beitstadfjorden and Frohavet constrain the uppermost Unit A to Callovian age (Melke Formation equivalent). The underlying Units B and C are thought to be equivalent to the offshore Fangst Group. In the Edøyfjorden Basin, a 1 m-long core comprises coarse-grained sediments possibly of Early-Middle Jurassic age, but this age assignment is uncertain.

Erratics of Cretaceous rocks have not been found along the shores of the studied basins. This may either reflect a lack of Cretaceous rocks available for erosion, or be due to destruction of Cretaceous rock fragments (possibly shale) by the eroding glaciers. Permo-Triassic rocks may occur below some of the Jurassic successions, and probably also in small, isolated basins northeast of the Frohavet Basin (Thorsnes 1995).

Blocks from Beitstadfjorden include iron-rich sand- and siltstones rich in plant fragments, interpreted to have been deposited in river channels and on flood plains (Oftedahl 1972). It is also noteworthy that reworked Middle Jurassic to Early Cretaceous dinoflagellate cysts have been found in Holocene sediments in Verdalsbukta and outside the Tautra ridge in the Trondheimsfjord (Scholze 1986), suggesting that not only Middle Jurassic, but also younger Mesozoic marine sediments were deposited farther eastwards. Blocks from Frohavet are dominated by well-sorted sandstones with marine fossils, interpreted

to represent shallow-marine deposits. It is assumed that in the Middle Jurassic there was a NW–SE transition from a continental to a shallow-marine environment in Mid Norway (Bøe 1991, Sommaruga and Bøe 2002). In the Late Jurassic much of the present coastal area was covered by a shallow sea. Further offshore, depths were more than 2000 m (e.g., Jongepier et al. 1996, Færseth and Lien 2002).

Organic matter maturation in erratic blocks from Beitstadfjorden suggests a burial depth of 1.8–2.3 km (Weisz 1992). During the Late Tertiary to Pleistocene, as much as 1000 m of Jurassic and younger sediments may have been eroded and only the Middle Jurassic and possibly older Mesozoic sediments have been preserved in the deepest half-grabens.

Western and Southern Norway

Permo-Triassic and Mid-Late Jurassic faulting in the North Sea occurred along approximately N–S-trending and at a later stage along NE–SW-trending faults (Færseth et al. 1997). Many onshore lineaments in West Norway have similar, coast-parallel trends. Some of these are fracture zones, while others have developed into faults with significant offsets.

The N–S to NNW–SSE-trending faults and fracture zones transect NE–SW-trending extensional faults that are related to Devonian extension of the thickened Caledonian crust (Fossen 2000). However, some of the NE–SW-trending faults also appear to have been reactivated in the Mesozoic, for instance the Lærdal-Gjende Fault (Andersen et al. 1999) and faults in the Sunnfjord region (Eide et al. 1997). In the coastal area, some of the fractures have been intruded by basaltic magma. Dykes (Figure 9) are up to two metres thick (Færseth et al. 1976) and gently altered by hydrothermal activity. K–Ar dating of some of the dykes gives two groups of ages; Permian and Triassic, in addition to a single Jurassic age (Færseth et al. 1976). More precise Ar–Ar dating of amphiboles in some of the dykes has given consistent Triassic ages of around 220 Ma, also for the dyke yielding a Jurassic K–Ar age (Fossen and Dunlap 1999). These ages agree with the general assumption that the first rifting phase in the adjacent North Sea basin initiated in the Permian and lasted into the Triassic. Furthermore, kinematic analysis indicates E–W to ENE–WSW extension during dyke intrusion (Fossen 1998, Valle et al. 2002), which is consistent with the North Sea Permo-Triassic rifting. The coast-parallel dykes transect older, mostly NE–SW-trending faults. The latter are typically affected by epidote mineralisation and conform to NW–SE Devonian extension in West Norway.

Figure 9. Triassic dyke crosscutting gneiss. Tofterøy, West Norway.

Along the coast, west-dipping Jurassic and Cretaceous strata overlay a peneplaned basement surface. These sediments extended eastward onto the Norwegian mainland, but were eroded during the Tertiary and Quaternary.

Bjorøy tunnel

In 1994, Jurassic sediments were encountered in a fault zone during construction of the subsea Bjorøy tunnel between Bjorøy (Figure 1) and the mainland southwest of Bergen (Fossen et al. 1997). The sediments, named the Bjorøy Formation, are strongly affected by fault movements, as seen by the broken and dismembered occurrence of the layers and their steep dips. Although the primary stratigraphic relations have been obscured by the fault movements, cores cut during the tunnelling operations show a gradual transition from granitic basement gneiss to feldspathic and polymict conglomerate, grit and sandstone. The mostly angular clasts in these sediments stem from the basement gneisses, and the sedimentary facies is thought to represent gravel and sand deposited on weathered basement rocks. Furthermore, quartz-rich sandstone (Figure 10) and sand with small fragments of coal and occasional gneiss pebbles occur in depositional contact with conglomerate. Remnants of one or more coal layers, around 10 cm thick, are also found.

The age of the sedimentary rocks has been constrained by analyses of pollen and spores from coal fragments in both the sandstone and the unconsolidated sand, and the results consistently indicate an early to middle Oxfordian age. This makes the sediments time equivalent to the North Sea Fensfjord and Sognefjord Formations, which form reservoir sandstones in the Troll field some 80 km NW of the Bjorøy locality. Thus, the sediments were deposited during the Late Jurassic-Cretaceous

Figure 10. Three core samples of the Mesozoic Bjorøy Formation. Left: Breccia, interpreted as sedimentary, with sand vein (top). Middle: transition from grit to quartz-rich sandstone with a few small coal fragments. Right: sandstone with gneiss fragments. These and other samples from the Bjorøy tunnel in West Norway are part of the Natural History Collections at Bergen Museum, University of Bergen.

transgression, which culminated with the Cretaceous flooding of much of the Norwegian mainland (Riis 1996). Today, the sedimentary rocks of the Bjorøy Formation occur in a ~10 m thick zone within the Proterozoic basement, some 70 m below sea level in an area without any trace of post-Palaeozoic sedimentary rocks. It is a challenge to understand the exact mechanisms that brought these sediments to their present position, but the fault zone they occur in must have opened and trapped the lower part of the Mesozoic deposits that were deposited on the Proterozoic basement. As the fault moved, probably at the end of the Late Jurassic rifting phase but possibly also later, the sediments were deformed and dismembered. Selective cementation of the sandstone by means of quartz dissolution, a feature generally restricted to the deeper (>3 km) North Sea reservoirs, may be related to local hydrothermal heating along the Bjorøy fault zone.

Karmsundet basin

The Karmsundet basin (Figure1) has an areal extent of ca. 28 x 5 km, and contains a sedimentary succession with a thickness of up to 600 m (Bøe et al. 1992). The rocks are preserved in a half-graben with reflectors dipping 5–25º ESE (Figure 11). The Kvitsøy fault separates the sedimentary rocks of the half-graben from Precambrian and Cambro-Silurian metamorphic rocks to the east. The western boundary of the basin is an unconformity. The age of the rocks in the Karmsundet basin has not been determined, but a Jurassic age is probable as Jurassic rocks subcrop close to the coast west of Karmøy (Rokoengen and Sørensen 1990). In the southernmost part of the Karmsundet basin, a possible unconformity separates rocks of probable Jurassic age from rocks of assumed Late Palaeozoic age (Bøe et al. 1992).

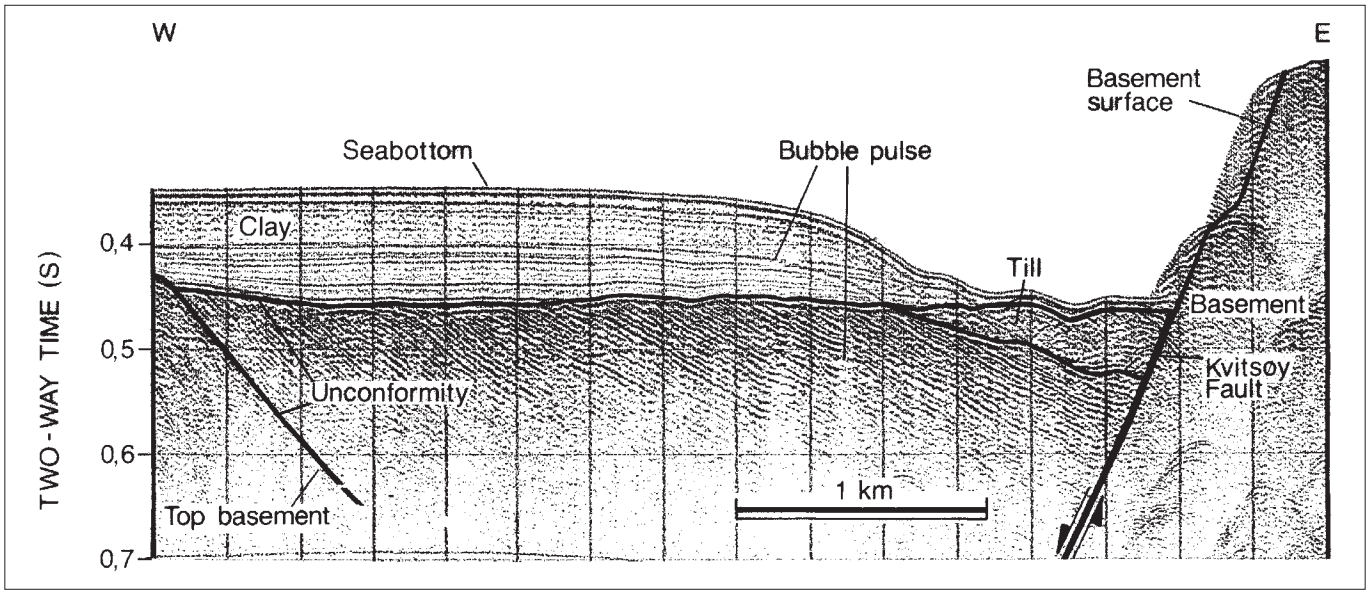

Figure 11. Seismic profile across the Karmsundet Basin. From Bøe et al. (1992).

Utsira

Upper Jurassic sedimentary rocks have been drilled north of Utsira (Figure 1) (Rokoengen et al. 1989, Rokoengen and Sørensen 1990). The succession is in lateral continuity with similar deposits on the shelf farther west. It is not preserved due to downfaulting, but rather on account of its position north of Utsira island that protected it from glacial erosion by the northward-moving Norwegian Channel Ice Stream in the Quaternary Period.

Lista basin

Sedimentary rocks of assumed Mesozoic age occur in the Lista basin (Holtedahl 1988) (Figure 1). The boundary between layered strata and older rocks, to the northeast, is marked by a major, NW–SE-trending normal fault outside the island of Hidra. Dredge samples and cores of Quaternary sediments contain flint, chalk, coal, sandstone, siltstone and limestone fragments with pollen and spores of Early Jurassic age. A Late Triassic-Early Jurassic age for the succession was suggested by Holtedahl (1988). He proposed that the sediments originally covered the Precambrian areas to the north of the Lista basin, and that the present surface is the result of exhumation of a sub-Triassic/Jurassic weathered surface. It has later been proposed that Mesozoic sediments occur beneath Quaternary sediments in the lowland areas of Lista (e.g., Bøe et al. 2000), but this has so far not been confirmed.

Summary

Smelror et al. (2001) published a detailed lithostratigraphic and sequence stratigraphic correlation of the Mesozoic succession on Andøya with age equivalent successions off Nordland and Troms (Figure 4). Such detailed correlations remain to be published for other nearshore/inshore Mesozoic basins. Although most of the coastal area has now been investigated in search for Mesozoic basins, at least at a reconnaissance scale, none of the basins, except for the one at Andøya, have been drilled and properly documented. This is a future major task that would lead to a much more thorough understanding of the Mesozoic and Cenozoic geological development of the Norwegian coastal zone.

Acknowledgements

Lisa Løseth is thanked for help in drawing Figure 1, Børre Davidsen for compiling Figure 2 and Irene Lundquist for drawing Figure 3. David Roberts, Roald B. Færseth, Mai Britt E. Mørk and Stephen Lippard are thanked for constructive comments on the manuscript.

References

Aarhus, N., Verdenius, J. and Birkelund, T. (1986) Biostratigraphy of a Lower Cretaceous section from Sklinnabanken, with some comments on the Andøya exposure. *Norsk geologisk Tidsskrift,* **66**, 17–43.

Aarhus, N., Bugge, T., Elvebakk, G., Fjerdingstad, V., Leith, T.L., Mørk, A., Rendall, H., Skarbø, O. and Weiss, H.M. (1987) Shallow Drilling Elf Aquitaine/Norsk Hydro/Statoil Barents Sea 1987. Main Data Report. *Continental Shelf and Petroleum Technology Research Institute (IKU) Report 21.3435.00/02/87*, 199 pp.

Andersen, T.B., Torsvik, T.H., Eide, E.A., Osmundsen, P.T. and Faleide, J.I. (1999) Permian and Mesozoic extensional faulting within the Caledonides of central Norway. *Journal of the Geological Society of London*, **156**, 1073–1080.

Birkelund, T., Thusu, B. and Vigran, J. (1978) JurassicCretaceous biostratigraphy of Norway, with comments on the British *Rasenia cymodoce* Zone. *Palaeontology*, **21**, 31–63.

Blystad, P., Brekke, H., Færseth, R.B., Larsen, B.T., Skogseid, J. and Tørudbakken, B. (1995) Structural elements of the *Norwegian continental shelf. Part II: the Norwegian Sea Region. Norwegian Petroleum Directorate Bulletin*, **8**, 1–45.

Brekke, H. (2000) The tectonic evolution of the Norwegian Sea continental margin with emphasis on the Vøring and Møre Basins. *In* Nøttvedt, A. (ed.) *Dynamics of the Norwegian margin,* Geological Society of London Special Publication, **167**, pp. 327–378.

Brekke, H. and Olaussen, S. (2006) Høyt hav og lave horisonter. In Ramberg, I.B., Bryhni, I. and Nøttvedt, A. (eds.) *Landet blir til—Norges geologi*, Norsk Geologisk Forening, Trondheim, pp. 416–439.

Brekke, H., Sjulstad, H.I., Magnus, C. and Williams, R.W. (2001) Sedimentary environments offshore Norway—an overview. *In* Martinsen, O.J. and Dreyer, T. (eds.) *Sedimentary Environments Offshore Norway—Palaeozoic to Recent*, Norwegian Petroleum Society Special Publication, **10**, pp. 7–37.

Bugge, T., Knarud, R. and Mørk, A. (1984) Bedrock geology on the mid-Norwegian continental shelf. *In* Norwegian *Petroleum Society (ed.) Petroleum Geology of the North European Margin,* Graham and Trotman, London, pp. 271–283.

Bugge, T., Elvebakk, G., Bakke, S., Fanavoll, S., Lippard, S.J., Leith, L., Mangerud, G., Möller, N., Nilsson, I., Rømuld, A., Schou, L., Vigran, J.O., Weiss, H.M. and Aarhus, N. (1989) Shallow drilling Barents Sea 1988. Main report. *Continental Shelf and Petroleum Technology Research Institute (IKU) Report 21.3444.00/03/89*, 348 pp.

Bugge, T., Leith, D.A., Mangerud, G., Ringås, J.E., Weiss, H.M., Leith, L., Ritter, U. and Vigran, J.O. (1993) Shallow drilling Helgeland 1992. Main report. *Continental Shelf and Petroleum Technology Research Institute (IKU) Report 23.1684.00/02/93*, 263 pp.

Bugge, T., Tveiten, B. and Bäckstrøm, S. (2001) The depositional history of the Cretaceous in the northeastern North Sea. In Martinsen, O.J. and Dreyer, T. (eds.) *Sedimentary Environments Offshore Norway—Palaeozoic to Recent*, Norwegian Petroleum Society Special Publication, **10**, pp. 279–291.

Bugge, T., Ringås, J.E., Leith, D.A., Mangerud, G., Weiss, H.M. and Leith, T.L. (2002) Upper Permian as a new play model on the Mid-Norwegian continental shelf; investigated by shallow stratigraphic drilling. *American Association of Petroleum Geologists Bulletin*, **2002**, 107–127.

Bøe, R. (1991) Structure and seismic stratigraphy of the innermost mid-Norwegian continental shelf: an example from the Frohavet area. *Marine and Petroleum Geology*, **8**, 140–151.

Bøe, R. and Bjerkli, K. (1989) Mesozoic sedimentary rocks in Edøyfjorden and Beitstadfjorden, Central Norway: Implications for the structural history of the Møre-Trøndelag fault zone. *Marine Geology*, **87**, 287–299.

Bøe, R. and Skilbrei, J.R. (1998) Structure and seismic stratigraphy of the Griptarane area, Møre Basin margin, mid-Norway continental shelf. *Marine Geology*, **147**, 85–107.

Bøe, R., Sørensen, S. and Hovland, M. (1992) The Karmsundet Basin, SW Norway: stratigraphy, structure and neotectonic activity. *Norsk Geologisk Tidsskrift*, **72**, 281–283.

Bøe, R., Rise, L. and Brekke, H. (2000) Berggrunnsgeologisk kart over den norske delen av Skagerrak og Nordsjøen mellom Kristiansand og Karmøy. *Norges geologiske undersøkelse Rapport 2000.010*, 10 pp.

Bøe, R., Mørk, M.B.E., Roberts, D. and Vigran, J.O. (2005) Possible Mesozoic sediments in fault and brecciation zones in Frøyfjorden, Mid Norway. *Norges geologiske undersøkelse Bulletin,* **443**, 29–35.

Bøe, R., Smelror, M., Davidsen, B. and Walderhaug, O. (2008) Nearshore Mesozoic basins off Nordland, Norway: Structure, age and sedimentary environment. *Marine and Petroleum Geology*, **25**, 235–253.

Carstens, C.W. (1929) Brunkullfund på Tun, Verran. *Det Kongelige Norske Videnskabers Selskabs Skrifter*, **2**, 32–33.

Dalland, A. (1981) Mesozoic sedimentary succession at Andøy, northern Norway and relation to structural development of the North Atlantic Area. *Canadian Society of Petroleum Geologists Memoir*, **7**, 563–584.

Dalland, A., Worsley, D. and Ofstad, K. (1988) A lithostratigraphic scheme for the Mesozoic and Cenozoic succession offshore mid- and northern Norway. *Norwegian Petroleum Directorate Bulletin*, **4**, 65 pp.

Dallmann, W.K. (ed.) (1999) *Lithostratigraphic Lexicon of Svalbard*, Norsk Polarinstitutt, Tromsø, 318 pp.

Davidsen, B., Smelror, M. and Ottesen, D. (2001a) Et nyoppdaget mesozoisk basseng i Sortlandsundet, Vesterålen. *Geonytt 2001, Geological Society of Norway Annual Meeting, Oslo, 8.–10. January 2001*, pp. 42–43.

Davidsen, B., Sommaruga, A. and Bøe, R. (2001b) Final report: sedimentation, tectonics and uplift in Vesterålen. Phase I—localizing near-shore faults and Mesozoic sediment basins. *NGU Report 2001.011*, 16 pp.

Eide, E.A., Torsvik, T.H. and Andersen, T.B. (1997) Absolute dating of brittle fault movements: late Permian and late Jurassic extensional fault breccias in western Norway. *Terra Nova,* **9**, 135–139.

Evans, D., Graham, C., Armour, A. and Bathurst, P. (2003) T*he millennium atlas: petroleum geology of the Central and Northern North Sea*, Geological Society of London, 990 pp.

Fjerdingstad, V., Mørk, A., Vigran, J.O., Bugge, T., Fanavoll, S. and Leith, L. (1985) Shallow drilling Barents Sea 1984. *Continental Shelf and Petroleum Technology Research Institute (IKU) Report 01.0217.00/01/85*, 142 pp.

Fossen, H. (1998) Advances in understanding the post-Caledonian structural evolution of the Bergen area, West Norway. *Norsk Geologisk Tidsskrift*, **78**, 33–46.

Fossen, H. (2000) Extensional tectonics in the Caledonides: synorogenic or postorogenic? *Tectonics*, **19**, 213–224.

Fossen, H. and Dunlap, W.J. (1999) On the age and tectonic significance of Permo-Triassic dikes in the Bergen-Sunnhordland region, southwestern Norway. *Norsk Geologisk Tidsskrift*, **79**, 169–178.

Fossen, H., Mangerud, G., Hesthammer, J., Bugge, T. and Gabrielsen, R.H. (1997) The Bjorøy Formation: a newly discovered occurrence of Jurassic sediments in the Bergen Arc System. *Norsk Geologisk Tidsskrift*, **77**, 269–287.

Fürsich, F.T. and Thomsen, E. (2005) Jurassic biota and biofacies in erratics from the Sortland area, Vesterålen, northern Norway. *Norges geologiske undersøkelse Bulletin*, **443**, 37–53.

Færseth, R.B. (1996) Interaction of Permo-Triassic and Jurassic extensional fault-blocks during the development of the northern North Sea. *Journal of the Geological Society of London*, **153**, 931–944.

Færseth, R.B. and Lien, T. (2002) Cretaceous evolution in the Norwegian Sea—a period of tectonic quiescence. *Marine and Petroleum Geology*, **19**, 1005–1027.

Færseth, R.B., Macintyre, R.M. and Naterstad, J. (1976) Mesozoic alkaline dykes in the Sunnhordland region, western Norway: ages, geochemistry and regional significance. *Lithos,* **9**, 331–345.

Færseth, R.B., Gabrielsen, R.H. and Hurich, C.A. (1995) The influence of basement in structuring of the North Sea Basin, offshore Southwest Norway. *Norsk Geologisk Tidsskrift*, **75**, 105–119.

Færseth, R.B., Knudsen, B.E., Liljedahl, T., Midbø, P.S. and Søderstrøm, B. (1997) Oblique rifting and sequential faulting in the Jurassic development of the northern North Sea. *Journal of Structural Geology,* **19**, 1285–1302.

Gabrielsen, R.H, Færseth, R.B., Jensen, L.N., Kalheim, J.E. and Riis, F. (1990) Structural elements of the Norwegian continental shelf. Part I: The Barents Sea Region. *Norwegian Petroleum Directorate Bulletin*, **6**, 1–33.

Gabrielsen, R.H., Odinsen, T. and Grunnaleite, I. (1999) Structuring of the northern Viking Graben and the Møre Basin; the influence of basement structural grain, and the particular role of the Møre-Trøndelag Fault Complex. *Marine and Petroleum Geology*, **16**, 443–465.

Grønlie, A. and Roberts, D. (1989) Resurgent strike-slip duplex development along the Hitra-Snåsa and Verran Faults, Møre-Trøndelag Fault Zone, Central Norway. *Journal of Structural Geology*, **11**, 295–305.

Grønlie, A., Naeser, C.W., Naeser, N.D., Mitchell, J.G., Sturt, B.A. and Ineson, P.R. (1994) Fission track and K-Ar dating of tectonic activity in a transect across the Møre-Trøndelag Fault Zone, central Norway. *Norsk Geologisk Tidsskrift*, **74,** 24–34.

Hansen, J.W., Bakke, S., Løseth, H., Mørk, A., Mørk, M.B.E., Rise, L., Smelror, M., Verdenius, J.G., Vigran, J.O. and Weiss, H.M. (1992) Shallow drilling Nordland VI and VII 1991. Main report. *Continental Shelf and Petroleum Technology Research Institute (IKU) Report 23.1594.00/02/92,* 390 pp.

Henningsen, T. (2006) Fiskeøgler besøker Andøya. *In* Ramberg, I.B., Bryhni, I. and Nøttvedt, A. (eds.) *Landet blir til—Norges geologi*, Norsk Geologisk Forening, Trondheim, p. 375.

Holtedahl, H. (1988) Bedrock geology and Quaternary sediments in the Lista basin, S. Norway. *Norsk Geologisk Tidsskrift*, **68**, 1–20.

Holtedahl, H. (1993) *Marine geology of the Norwegian continental margin*, Norges geologiske undersøkelse Special Publication, **6**, 150 pp.

Horn, G. (1931) Über kohlen-gerölle in Norwegen. *Norsk Geologisk Tidsskrift*, **12**, 341–361.

Husmo, T., Hamar, G.P., Høiland, O., Johannesen, E.P., Rømuld, A., Spencer, A.M. and Tritterton, R. (2002) Lower and middle Jurassic. *In* Evans, D., Armour, A. and Bathurst, P. (eds.) *The Millennium Atlas: petroleum geology of the central and northern North Sea*, Geological Society of London, pp. 129–155.

Johansen, M., Poulsen, H., Skjæran, H., Straume, T. and Thorsplass, J.O. (1988) Froanbassengets Dannelse og Jurassiske Sedimenter. *Report, Norwegian Institute of Technology (NTH)*, 103 pp.

Jongepier, K., Rui, J.C. and Grue, K. (1996) Triassic to Early Cretaceous stratigraphic and structural development of the northeastern Møre Basin, off Mid-Norway. *Norsk Geologisk Tidsskrift*, **76**, 199–214.

Karputz, M.R., Roberts, D., Olesen O., Gabrielsen, R.H. and Herrevold, T. (1993) Application of multiple data sets to structural studies on Varanger Peninsula, Northern Norway. *International Journal of Remote Sensing*, **14**, 979–1003.

Kjerulf, T. (1870) Undersøgelse av Nogle Kulslags og Torv. *Videnskabselskabet i Christiania Forhandlingar*, pp. 404–413.

Lien T. (2005) From rifting to drifting: effects on the development of deep-water hydrocarbon reservoirs in a passive margin setting, Norwegian Sea. *Norwegian Journal of Geology*, **85**, 319–332.

Lippard, S. and Roberts, D. (1987) Fault systems in Caledonian Finnmark and the southern Barents Sea. *Norges geologiske undersøkelse Bulletin*, **410**, 55–64.

Løseth, H. and Tveten, E. (1996) Post-Caledonian structural evolution of the Lofoten and Vesterålen offshore and onshore areas. *Norsk Geologisk Tidsskrift*, **76**, 215–230.

Manum, S.B. (1964) Nytt om Verran-kullene. *Fossil-Nytt*, **3**, 1–2.

Manum, S.B., Bose, M.N. and Vigran, J.O. (1991) The Jurassic flora of Andøya, northern Norway. *Review of Palaeobotany and Palynology*, **68**, 233–256.

Martinsen, O. and Dreyer, T. (eds.) (2001) *Sedimentary environments offshore Norway—Palaeozoic to Recent*,Norwegian Petroleum Society Special Publication, **10**, 490 pp.

Martinius, A.W., Kaas, I., Næss, A., Helgesen, G., Kjærefjord, J.M. and Leith, D.A. (2001) Sedimentology of the heterolithic and tide-dominated Tilje formation (Early Jurassic, Halten Terrace, offshore mid-Norway). *In* Martinsen, O.J. and Dreyer, T. (eds.) *Sedimentary environments offshore Norway—Palaeozoic to Recent*,Norwegian Petroleum Society Special Publication, **10**, pp. 103–144.

Müller, R., Nystuen, J.P., Eide, F. and Lie, H. (2005) Late Permian to Triassic basin infill history and palaeogeography of the Mid-Norwegian shelf—East Greenland region. *In* Wandås, B.T.G., Nystuen, J.P., Eide, E. and Gradstein, F.M. (eds.) *Onshore-offshore relationships on the North Atlantic Margin.*, Norwegian Petroleum Society Special Publication, **12**, pp. 155–189.

Mørk, A., Aarhus, N., Bugge, T. and Mills, N. (1983) Shallow drilling of Mesozoic rocks off Helgeland 1982. *Continental Shelf and Petroleum Technology Research Institute (IKU) Report P–248/1/83*, 332 pp.

Mørk, M.B.E., Vigran, J.O., Smelror, M., Fjredingstad, V. and Bøe, R. (2003) Mesozoic mudstone compositions and the role of kaolinite weathering—a view from shallow cores in the Norwegian Sea (Møre to Troms). *Norwegian Journal of Geology*, **83**, 61–78.

Nordhagen, R. (1921) Fossilførende blokker fra Juratiden på Froøyene utenfor Trondheimsfjorden. *Naturen*, **45**, 110–115.

Nystuen, J.P., Müller, R., Mørk, A. and Nøttvedt, A. (2006) Fra ørken til elveslette—fra land til hav. *In* Ramberg, I.B., Bryhni, I. and Nøttvedt, A. (eds.) *Landet blir til—Norges geologi*, Norsk Geologisk Forening, Trondheim, pp. 328–353.

Nøttvedt, A., Cecchi, M., Gjelberg, J.G., Kristensen, S.E., Lønøy, A., Rasmussen, A., Rasmussen, E., Skott, P.H. and van Veen, P.M. (1993) Svalbard-Barents Sea correlation: a short review. *In* Vorren, T.O., Bergsager, E., Dahl-Stamnes, Ø.A., Holter, E., Johansen, B., Lie, E. and Lund, T.B. (eds.) *Arctic Geology and Petroleum Potential.*, Norwegian Petroleum Society Special Publication, **2**, pp. 363–375.

Odinsen, T., Reemst, P., Beek, P.V.D., Faleide, J.I. and Gabrielsen, R.H. (2000) Permo-Triassic and Jurassic extension in the northern North Sea: results from tectonostratigraphic forward modelling. *In* Nøttvedt, A. (ed.) *Dynamics of the Norwegian margin*, Geological Society of London Special Publication, **167**, pp. 83–103.

Oftedahl, C. (1972) A sideritic ironstone of Jurassic age in Beitstadfjorden, Trøndelag. *Norsk Geologisk Tidsskrift*, **52**, 123–134.

Oftedahl, C. (1975) Middle Jurassic graben tectonics in Mid-Norway. *In* Norwegian Petroleum Society (ed.) *Jurassic Northern North Sea*, pp. 1–13.

Olesen, O., Dehls, J.F., Ebbing, J., Henriksen, H., Kihle, O. and Lundin, E. (2007) Aeromagnetic mapping of deep-weathered fracture zones in the Oslo Region—a new tool for improved planning of tunnels. *Norwegian Journal of Geology*, **87**, 253–267.

Osmundsen, P.T., Sommaruga, S., Skilbrei, J.S. and Olesen, O. (2002) Deep structure of the Mid Norway rifted margin. *Norwegian Journal of Geology*, **82**, 205–224.

Osmundsen, P.T., Eide, E.A., Haabesland, N.E., Roberts, D., Andersen, T.B., Kendrick, M., Bingen, B., Braathen, A. and Redfield, T.F. (2006) Kinematics of the Høybakken detachment zone and the Møre-Trøndelag Fault Complex, central Norway. *Journal of the Geological Society of London*, **163**, 303–318.

Ramberg, I.B., Bryhni, I. and Nøttvedt, A. (eds.) (2006) *Landet blir til—Norges geologi*, Norsk Geologisk Forening, Trondheim, 608 pp.

Riis, F. (1996) Quantification of Cenozoic vertical movements of Scandinavia by correlation of morphological surfaces with offshore data. *Global Change*, **12**, 331–357.

Roberts, D. and Lippard, S. (2005) Inferred Mesozoic faulting in Finnmark: current status and offshore links. *Norges geologiske undersøkelse Bulletin*, **443**, 55–60.

Rokoengen, K. and Sørensen, S. (1990) Late Jurassic sedimentary bedrock north of Utsira, offshore western Norway. *Norsk Geologisk Tidsskrift*, **70**, 61–63.

Rokoengen, K., Bakke, S., Elvebakk, G., Rise, L., Weiss, H. and Aarhus, N. (1989) Shallow drilling Stord Basin: Main report. *Continental Shelf and Petroleum Technology Research Institute (IKU) report 21.3459.00/04/89*, 89 pp.

Skarbø, O., Bakke, S., Jacobsen, T., Krokstad, W., Lundschien, B., Myhr, M.B., Rise, L., Schou, L., Smelror, M., Verdenius, J., Vigran, J.O. and Århus, N. (1988) Shallow drilling off Møre-Trøndelag 1988. Main report. *Continental Shelf and Petroleum Technology Research Institute (IKU) Report 21.3434/00/03/88*, 289 pp.

Scholze, A. (1986) *En palynologisk og maringeologisk undersøkelse av Holocene sedimenter fra Trondheimsfjorden*. Cand.scient-thesis, University of Oslo, 117 pp (in Norwegian).

Smelror, M., Jacobsen, T., Rokoengen, K., Bakke, S., Bøe, R., Goll, R.M., Lippard, S.J., Mørk, A., Rise, L., Vigran, J.O., Weiss, H.M. and Aarhus, N. (1989) Shallow drilling Farsund Subbasin 1989. Main report. *Continental Shelf and Petroleum Technology Research Institute (IKU) Report 21.3460.00/04/89*, 242 pp.

Smelror, M., Jacobsen, T., Rise, L., Skarbø, O., Verdenius, J.G. and Vigran, J.O. (1994) Jurassic to Cretaceous stratigraphy of shallow cores on the Møre Basin Margin, Mid-Norway. *Norsk Geologisk Tidsskrift*, **74**, 89–107.

Smelror, M., Mørk, A., Monteil, E., Rutledge, D. and Leereveld, H. (1998) The Klippfisk Formation—a new lithostratigraphic unit of Lower Cretaceous platform carbonates on the Western Barents Shelf. *Polar Research*, **17**, 181–202.

Smelror, M., Mørk, A., Mørk, M.B.E., Weiss, H.M. and Løseth, H. (2001) Middle Jurassic-Lower Cretaceous transgressive-regressive sequences and facies distribution off northern Nordland and Troms, Norway. *In* Martinsen, O.J. and Dreyer, T. (eds.) *Sedimentary environments offshore Norway—Palaeozoic to Recent*, Norwegian Petroleum Society Special Publication, **10**, pp. 211–232.

Smelror, M., Petrov, O.V., Larsen, G.B. and Werner, S. (eds.) (2009) *Atlas—Geological History of the Barents Sea*, Geological Survey of Norway, Trondheim, 135 pp.

Sommeruga, A. and Bøe, R. (2002) Geometry and subcrop maps of shallow Jurassic basins along the Mid-Norway coast. *Marine and Petroleum Geology*, **19**, 1029–1042.

Steel, R. and Ryseth, A. (1990) The Triassic-Early Jurassic succession in the northern North Sea: megasequence stratigraphy and intra-Triassic tectonics. *In* Hardman, R.P.F. and Brooks, J. (eds.) *Tectonic events responsible for Britain's Oil and Gas Reserves*., Geological Society of London Special Publication, **55**, pp. 139–168.

Sturt, B.A., Dalland, A. and Mitchell, J.L. (1979) The age of the sub Mid-Jurassic tropical weathering profile of Andøya, Northern Norway, and the implications for the Late Palaeozoic palaeogeography in the North Atlantic region. *Geologische Rundshau*, **68**, 523–542.

Sættem, J., Aarhus, N., Elvebakk, G., Leith, L. and Vigran, J.O. (1985) Shallow seismic and sampling off Troms 1984. *Continental Shelf and Petroleum Technology Research Institute (IKU) Report 04.1224.00/01/85*, 63 pp.

Thorsnes, T. (1995) Structural setting of two Mesozoic half-grabens of the coast of Trøndelag, Mid-Norwegian shelf. *Norges geologiske undersøkelse Bulletin*, **427**, 68–71.

Valle, P., Færseth, R.B. and Fossen, H. (2002) Devonian-Triassic brittle deformation based on dyke geometry and fault kinematics in the Sunnhordland region, SW Norway. *Norsk Geologisk Tidsskrift*, **82**, 3–17.

Vigran, J.O. (1970) Fragments of a Middle Jurassic flora from northern Trøndelag, Norway. *Norsk Geologisk Tidsskrift*, **50**, 193–214.

Wandås, B.T.G., Nystuen, J.P., Eide, E.A. and Gradstein, F. (eds.) (2005) *Onshore-offshore relationships on the North Atlantic Margin*., Norwegian Petroleum Society Special Publication, **12**, 305 pp.

Weisz, G. (1992) *An investigation of Jurassic coals from Haltenbanken and Beistadfjorden. A comparison of composition and maturity.* Diploma thesis, Norwegian Institute of Technology (NTH), Norway, 79 pp.

Zakharov, V.A., Surlyk, F. and Dalland, A. (1981) Upper Jurassic-Lower Cretaceous *Buchia* from Andøya, northern Norway. *Norsk Geologisk Tidsskrift*, **61**, 261–269.

Zwaan, B., Fareth, E. and Grogan, P.W. (1998) Trømsø, bedrock geological map, scale 1:250.000, Norges geologiske undersøkelse.

Ørvig, T. (1960) The Jurassic and Cretaceous on Andøya in northern Norway. *In* Holtedahl, O. (ed.) *Geology of Norway*, Norges geologiske undersøkelse, **208**, pp. 344–350.

RESEARCH ARTICLE

Regional similarities in the distributions of well yield from crystalline rocks in Fennoscandia

David Banks[1,6,*], Pål Gundersen[2], Gunnar Gustafson[3], Jorma Mäkelä[4], Geir Morland[5]

[1]*Holymoor Consultancy Ltd., 8 Heaton Street, Chesterfield, Derbyshire, S40 3AQ, United Kingdom.*
[2]*Norges Geologiske Undersøkelse, 7491 Trondheim, Norway.*
[3]*Department of GEO Engineering, Chalmers University of Technology, SE–41296, Göteborg, Sweden.*
[4]*Central Finland Centre for Economic Development, Transport and the Environment, P.O. Box 250, FI-40101 Jyväskylä, Finland.*
[5]*NorChip AS, Industriveien 8, 3490 Klokkarstua, Norway.*
[6]*HERO Group, School of Civil Engineering and Geoscience, Newcastle University, Newcastle-upon-Tyne, NE1 7RU, United Kingdom.*
[*]*david@holymoor.co.uk*

Well yields from Precambrian and Palaeozoic bedrock in Norway, Sweden and Finland exhibit very similar and approximately log-normal distributions: all three data sets exhibit a median yield of 600–700 L hr^{-1}, despite the differences in climate and lithology. This similarity is tentatively reflected on a larger geographical scale by a meta-analysis of the international data sets on crystalline rock aquifers from other recently glaciated areas (i.e., without a thick regolith of weathered rock). An heuristic treatment of the Fennoscandian data sets suggests that this median yield is consistent with the following bulk properties of shallow (to c. 70–80 m depth) crystalline bedrock: transmissivity of 0.56 ± 0.30 $m^2 d^{-1}$ (6.4 ± 3.4 x 10^{-6} $m^2 s^{-1}$) and hydraulic conductivity of around 1.1 (± 0.6) x 10^{-7} m s^{-1}.

Objective

The behaviour of fractured, crystalline rock aquifers is often regarded as being extremely complex, requiring a consideration of discontinuous flow systems, anisotropy and heterogeneity. Emphasis is often placed on the importance of local tectonic, topographic and weathering controls for the development of transmissivity. Without wishing to detract from the validity of these 'complex' approaches, this paper considers well yield data at regional and national scales, to demonstrate that large data sets from such aquifers exhibit considerable similarity in statistical distribution, despite apparent differences in lithology and climate. This paper discusses the implications of this finding and heuristically attempts to deduce what this may imply about the distributions of transmissivity in crystalline rock aquifers.

The authors specifically consider crystalline bedrock aquifers which are dominated by tectonically controlled fracture systems: i.e., crystalline bedrock in recently glaciated terrain, where geological time has not been sufficient to permit the development of a significant overlying weathered regolith or saprolite. Such a regolith is characteristic of crystalline bedrock in temperate/tropical climates (e.g., Africa and India and also parts of southern and central Europe) and its properties tend towards a conventional 'porous medium' aquifer. In regions where it overlies a true fractured crystalline bedrock aquifer, the presence of regolith may be expected to modify the behaviour and prop-

Banks, D., Gundersen, P., Gustafson, G., Mäkelä, J. and Morland, G. (2010) Regional similarities in the distributions of well yield from crystalline rocks in Fennoscandia. *Norges geologiske undersøkelse Bulletin*, **450**, 33–47.

erties of the bedrock aquifer system. Nevertheless, towards the conclusion of this paper, the findings from recently glaciated Fennoscandian and North American crystalline rock aquifers are tentatively compared to tropical crystalline rock terrains to ascertain whether any of the conclusions from the former may be transferable to the latter.

Introduction

It is widely accepted that wells in poorly weathered, fractured, crystalline bedrock aquifers have groundwater yields that are impossible to predict deterministically. Many researchers (Rohr-Torp 1994, Henriksen 1995, 2003, 2006, Sander 1997, 2007, Morland 1997, Henriksen and Braathen 2006) have attempted to correlate well yields in such terrains with factors such as lithology, topography, proximity to lineaments and postglacial isostatic rebound and have found some degree of tentative correlation. Often, however, the degree of correlation has been less than impressive—to cite a few of these articles:

"Results from correlation studies between mapped lineaments and well capacities have been ambiguous and demonstrate that lineaments alone cannot be used for water well siting." (Sander 1997).

"The results of this exploratory data analysis do not indicate any clear trends in well yield with regional gradients.... a simple correlation based on the relationships between two variables would not be sufficient to describe the observed regional variations in well yields." (Henriksen 2003).

"The testing of the two hypotheses" [i.e., regarding correlation between well yield and position relative to a lineament] *"does not give a clear and unequivocal answer in support of the two assumptions about groundwater flow in the study area."* (Henriksen and Braathen 2006).

"The hunt for major lineaments and lineament intersections as targets can be discouraging..." (Sander 2007).

It thus remains an important observation that, while one can subdivide a set of water wells on the basis of an attribute such as lithology or tectonic setting, the systematic differences in groundwater yield between subsets remain rather modest and the variation *within* each subset is enormous. Because of this, several authors have argued that it is more meaningful to make probabilistic assessments of well yield, on the basis of nonparametric statistics, rather than deterministic predictions (Gustafson 2002, Banks et al. 2005). Banks and Robins (2002) have likened well drilling in such terrain to a strategic game with a high element of chance, such as poker, rather than to a deterministic battle of wits, such as chess. Intriguingly, Braester and Barak (1991) explicitly considered drilling in fractured rock terrain as a two-player, zero-sum game (a mathematical term denoting a game where the gains of one player balance the losses of another), where the well-driller pits his luck against Mother Nature.

If one wishes to pursue correlations between well yields and geological, tectonic or lithological factors, it is beyond doubt that large, quality-controlled data sets and appropriate statistical techniques and tools are essential. However, it can be argued that the search for such correlations has overshadowed the significance of the far more interesting observation that the frequency distributions of water well yields in crystalline bedrock aquifers from nations such as Norway, Sweden and Finland are remarkably similar, irrespective of varying climate, tectonic setting, Quaternary history and lithology. Indeed, Krásný and Sharp (2007) go further and state that transmissivity distributions are rather similar in near-surface crystalline rock aquifers in many other parts of the world, including Korea, Poland, the Czech Republic and Ghana.

This paper will systematically compare, for the first time, the overall statistical distribution of well yields within the Fennoscandian nations (Norway, Sweden, and Finland) (Figure 1).

Figure 1. Map of Norway, Finland and Sweden. Showing Central Finland, Skåne (Scania) and the Tornqvist Zone (TZ).

The distribution of well yields in databases

Most nations attempt to collect details of the location, penetrated geology, construction and production data of water wells in databases, with varying degrees of success. A good well data-

base is, naturally, a prerequisite for any statistical analysis of well yields. Such a database should ideally be:

(1) Large: in order to provide a good degree of confidence in calculated mean, median or percentile yields.
(2) Representative: there is a clear danger that 'failed' (i.e., poorly yielding) wells will tend to be under-reported to national databases, relative to successful wells that are eventually taken into production.
(3) Reliable: yield data, often of variable quality, should ideally be quality-filtered to secure reliable statistical analysis (e.g., Morland 1997, Henriksen 2008).

In Scandinavia, and especially in Norway and Sweden, these criteria are fulfilled (albeit imperfectly) to a greater degree than in many other countries. The Scandinavian nations generally have a culture that prizes the curation of information. The databases hosted by the national Geological Surveys of Norway (NGU) and Sweden (SGU) contain tens of thousands of records of crystalline rock water wells. (The Geological Survey of Finland (GTK) has a nationwide database of a few thousand drilled wells with comprehensive water quality information but, unfortunately, sparse well yield data.) Furthermore, because the nations are rather small and the numbers of operational drilling companies limited, the Surveys have often been able to establish rather good relationships with the most important drillers to ensure representative reporting. Of course, this does not rule out the possibility of 'failed'/poorly yielding wells being underrepresented, especially in historic data, but the fact that most hard rock wells are drilled for individual households (which may only have a requirement of <100 L hr^{-1} water) means that a well has to be very poorly yielding indeed to be deemed a 'failure'. One must also accept the possibility that unscrupulous drillers (who are surely in a small minority!) may 'inflate' well yields, with confidence that a householder will seldom independently put these to the test. Nevertheless, one may argue that the Swedish and Norwegian databases are amongst the best and most representative databases of crystalline bedrock wells available today. In Finland, as in Norway and Sweden, crystalline bedrock aquifers are a major source of groundwater supply in rural areas (Mäkelä 1993). While no national Finnish database has been constructed and statistically analysed in the same way that Norwegian and Swedish data have been, representative regional databases have been examined in parts of Finland (Rönkä 1993).

Despite the different lithologies, climates and tectonic histories of Sweden, Finland and Norway, it is remarkable that the data distributions for well yield from crystalline bedrock databases in the three nations are very similar (Figure 2), all with a median well yield of 600–700 L hr^{-1}. Note that Figure 2 (and Figure 4) has a probability scale on the y-axis and a logarithmic scale on the x-axis. On such log-probability plots, a log-normal distribution yields a straight line.

Morland (1997) was responsible for the first comprehensive statistical analysis of the Norwegian crystalline bedrock well database in recent years. After rigorous quality control, he ended

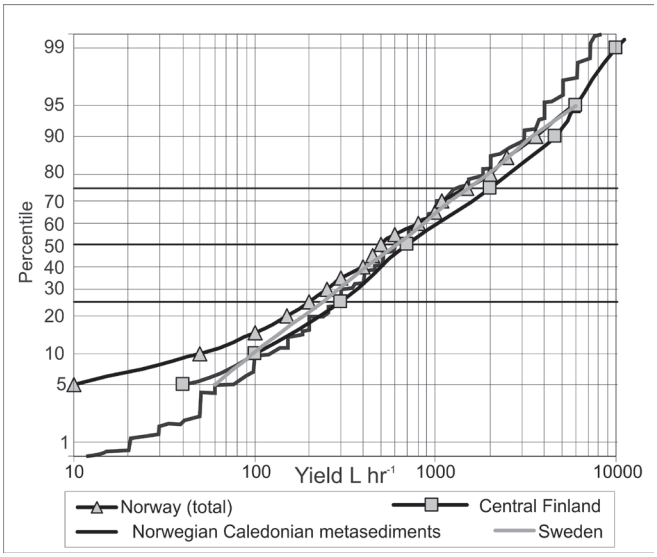

Figure 2. Comparison of distribution of short term well yield in crystalline rocks of the three Fennoscandian nations. Note the probability scale on the y-axis and the log-transformed x-axis. On such log-probability plots, a log-normal distribution yields a straight line.

- *Swedish hard rock drilled wells (N=59,000, derived from Gustafson 2002),*
- *Norwegian wells in Caledonian metasediments (Rock Group 74 in Table 1 and Figure 3, from Morland 1997, N=2098). The median yield of this Group is identical to that of Morland's total data set.*
- *drilled wells in Central Finland (Table 3, N=1297)*
- *Norway (total): Norwegian wells in crystalline rock (N=26,811, from the Geological Survey of Norway's database in March 2008).*

up with a set of 12,757 records. He subdivided the records on the basis of lithology and found that, while a few specific lithologies (e.g., the Permian lavas of the Oslo Rift, some sandstone and marble lithologies) (Table 1) exhibited significantly higher yields, the bulk of the lithologies had median well yields of several hundred L hr^{-1}. He found, moreover, that *within* each lithology there was a huge range in well yield, from effectively 'dry' (nominally 10 L hr^{-1} or less) to >10,000 L hr^{-1} (Figure 3).

Every crystalline bedrock lithology can therefore effectively be regarded as an aquifer, capable of supporting water wells yielding economically viable quantities of water. One can speculate that the reason that most lithologies exhibit remarkably similar yield distributions (Figure 3, Krásný and Sharp 2007) is that they have similar, silicate-based matrices with similar geomechanical properties. They may also have been subject to broadly similar recent tectonic stress fields and post-glacial stress-release histories (which are likely to be far more important for hydraulic properties than ancient geological stress histories) (Zoback 1992, Banks et al. 1994). Thus, from a regional point of view, they contain a population of fractures with similar distributions of size and aperture.

One may further speculate that the small differences in median yield between lithologies reflect differences in weathering and geomechanical properties: typically somewhat higher median yields and hydraulic conductivities are found in felsic rocks (e.g., Bäckblom et al. 1997, Olofsson et al. 2001, Knutsson

Table 1. Norwegian lithological codes employed in Figure 1 (after Sigmond 1992), arranged in order of declining median well yield (according to Morland 1997).

Lithological group	Description
57	Permo-Carboniferous volcanic and some sedimentary rocks. Oslo Rift region
79	Late Proterozoic tillite
75	Cambro-Silurian limestone and marble
54	Intrusive igneous rocks of Permian age. Oslo Rift region
67	Early Devonian sedimentary rocks: mainly sandstone and conglomerate
81	Late Proterozoic limestone, mudstone, sandstone
98	Autochthonous Proterozoic gneiss, migmatite, foliated granite and amphibolite
97	Autochthonous Proterozoic metarhyolite and metarhyodacite
87	Proterozoic granite/tonalite in the Caledonian belt
80	Late Proterozoic sandstone and conglomerate, with metaargillites and volcanics
85	Various Proterozoic metamorphic rocks in the Caledonian nappes
74	Cambro-Silurian metasediments. Caledonian belt and Oslo rift area
92	Autochthonous Proterozoic granite to tonalite
88	Proterozoic gabbro, diorite, amphibolite in the Caledonian belt
82	Late Proterozoic sandstone (meta-arkose) and mica schists
95	Autochthonous Proterozoic metasandstone, mica schists, conglomerate, gneiss
96	Autochthonous Proterozoic metabasalt, meta-andesite and amphibolite
94	Autochthonous Proterozoic gabbro, amphibolite and ultramafics
90	Proterozoic metasediments, metavolcanics and gneiss in the Caledonian belt
91	Proterozoic gneiss, migmatite, foliated granite, amphibolites—NW gneiss region
76	Cambro-Silurian greenstone, greenschists, amphibolite and meta-andesite
86	Proterozoic charnockite to anorthosite in the Caledonian nappes
64	Devonian sedimentary rocks: mainly sandstone and conglomerate
71	Caledonian (Ordovian-Silurian) granite to tonalite.
72	Late Proterozoic–Silurian gabbro, diorite and ultramafics in the Caledonian belt

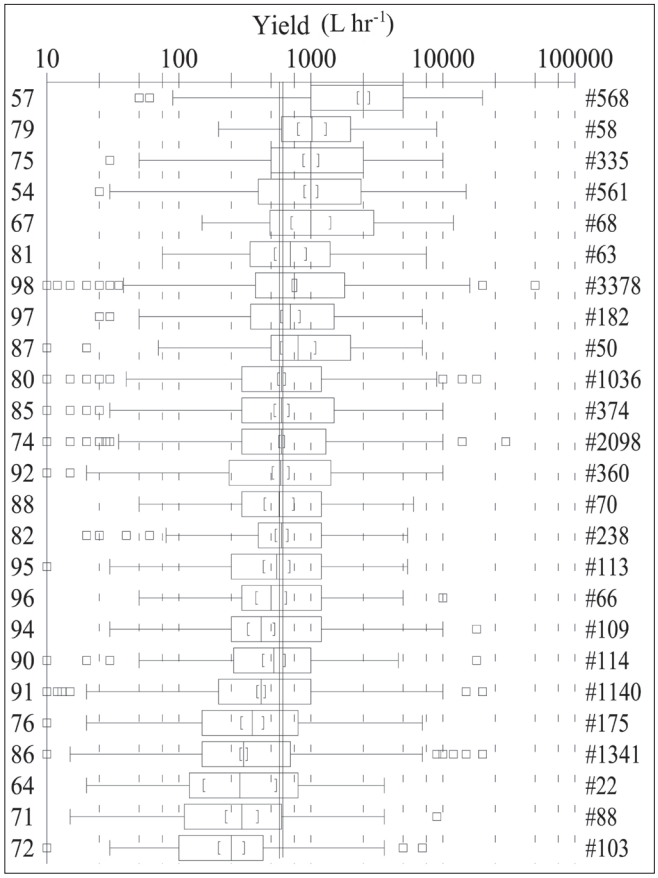

Figure 3. Boxplots showing distribution of well yields within each Norwegian hard-rock lithology (after Morland 1997). The lithological key is shown in Table 1.

2008), such as quartzites and granites, which are more brittle and might support larger-aperture, non-self-healing fractures. Lower median yields are typically reported from mafic rocks (e.g., gabbros), anorthosites and shales, which are regarded as being more readily weathered and more ductile and can accommodate strain by larger numbers of smaller or self-healing fractures. The term 'self-healing' refers to fractures in rocks exhibiting ductile or plastic deformation, where fracture apertures can be irreversibly reduced under appropriate ambient stress fields by movement of e.g., clay platelets.

The high median yields of lithologies such as the Permian sedimentary rocks and lavas (Table 1, Figure 3) can be explained by the fact that groundwater flow occurs, at least partially, through primary features—intergranular pore spaces, chilled/cracked margins or vesicles.

Regardless of the possible explanations for the modest degree of lithological dependence of yield, Morland (1997) found that the median yield of 12,757 Norwegian crystalline bedrock wells was 600 L hr^{-1} (± 17 L hr^{-1} at a 95% confidence level), with 25%- and 75%-ile values of 300 L hr^{-1} and 1500 L hr^{-1}

(Morland *pers. comm.*). The median depth of the wells was 52 m. Since Morland's (1997) analysis, NGU has expended considerable effort on acquiring high-quality data from drillers: the current database (as of March 2008) contains 26,811 records of bedrock well yields, with a median yield of 500 L hr^{-1} and lower and upper quartile yields of 200 and 1500 L hr^{-1} (Figure 2). It is suspected that the differences between the 1997 and 2008 analyses may reflect the ways in which 'zero' entries in the database have been handled.

Fagerlind (1986) and Gustafson (2002) document the findings from a statistical analysis of the Swedish data set, performed in around 1986. They, too, found that the median yield was 600 L hr^{-1} from a data set of 59,000 wells. The 25% and 75% percentiles are reported as 270 and 1800 L hr^{-1}, respectively (Figures 2 and 4), and the median depth of the wells was 64 m. For wells drilled in late 1987 and 1988 (N=6630), the median depth and yield were slightly higher at 75 m and 700 L hr^{-1} (Fagerlind 1989). Some systematic differences in median yield according to lithology can be identified (Struckmeier 1993, Olofsson et al. 2001, Knutsson 2008) and there are some Swedish regions (e.g., Skåne or Scania, as it is sometimes known in English, near the Tornqvist Zone) where Precambrian basement rocks appear to exhibit higher well yields than elsewhere (Table 2, Figure 1).

In Finland, current yield data are not available from any national database. However, examination of a regional database (which is regularly updated) of crystalline rock wells, drilled between 1947 and 2007 in Central Finland, reveals a median yield of 700 L hr^{-1} (N=1297) with 25%- and 75%-ile yields at 300 and 2000 L hr^{-1} (Figure 2). The median depth for the boreholes in the data set is 73 m (N=1996) with 25%- and 75%-ile depths of 46 and 109 m (Mäkelä 1994 and recent output from updated database). The mean yield is 1592 L hr^{-1}, demonstrating

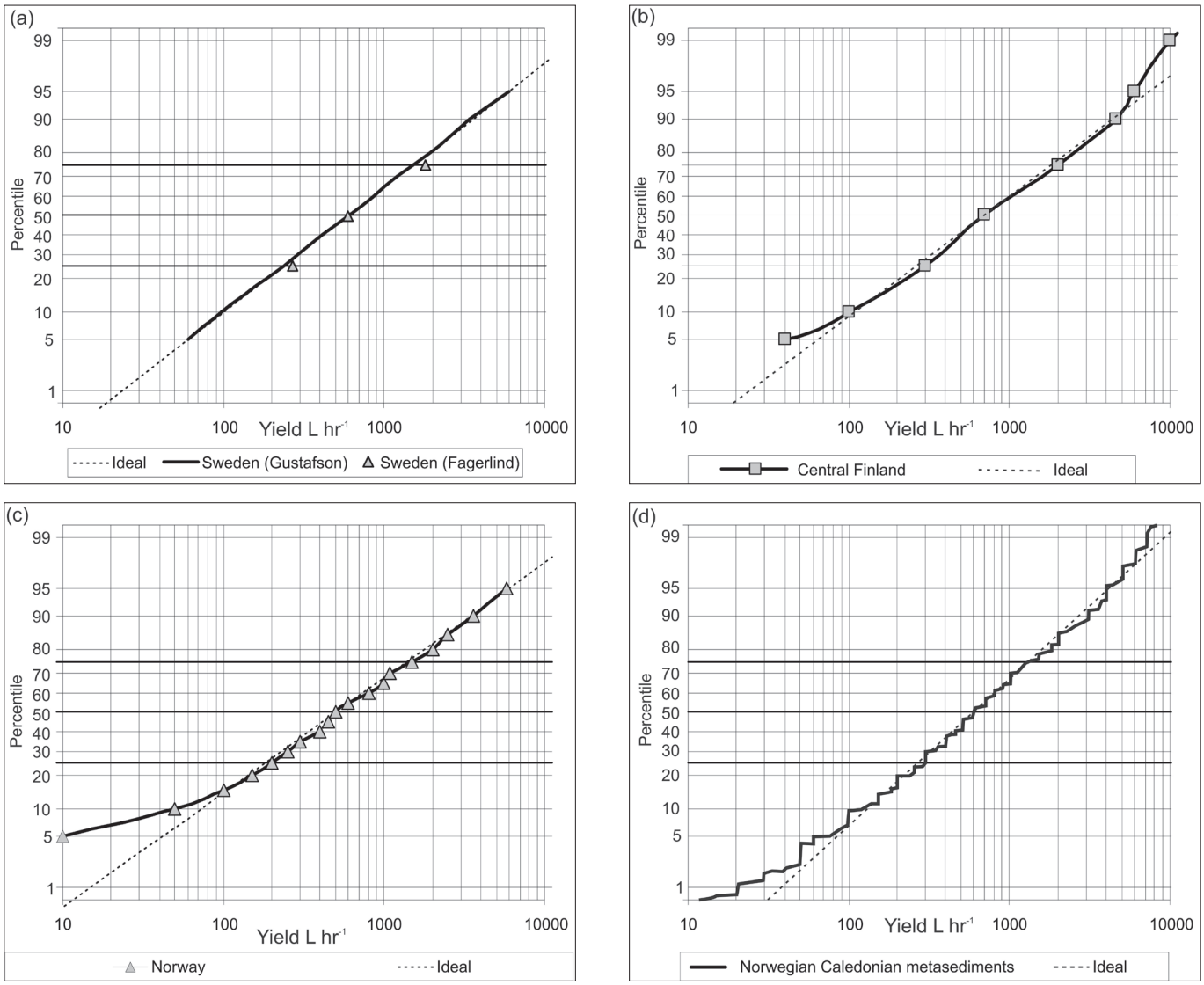

Figure 4. Distributions of short term well yield from the same data sets as Figure 2. Real data are compared with idealised log-normal distributions (indicated by dashed lines), as follows: (geometric mean=median ± log-transformed standard deviation): (a) 600 ± 0.602 L hr^{-1}; (b) 700 ± 0.623 L hr^{-1}; (c) 500 ± 0.652 L hr^{-1}; (d) 600 ± 0.511 L hr^{-1}. Note that Figure 4a displays data from both Fagerlind (1986) and Gustafson (2002). On such log-probability plots, a log-normal distribution yields a straight line.

Table 2. Median hydraulic conductivities (m s^{-1}) of drilled wells in different counties of Sweden.

County (län)	N	Median hydraulic conductivity (m s^{-1})	Reference
Jönköping	3,500	5.0×10^{-8}	Gierup et al. (1999a)
Västra Götaland	21,000	4.2×10^{-8}	Antal et al. (1999a)
Västmanland	4,200	5.7×10^{-8}	Bergman et al. (1999b)
Dalarna *	5,000	5.5×10^{-8}	Gierup et al. (1999c)
Skåne *	4,000	2.74×10^{-7}	Gierup et al. (1999d)
Jämtland *	1,000	9.0×10^{-8}	Antal et al. (1999c)
Örebro	4,900	4.3×10^{-8}	Bergman et al. (1999a)
Värmland	7,000	5.6×10^{-8}	Fredén et al. (1999)
Kronoberg	1,800	9.3×10^{-8}	Gierup et al. (1999b)
Halland	4,000	5.4×10^{-8}	Antal et al. (1999b)
Norrbotten*	2,700	5.0×10^{-8}	Bergman et al. (1998)
Västernorrland	3,400	3.9×10^{-8}	Antal et al. (1998f)
Uppsala	7,000	5.9×10^{-8}	Antal et al. (1998a)
Stockholm	15,000	2.2×10^{-8}	Antal et al. (1998e)
Södermanland	4,200	2.2×10^{-8}	Antal et al. (1998d)
Kalmar	2,500	5.9×10^{-8}	Antal et al. (1998b)
Blekinge	2,100	8.3×10^{-8}	Antal et al. (1998c)
Sum	93,300		
Arithmetic mean		6.75×10^{-8}	
Weighted mean		5.54×10^{-8}	

**In some counties with later (e.g., Mesozoic and Caledonian) cover rocks, only wells drilled in pre-Caledonian basement (*urberg*) are considered.*

Table 3. Statistics for drilled wells in Central Finland, supplied by the database of the Central Finland Regional Environment Centre (now the Central Finland Centre for Economic Development, Transport and the Environment).

	Parameter	Depth	Yield	Yield	Yield	Yield	Yield	Yield
	Subset	All wells 1947-2007	All wells 1947-2007	Granite	Granodiorite	Other intrusive rocks	Subvolcanic / volcanic rocks	Mica gneiss and schist
	Unit	m	L hr^{-1}	L hr^{-1}	L hr^{-1}	L hr^{-1}	L hr^{-1}	L hr^{-1}
	Database date	24/10/2007	24/10/2007	27/11/2007	27/11/2007	27/11/2007	27/11/2007	27/11/2007
Percentile	0 (minimum)	9	0	0	0	0	0	0
	1	15	0	0	0	1	0	0
	5	23	40	50	40	15	20	30
	10	31	100	100	100	70	83	150
	25 (1st quartile)	46	300	300	300	240	300	500
	50 (median)	73	700	700	600	650	700	864
	75 (3rd quartile)	109	2000	2000	1800	2000	2000	2400
	90	151	4600	4000	4800	5000	4200	4800
	95	181	6000	6000	6000	8000	5000	6850
	99	247	10000	10000	9000	20000	10000	10000
	100 (maximum)	505	24000	24000	20000	20000	10000	10000
	N	1996	1297	393	562	144	85	101
	Mean	84	1592	1574	1531	1869	1498	1768
	Median	73	700	700	600	650	700	864
	Mode	40	500	500	500	500	600	600

the skewed character of the data set towards low yields. There is relatively little variation with lithology (Table 3).

Rönkä's (1983) data for 368 Finnish drilled wells resulted in an arithmetic mean yield of a similar magnitude to the Central Finnish data set—1188 L hr^{-1}—with relatively little lithological dependence. The average depth of wells in his data set was 60 m (N=385). The data of Laakso (1966) consisted of cable-tool wells drilled by a single firm, mainly in the 1950s, with an average depth of 68 m and an arithmetic mean yield of 2460 L hr^{-1} (N=1108). Hyyppä (1984) considered (for water quality purposes) a data set of 908 wells around Finland, and recorded an average depth of 48 m. Lahermo (1970, 1971) has studied drilled wells in Finnish Lapland and in the rapakivi granite area of southeastern Finland. The average depth of wells was 33 and 65 m, respectively, and the average yield of wells 2050 and 3200 L hr^{-1}, respectively (N=213 and 147).

At this stage, it is worth noting that these well yields are almost always estimated on the basis of short-term pumping or air-lift tests, short-term recovery tests or estimates of water 'blown out' of boreholes during down-the-hole-hammer compressed-air drilling. Such short-term tests are thus not representative of a large aquifer volume, but of the relatively small number of fractures that transmit water to the well from some form of broader water fracture network/aquifer storage. The yields would thus be expected to be determined by the transmissivity of these 'feeder fractures' in the limited zone of rock intersected by the well (Banks 1992).

Log-normal distributions

It is widely accepted that the distributions of physical dimensions of fractures (aperture, length) within a population (a fracture set) are typically approximately log-normally distributed (Banks et al. 1996). Power-law distributions are also sometimes considered more appropriate (de Dreuzy et al. 2002) for the distribution of fracture dimensions but, as Mitzenmacher (2004) demonstrates, power-law and log-normal distributions are often very difficult to distinguish, especially at the upper end (at the lower end, differences may be significant, however).

The origin of log-normal distributions in nature is often due to multiplicative or branching processes (Limpert et al. 2001, Mitzenmacher 2004). Bershadskii (2000) has demonstrated that the branching and fragmentation of fractures during their propagation can result in just such a distribution.

If we accept that fracture apertures are approximately log-normally or power-law distributed, it is then a short step to accepting that fracture transmissivities are similarly distributed, given that the transmissivity (T_f) of an ideal (smooth, plane-parallel) fracture is given by the equation (Snow 1969, Walsh 1981):

$$T_f = \frac{\rho g b^3}{12\mu} \quad (1)$$

where ρ is the density of water, g is the acceleration due to gravity, b is the fracture aperture and μ is the dynamic viscosity of water. Given a Poisson or negative binomial distribution of fracture frequency and a power-law or log-normal distribution of fracture transmissivity, we should not be wholly surprised to find an approximately log-normal distribution of yields in databases of boreholes drilled in hard rock aquifers (e.g., Moore et al. 2002, Figure 4). This is understandable if we consider the observations that:

- the yields documented in such databases are typically short-term yields and are probably controlled by the transmissivity of the 'feeder' fractures in the immediate vicinity of the borehole, rather than the properties of the broader aquifer fracture network storage (including connectivity) or the available recharge. It is these fractures which connect the well to a wider network of fracture storage and are usually the limiting factor for a crystalline bedrock well's yield in the short term and in the case of relatively poorly yielding wells (Banks 1992).
- the yield of wells in crystalline bedrock aquifers is typically dominated by groundwater inflow from a very small number (or sometimes just one) of fractures (e.g., Carlsson and Olsson 1977), which itself is a consequence of a fracture transmissivity distribution skewed towards low yields. Such an observation argues against the utility of the concept of hydraulic conductivity (an *intrinsic* property that presupposes a continuum approach) when describing properties derived from single boreholes, while the extrinsic (fracture-specific) concept of transmissivity is more tenable.

In this study, we have regarded transmissivity as the primary hydraulic property that can be estimated from consideration of well yields. In most simple hydraulic analysis methods (e.g., Theis 1935, Cooper and Jacob 1946, Logan 1964), transmissivity is proportionately related to specific capacity (the ratio of yield to drawdown) and it is specific capacity that can be inferred from the well yield data considered in this paper. Average hydraulic conductivity can be regarded as a secondary parameter calculated as transmissivity divided by the thickness of the tested interval.

Moore et al. (2002) regard the distribution of yields in their New Hampshire data set as log-normally distributed, while Banks (1998) has used Norwegian data to demonstrate that the yields of wells from individual crystalline rock lithologies are indistinguishable from a log-normal distribution at a 95% confidence level. Previous studies have indicated yield data from Central Finland to be approximately log-normally distributed (Mäkelä 1994). Morland's (1997) and Fagerlind's (1986) full raw data sets for Norway and Sweden have not been available for rigorous statistical testing within this study, but examination of Figure 4 reveals approximately straight lines on probability-logarithmic plots, indicating that the distributions are close to log-normal, at least over their central portions. The Central Finnish data set has been log-transformed and tested for nor-

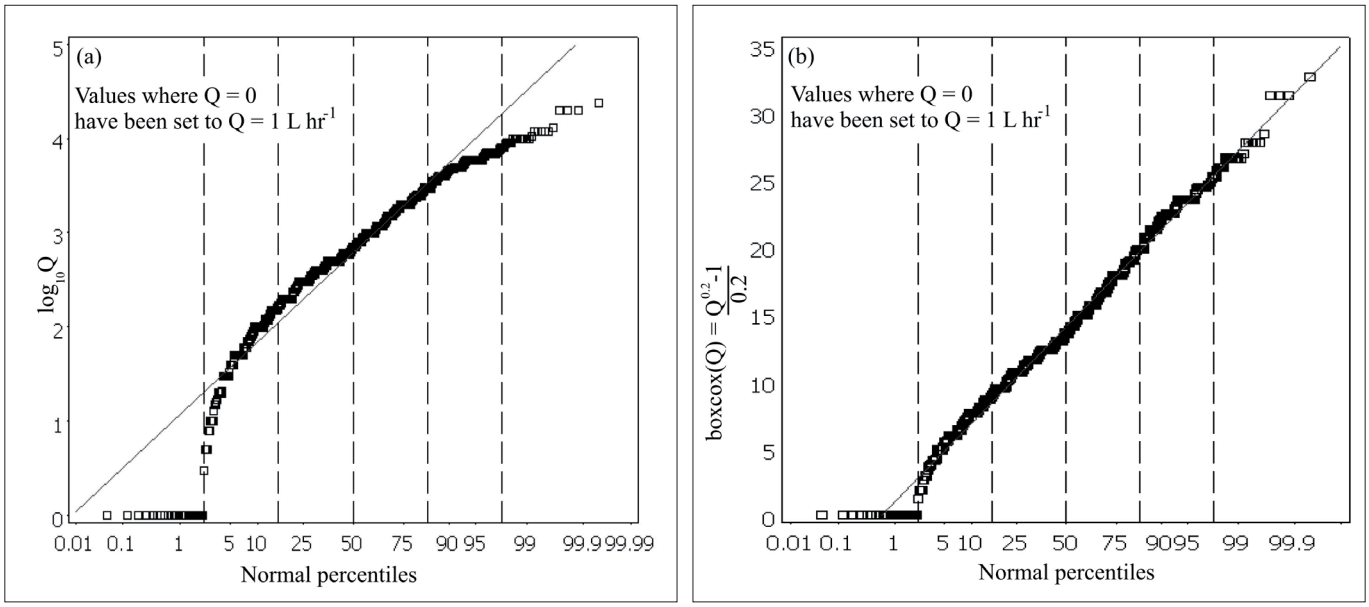

Figure 5. (a) Logarithmically transformed and (b) Box-Cox transformed yield (Q) distribution of the Central Finnish drilled well data set (N=1300, as of 29/3/10), plotted against a normalised probability axis. Figure 5a is essentially similar to Figure 4b, although plotted on different axes (and with detail omitted at the extremes of the distribution in Figure 4b). The Box-Cox transformation was $(Q^{0.2}-1)/0.2$*. A linear relationship indicates that the Box-Cox transformed distribution closely approaches normality. The Box-Cox transformed distribution can be compared favourably, in terms of normality, with the log-transformed data set, which deviates from normality at both low and high yields. Yields of 0 L hr*$^{-1}$ *have been set to a nominal value of 1 L hr*$^{-1}$*.*

mality using the Shapiro-Wilk and Kolmogorov-Smirnov tests. The former test yielded a W-value of 0.916 and the latter a D-value of 0.103, respectively (N=1300), which were not adequate to support a hypothesis of log-normality at a 95% confidence level. These relatively rigorous statistical tests require a good fit across the entire distribution to be satisfied, while, in the Finnish data set, the deviations from log-normality occurred at the extremes of the distribution, with the main, central portion of the data closely resembling log-normality (Figure 5a). As with fracture dimensions (see above), there is some debate as to whether a power-law distribution is more appropriate for well yields and hydraulic properties of crystalline rocks. Gustafson and Fransson (2006) argue for a power law distribution of fracture transmissivities. The Central Finnish data set has also been Box-Cox transformed, using a power law algorithm, and tested for normality using the same tests, yielding a W-value of 0.991 and a D-value of 0.0611 (Figure 5b). Although these values were still not wholly adequate to demonstrate a normalising transformation, the power-law transformation is qualitatively far more convincing than the logarithmic transformation, with a much better fit to the tails of the distribution.

An heuristic approach to median transmissivity and hydraulic conductivity

It has been very common in nations dominated by poorly weathered crystalline rock aquifers to use well yield as a proxy for aquifer transmissivity (Jetel and Krásný 1968, Krásný 1975, Carlsson and Carlstedt 1976, Wladis and Gustafson 1999). Furthermore, several geotechnical methods for determining the hydraulic conductivity of intervals of hard rock borehole essentially measure the flow of water between borehole and aquifer for a given pressure differential. The authors have thus undertaken an heuristic approach (i.e., an analysis undertaken in the spirit of scientific 'playfulness' and discovery, on the explicit understanding that some of the underlying assumptions and conceptual models are grossly oversimplified) to ascertain whether the observed distributions of well yield can be explained by a characteristic distribution of transmissivity.

Banks (1992) examined a large variety of published relationships between crystalline rock well yield and apparent transmissivity T_a and found that most were of the form:

$$T_a = \frac{1}{\alpha}\frac{Q}{s} \qquad (2)$$

where Q/s is the short-term specific capacity (ratio of yield Q to drawdown s) and α is a constant. Banks (1992) concluded with recommending a value of α=0.9, although Wladis and Gustafson (1999) suggest a somewhat lower value of α=0.45 from Swedish studies. For the purposes of this paper, we will assume a value of α=0.7 ± 0.2 (the error margins cited in this paper should be regarded as estimates of limits of confidence; the value cited here is selected to span the majority of α values suggested in the above studies).

If we know the yield of a well in crystalline bedrock, we can thus make an estimate of the apparent aquifer transmissivity, provided we can estimate the drawdown in the well corresponding to that yield. Let us assume that the depth to rest water level

in a crystalline bedrock borehole is d_o and the depth of the well is D. In low-yielding crystalline bedrock wells in Scandinavia, it is common practice to measure yield by one of the following methods:

1) the amount of water blown out of the well over a modest period of time by compressed air introduced at the base of the hole on completion of drilling (in which case the 'drawdown' can be taken to be the depth of the well minus the rest water level; i.e., $[D–d_o]$).
2) a recovery test, where the hole is emptied by a pump near the base of the well, the well is 'skim pumped' at that level for a short period and thereafter the inflow (Q) is determined as:
   $Q = \pi * r_w^2 * (\Delta h/\Delta t)$ by Banks (1992) (3)
   by measuring the recovery of the water level Δh over a given time interval Δt, where r_w is the radius of the drilled well. In this case, the appropriate measure of drawdown to associate with the yield is probably around $^2/_3(D\text{-}d_o)$ (i.e., we are assuming that the interval over which recovery is measured is 2/3 down the borehole, relative to rest water level).
3) a pumping test, where a submersible pump cuts in and out in response to water level recovery in the borehole following a short period of pumping. Again, it is suggested that an appropriate measure of drawdown is probably around $^1/_2(D\text{-}d_o)$ to $^2/_3(D\text{-}d_o)$.

The vast majority of wells in the Scandinavian bedrock well databases are drilled boreholes. The depth of these crystalline rock boreholes is commonly between 40 and 100 m, with depths of around 70 m being typical. The rest water level is typically rather near the surface (0–15 m), as a water table which closely follows the topography is a characteristic of low permeability crystalline rock terrain (Banks and Robins 2002). A typical value of $(D\text{-}d_o)$ can thus be estimated as 60 ± 10 m. A typical value of drawdown is thus $^2/_3(D\text{-}d_o)$=40 ± 7 m.

Clearly, the value of T_a has rather little meaning for a single well, but if we consider a large enough data set, we are in a position to estimate the median apparent transmissivity of crystalline hard rock aquifers in Fennoscandia. We may assume:

1) the median well yield in such aquifers is 650 ± 50 L hr^{-1} = 15.6 ± 1.2 m^3 d^{-1}
2) the corresponding drawdown is estimated as 40 ± 7 m.
3) the constant of proportionality α= 0.7 ± 0.2

Equation (2) thus provides us with a median value of transmissivity of T_a = 0.56 ± 0.30 m^2 d^{-1} = 6.4 x 10^{-6} ± 3.4 x 10^{-6} m^2 s^{-1}.

Statistically, this method is flawed, as it assumes that the expected value of specific capacity is simply the ratio between the expected value of the yield and that of drawdown (which is related to depth). It thus effectively assumes that there is no correlation between yield and depth. In fact, there is known to be a dependence of yield on depth due to at least two factors: (a) the observation that borehole depths are generally shallower in 'better' crystalline rock aquifers, as the driller often stops drilling once adequate water has been achieved (Rönkä 1993, Morland 1997), and (b) the total effective transmissivity of the aquifer increases with drilled depth, although the transmissivity of individual fractures tends to decrease with drilled depth in a nonlinear manner (see below). As these relationships are not necessarily linear and are different in nature (the first being a 'drilling-psychological' factor and the second geotectonic in nature), any correlation between depth and yield has been ignored in the above estimate.

Bulk transmissivity

For networks of fractures, whose dimensions are log-normally or power-law distributed, many researchers have argued that, at scales in excess of a given threshold (the 'Representative Elementary Volume (REV)'), the bulk transmissivity of the network (i.e., its overall ability to transmit water in response to head gradients) is best described by the geometric mean of the transmissivities (or hydraulic conductivities) of the individual fracture elements (e.g., de Dreuzy et al. 2002, Hunt 2005). The REV can be regarded as the volume/dimension at which there are only small changes in bulk hydraulic conductivity for small changes in sample size or sample location. It is a concept that is not limited to fractured rock aquifers, but which can also be applied to other forms of aquifer heterogeneity. For 2D isotropic systems, Renard and de Marsily (1997) and Renard et al. (2000) regard the geometric mean of permeabilities as being a good solution to bulk permeability and for 3D systems as being a plausible, though not perfect, estimate.

Moreover, for a distribution of fracture transmissivities or hydraulic conductivities that is approximately log-normal, the median value of that distribution will closely approximate the geometric mean (an observation empirically confirmed by researchers such as Broch and Kjøholt 1994). We can thus conclude that our estimated median value of transmissivity of 0.56 m^2 d^{-1} essentially represents the bulk transmissivity of the upper 70–80 m of crystalline bedrock that are penetrated by typical Scandinavian hard rock wells.

We should, of course, bear in mind that the transmissivity represented by these relatively shallow bedrock wells will only be a proportion of the total transmissivity of the rock 'column'. Swedish work suggests that crystalline bedrock hydraulic conductivity (measured as $\overline{K}$: the transmissivity divided by the tested interval of a borehole) decreases strongly with depth according to the relationship of the type shown in Figure 6 (which is derived specifically for a site as Oskarshamn in Sweden by SKB 2006). If such a relationship is more universally applicable, it would imply that the bulk transmissivity of the portion of aquifer down to 100 m may only account for 45% of the total transmissivity of the rock mass. Moreover, the upper 70

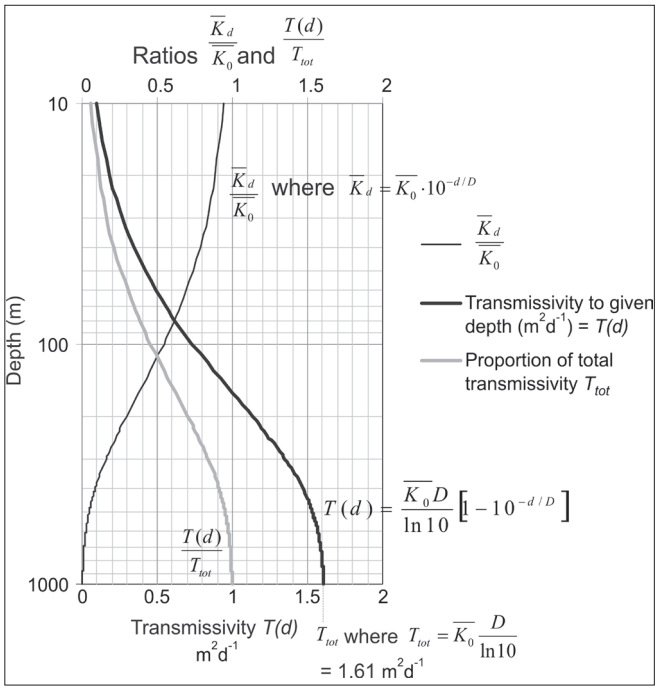

Figure 6. A simple empirically based model for development of average bulk hydraulic conductivity ($\overline{K}_d$) with depth (d), developed by SKB (2006) for a crystalline rock site at Oskarshamn, Sweden, where K_d decreases by a factor of 10 every D=380 m. $\overline{K}_0$ is the surficial average bulk hydraulic conductivity at d=0. T(d) is the transmissivity of the rock integrated down to depth d, while T_{tot} is the total transmissivity of the rock mass (to d=∞). A value of $\overline{K}_0$ of 0.0098 m d^{-1} has been selected, which yields a value of T(d)=0.56 m^2 d^{-1} for d=70 m.

m and 50 m represent only 35% and 26% of the total transmissivity, respectively. Here, the 'total transmissivity' should be understood as the sum of the fracture transmissivity down to an (unspecified) depth where fractures are effectively hydraulically 'closed' by the ambient stress field.

It is tempting to endeavour to convert our estimate of bulk apparent transmissivity to a value of bulk hydraulic conductivity K_b. We should here note that, at small scales, hydraulic conductivity is usually regarded as scale-dependent (Brace 1984, Clauser 1992). Only above a given REV (which Gustafson, 1986, estimates as being at least 1000 m^3) do we find that we can begin to consider a consistent value of bulk hydraulic conductivity, which can be considered 'equivalent' to the hydraulic conductivity of an analogous porous medium and which is not highly dependent on scale or location (Renard and de Marsily 1997). If the typical saturated depth (i.e., the section of rock hydraulically 'tested') of a Scandinavian water well borehole is around 60 m, it is possible to say that an estimated geometric mean transmissivity of 0.56 ± 0.30 m^2 d^{-1} is compatible with an equivalent bulk hydraulic conductivity of 1.1 (± 0.6) x 10^{-7} m s^{-1}.

Given the strong depth-dependence of hydraulic conductivity in crystalline bedrock (see above), and the significant variation in well yield in our datasets, we should be very sceptical about the significance of this interpretation of bulk hydraulic conductivity. Nevertheless, our estimate falls squarely within the range reported as being typical of shallow crystalline bedrock from a number of international sources (Table 4). Furthermore it is only a little higher than (and within the margin of uncertainty of) the typical median values estimated for hydraulic conductivity from Swedish bedrock boreholes (Table 2). This slight discrepancy with the Swedish data in Table 2 may, in fact, be consistent with the Swedish practice of estimating hydraulic conductivity by dividing yield by $(depth)^2$ rather than by (depth x drawdown). In other words, Swedish practice has assumed that drawdown is almost equal to the saturated depth of the borehole (Follin et al. 1999), whereas this study has assumed that drawdown is 2/3 of the saturated depth.

Comparison with other international data sets

It is hoped that this paper will stimulate discussion and encourage other nations to collate and publish statistical summaries of yield data from water wells in hard rock aquifers. We hope that this will allow us to ascertain if the consistency of yield distributions in wells from Fennoscandia is reproduced from other tectonic settings and other climates, or whether well yield distributions are significantly influenced by other factors, such as recent weathering environment (Banks et al. 1998). Some data are already published from other crystalline bedrock regions of the world (Table 4), which offer a tantalising suggestion that the 'median yield=600–700 L hr^{-1}' rule may have broader application than just Fennoscandia, as Krásný and Sharp (2007) have suggested. It was noted, in the Introduction, that the conclusions of this paper might only be expected to be valid in recently glaciated crystalline bedrock terrain—i.e., in true fractured aquifers, where a porous, permeable, weathered regolith aquifer is absent. Nevertheless, some of the case studies in Table 4 seem to suggest that, even where a weathered regolith could be expected, some of the observations regarding well yield distribution seem (surprisingly) to be valid.

Conclusions

The two main (and admittedly provocative) conclusions of this paper are:

1) Wells drilled in crystalline bedrock in recently glaciated, relatively unweathered terrain in Fennoscandia exhibit a wide range of yields. The distribution of these yields exhibits, however, a consistent median value of 600–700 L hr^{-1}. Analysis of subsets of data according to factors such as lithology, topography, proximity to lineaments etc., often reveals a relatively weak correlation with such factors. The ability to deliver realistic and helpful prognoses when prospecting for groundwater in such terrain thus requires an understanding of statistics every bit as much as skills in identifying deter-

Table 4. Hydraulic properties of crystalline rock terrains cited in worldwide literature and compared with Fennoscandian values (this paper).

Parameter Fennoscandian result (this paper)	Location	Result	Reference
Median well yield 600–700 L hr^{-1}	**Northern terrains**		
	3000 wells, British Columbia, Canada	Median well yields from 340 to 1150 L hr^{-1} in different lithological groups (see Figure 3). Median of 700–900 L hr^{-1} typical.	Kohut (2006)
	196 boreholes in igneous and metamorphic rocks, Manitoba, Canada	Median yield = 700 L hr^{-1}	Betcher et al. (1995)
	433 boreholes in metamorphic bedrock (excluding limestone), southern Vancouver Island, Canada	Median yield = 900 L hr^{-1}	Kenny et al. (2006)
	Caledonian (Appalachian) terrain of Maine, USA	Median yield = 3 to 6 US gallons/minute (680 to 1360 L hr-1) for different map sheets	Maine Geological Survey (2007)
	Domestic bedrock wells, Maine, USA	Median yield = 4 US gallons min^{-1} = c. 900 L hr^{-1}	Maine State Planning Office (2001)
	20,308 drilled wells in New Hampshire, USA	Median yield = 6 US gallons/min^{-1} = 1360 L hr^{-1}	Moore et al. (2002)
	Tropical terrains		
	Crystalline basement, eastern Chad	Overall well 'success rate' of 30–40% and a median yield of 1500–2000 L hr-1 in 'successful' wells	Well database held in N'djamena. Cited in Misstear et al. (2006)
	Masvingo, Zimbabwe	30–40% of wells have yields less than 360 L hr^{-1}	Wright (1989), Herbert et al. (1993)
	Drilled wells, northern Niger	Median yield varies from 430 to 2010 L hr^{-1} in different lithological groups (see Figure 3).	Barratt and Puyoo (1984)
	536 wells in Precambrian gneisses and schists, Kandy region, Sri Lanka (median depth = 76 m)	Median yield = 780 L hr^{-1}	Johansson (2005)
	380 wells in Precambrian basement, NE Brazil	Median yield = 1800 L hr^{-1}	Rebouças (1999)
Bulk transmissivity 0.56 ± 0.30 m^2 d^{-1}	22 drilled wells, Uganda (regolith excluded by casing)	Median transmissivity = 0.8 m^2 d^{-1}	Howard et al. (1992)
Bulk hydraulic conductivity. 1.1 ± 0.6 x 10^{-7} m s^{-1}	**Northern terrains**		
	To depths of 1 km, Europe and Canada	Typical bulk conductivity = 10^{-6} to 10^{-8} m s^{-1}	Stober and Bucher (2007)
	c. 140,000 wells in Norway and Sweden	'Average' conductivity = 10^{-6} to 10^{-8} m s-1	Henriksen's (2008) Figure 7
	Upper few hundred metres of Canadian shield, Canada	10^{-6} to 10^{-8} m s^{-1}	Dickin et al. (1984).
	To 100 m depth, Altnabreac, Scotland	Range = 10^{-6} to 10^{-8} m s^{-1}	Mather and Sargent (1986)
	Central European terrains		
	Harz Mountains, Germany	Regional conductivity = 3.0 x 10^{-7} m s^{-1}	Maloszewski et al. (1999)
	Drainage study at 170 m depth, Limoges, France	'Average' conductivity = 10^{-7} to 10^{-8} m s^{-1}	Mather and Sargent (1986)

ministic geological factors (Banks et al. 2005).

2) The approximately log-normal distribution of well yields in crystalline bedrock terrain, coupled with a median yield of some 600-–700 L hr^{-1}, implies that the bulk transmissivity of the upper 70–80 m or so of Fennoscandian crystalline bedrock crust is around 0.56 ± 0.30 m^2 d^{-1}, although this may only represent around one third of the total transmissivity of the full depth of the rock mass. Considering a typical saturated depth of a borehole, leads us to estimate the bulk hydraulic conductivity of a similar aquifer interval to be around 1 x 10^{-7} m s^{-1}. This last estimate must be treated with considerable scepticism, given the strong depth dependence of hydraulic conductivity and the varying depth of wells used in the analysis.

Knowledge of the statistical distribution of hydraulic properties of crystalline bedrock is a prerequisite for a cost-effective drilling strategy in such aquifers. Knowledge of bulk transmissivity will also have relevance to assessing the water balance and available water resources of bedrock aquifer catchments and to the assessment of the significance of advection of heat with groundwater in the underground thermal energy storage (UTES) systems that are becoming increasingly common throughout Scandinavia.

Acknowledgements

The authors wish to thank Ritva Britschgi of the Finnish Environment Institute (Suomen ympäristökeskus) for her interest and enthusiasm during the preparation of this paper. They also thank Nick Robins of the British Geological Survey and Dr. Noelle Odling of Leeds University for their comments and constructive reviews of the manuscript.

References

Antal, I., Bergman, S., Gierup, J., Persson, C. and Thunholm, B. (1998a) Översiktsstudie av Uppsala län. Geologiska förutsättningar. *SKB Report*, **R–98–32**, 49pp.

Antal, I., Bergman, S., Gierup, J., Rudmark, L., Thunholm, B. and Wahlgren, C.H. (1998b) Översiktsstudie av Kalmar län. Geologiska förutsättningar. *SKB Report*, **R–98–24**, 48pp.

Antal, I., Bergman, T., Gierup, J., Persson, M., Thunholm, B. and Wahlgren, C.H. (1998c) Översiktsstudie av Blekinge län. Geologiska förutsättningar. *SKB Report*, **R–98–22**, 45pp.

Antal, I., Bergman, T., Persson, C., Stephens, M., Thunholm, B. and Åsman, M. (1998d) Översiktsstudie av Södermanlands län. Geologiska förutsättningar. *SKB Report*, **R–98–28**, 49pp.

Antal, I., Bergman, T., Persson, C., Stephens, M., Thunholm, B. and Åsman, M. (1998e) Översiktsstudie av Stockholms län. Geologiska förutsättningar. *SKB Report*, **R–98–30**, 47pp.

Antal, I., Fredén, C., Gierup, J., Stølen, L.K. and Thunholm, B. (1998f) Översiktsstudie av Västernorrlands län. Geologiska förutsättningar. *SKB Report*, **R–98–36**, 48pp.

Antal, I., Berglund, J., Eliasson, T., Gierup, J., Hilldén, A., Stølen, L.K. and Thunholm, B. (1999a) Översiktsstudie av Västra Götalands län. Geologiska förutsättningar. *SKB Report*, **R–99–33**, 57pp.

Antal, I., Berglund, J., Gierup, J., Lundqvist, I., Påsse, T., Stølen, L.K., Thunholm, B. (1999b) Översiktsstudie av Hallands län. Geologiska förutsättningar. *SKB Report*, **R–99–17**, 45pp.

Antal, I., Bergman, S., Fredén, C., Gierup, J., Stølen, L.K. and Thunholm, B. (1999c) Översiktsstudie av Jämtlands län (urbergsdelen). Geologiska förutsättningar. *SKB Report*, **R–99–25**, 46pp.

Bäckblom, G., Gustafson, G., Stanfors, R. and Wikberg, P. (1997) ÄSPÖ HRL—geoscientific evaluation 1997/2. Results from pre-investigations and detailed site characterisation. Summary report. *SKB Technical Report*, **TR 97–03**.

Banks, D. (1992) Estimation of apparent transmissivity from capacity-testing of boreholes in bedrock aquifers. *Hydrogeology Journal*, **1(4)**, 5–19.

Banks. D, (1998) Predicting the probability distribution of yield from multiple boreholes in crystalline bedrock. *Ground Water*, **36**, 269–274.

Banks, D. and Robins, N. (2002) *An introduction to groundwater in crystalline bedrock*. Norges geologiske undersøkelse, Trondheim, 63 pp.

Banks. D., Rohr-Torp, E. and Skarphagen, H. (1994) Groundwater resources in hard rock; experiences from the Hvaler study, southeastern Norway. *Hydrogeology Journal*, **2(2)**, 33–42.

Banks, D., Odling, N., Skarphagen, H. and Rohr-Torp, E. (1996) Permeability and stress in crystalline rocks. *Terra Nova*, **8**, 228–235.

Banks, D., Reimann, C. and Skarphagen, H. (1998) The comparative hydrochemistry of two granitic island aquifers: the Isles of Scilly, UK and the Hvaler Islands, Norway. *The Science of the Total Environment*, **209**, 169–183.

Banks, D., Morland, G. and Frengstad, B. (2005) Use of non-parametric statistics as a tool for the hydraulic and hydrogeochemical characterization of hard rock aquifers. *Scottish Journal of Geology*, **41**, 69–79.

Barrat, J.M. and Puyoo, S. (1984) Analyse hydrogéologique par méthode statistique de la campagne 1000 forages au Niger. *BRGM (Bureau de Recherches Géologiques et Minières) Report*, **84**, SGN 309 EAW/AGE, 82 pp.

Bergman, S., Gierup, J., Kübler, L., Lagerbäck, R. and Thunholm, B. (1998) Översiktsstudie av Norrbottens län (urbergsdelen). Geologiska förutsättningar. *SKB Report*, **R–98–40**, 58pp.

Bergman, T., Fredén, C., Gierup, J., Kübler, L., Stephens, M., Stølen, L.K. and Thunholm, B. (1999a) Översiktsstudie av Örebro län. Geologiska förutsättningar. *SKB Report*, **R–99–23**, 49pp.

Bergman, T., Gierup, J., Kübler, L., Lindén, A., Stephens, M., Stølen, L.K. and Thunholm, B. (1999b) Översiktsstudie av Västmanlands län. Geologiska förutsättningar. *SKB Report*, **R–99–31**, 48pp.

Bershadskii, A. (2000) Multiscaling and localized instabilities in fracture, fragmentation, and growth processes. *European Physical Journal B*, **14**, 323–327.

Betcher, R., Grove, G. and Pupp, C. (1995) Groundwater in Manitoba: hydrogeology, quality concerns, management. *Environment Canada, National Hydrology Research Institute (NHRI) Contribution*, **CS–93017**, March 1995, 47 pp.

Brace, W.F. (1984) Permeability of crystalline rocks: new in situ measurements. *Journal of Geophysical Research*, **89(B6)**, 4327–4430.

Braester, C. and Barak, L. (1991) Searching for a fracture as a two-person zero-sum game. *Physica A—Theoretical and Stochastic Physics*, **175**, 1–8.

Broch, E. and Kjøholt, H. (1994) Verification of large-scale permeability tests in hard rocks. *Hydrogeology Journal*, **2(3)**, 9–16.

Carlsson, L. and Carlstedt, A. (1976) Estimation of transmissivity and permeability in Swedish bedrocks. *In* Proceedings of the Nordic Hydrological Conference, Reykjavik (August–Sept. 1976), 27–39. Reprinted in *Nordic Hydrology* (1977), **8**, 103–116.

Carlsson, A. and Olsson, T. (1977) Hydraulic properties of Swedish crystalline rocks. Hydraulic conductivity and its relation to depth. *Bulletin of the Geological Institutions of the University of Uppsala*, **NS7**, 71–84.

Clauser, C. (1992) Permeability of crystalline rocks. *EOS Transactions of the American Geophysical Union*, **73**, 233–240.

Cooper, H.H. and Jacob, C.E. (1946) A generalised graphical method for evaluating formation constants and summarizing well field history. *Transactions of the American Geophysical Union*, **27**, 526–534.

de Dreuzy, J.R., Davy, P. and Bour, O. (2002) Hydraulic properties of two-dimensional random fracture networks following power law distributions of length and aperture. *Water Resources Research*, **38**, 1276.

Dickin, R.C., Frape, S.K., Fritz, P., Leech, R.E.J. and Pearson, R. (1984) Groundwater chemistry to depths of 1000 m in low permeability granitic rocks of the Canadian Shield. *In* Pearson, R. (ed.) *Proceedings of the International Groundwater Symposium on Groundwater Resources Utilization and Contaminant Hydrogeology*, Montreal, Quebec, Canada, May 1984, Vol. II, 357–371.

Fagerlind, T. (1986) Kapaciteter i urbergsbrunnar. *Grundvatten (SGU Uppsala)*, **2**, 14–15.

Fagerlind, T. (1989) Aktuella brunnsuppgifter. *Grundvatten (SGU Uppsala)*, **1**, 6–9.

Follin, S., Årebäck, M., Stigsson, M., Isgren, F. and Jacks, G. (1999) Förstudie Tierp. Grundvattnets rörelse, kemi och långsiktiga förändringar. *SKB Rapport*, **R–99–57**, 84 pp.

Fredén, C., Gierup, J., Johansson, R., Stølen, L.K., Thunholm, B. and Wahlgren, C.H. (1999) Översiktsstudie av Värmlands län. Geologiska förutsättningar. *SKB Report*, **R–99–21**, 53pp.

Gierup, J., Johansson, R., Pamnert, M., Persson, M., Thunholm, B., Wahlgren, C.H. and Wikman, H. (1999a) Översiktsstudie av Jönköpings län; geologiska förutsättningar. *SKB Report*, **R–99–35**, 53pp.

Gierup, J., Johansson, R., Persson, M., Stølen, L.K., Thunholm, B., Wahlgren, C.H. and Wikman, H. (1999b) Översiktsstudie av Kronobergs län. Geologiska förutsättningar. *SKB Report*, **R–99–19**, 53pp.

Gierup, J., Kübler, L., Lindén, A., Ripa, M., Stephens, M., Stølen, L.K. and Thunholm, B. (1999c) Översiktsstudie av Dalarnas län (urbergsdelen). Geologiska förutsättningar. *SKB Report*, **R–99–29**, 48pp.

Gierup, J., Kübler, L., Pamnert, M., Persson, M., Thunholm, B., Wahlgren, C.H. and Wikman, H. (1999d) Översiktsstudie av Skåne län (urbergsdelen). Geologiska förutsättningar. *SKB Report*, **R–99–27**, 55pp.

Gustafson, G. (1986) Geohydrologiska förundersökningar i berg. Bakgrund–metodik–användning. *Stiftelsen Bergteknisk Forskning BeFo*, **84:1/86**, Stockholm.

Gustafson, G. (2002) Strategies for groundwater prospecting in hard rocks: a probabilistic approach. *Norges geologiske undersøkelse Bulletin*, **439**, 21–25.

Gustafson, G. and Fransson, Å. (2006) The use of the Pareto Distribution for fracture transmissivity assessment. *Hydrogeology Journal*, **14**, 15–20.

Henriksen, H. (1995) Relation between topography and borehole yield in boreholes in crystalline rocks, Sogn og Fjordane, Norway. *Ground Water*, **33**, 635–643.

Henriksen, H. (2003) The role of some regional factors in the assessment of well yields from hard-rock aquifers of Fennoscandia. *Hydrogeology Journal*, **11**, 628–645.

Henriksen, H. (2006) *The role of regional and local variables in the hydrogeology of the solid rocks of Fennoscandia*. PhD thesis, University of Bergen, Norway, 96 pp. + 6 original papers.

Henriksen, H. (2008) Late Quaternary regional geodynamics and hydraulic properties of the crystalline rocks of Fennoscandia. *Journal of Geodynamics*, **45**, 49–62.

Henriksen, H. and Braathen, A. (2006) Effects of fracture lineaments and in-situ rock stresses on groundwater flow in hard rocks: a case study from Sunnfjord, western Norway. *Hydrogeology Journal*, **14**, 444–461.

Herbert, R., Talbot, J.C. and Buckley, D.K. (1993) A study of hydraulic fracturing used on low yielding boreholes in the crystalline basement rocks of Masvingo Province, Zimbabwe. *In* Banks, S. and Banks, D. (eds.) *Hydrogeology of Hard Rocks*, Memoirs of the XXIVth Congress of the International Association of Hydrogeologists, 28th June–2nd July 1993, Ås (Oslo), Norway, pp. 698–716.

Howard, K.W.F., Hughes, M., Charlesworth, D.L. and Ngobi, G. (1992) Hydrogeologic evaluation of fracture permeability in crystalline basement aquifers of Uganda. *Hydrogeology Journal*, **1(1)**, 55–65.

Hunt, A.G. (2005) Percolation theory and the future of hydrogeology. *Hydrogeology Journal*, **13**, 202–205.

Hyyppä, J. (1984) Chemical composition of ground water in the bedrock of Finland [in Finnish with English summary]. *Nuclear Waste Commission of Finnish Power Companies Report*, **YJT–84–10**, 69 pp.

Jetel, J. and Krásný, J. (1968) Approximate aquifer characteristics in a regional hydrogeological study. *Vestnik Ústředniho Ústavu Geologického, Praha*, **43**, 459–461.

Johansson, D. (2005) *Influence of lineaments on the productivity of water supply boreholes in a hard rock terrain: a systematic approach in Pinga Oya Basin, Kandy, Sri Lanka*. MSc. thesis 2005:32, Department of Civil and Environmental Engineering, Chalmers University of Technology, Göteborg, Sweden.

Kenny, S., Wei, M. and Telmer, K. (2006) Factors controlling well yield in a fractured metamorphic bedrock aquifer, District of Highlands, Vancouver Island, British Columbia, Canada. *In* Sea to Sky Geotechnique 2006—the 59th Canadian Geotechnical Conference and the 7th Joint CGS/IAH–CNC Groundwater Specialty Conference, Vancouver, Canada, 1st–4th October 2006, pp. 1561–1568.

Kohut, A. (2006) Ground water availability and extension structures in fractured crystalline rocks, Southern Vancouver Island, British Columbia. *In* Sea to Sky Geotechnique 2006—the 59th Canadian Geotechnical Conference and the 7th Joint CGS/IAH–CNC Groundwater Specialty Conference, Vancouver, Canada, 1st–4th October 2006, pp. 1546–1551.

Knutsson, G. (2008) Hydrogeology in the Nordic countries. *Episodes*, **31(1)**, 1–7.

Krásný, J. (1975) Variation in transmissivity of crystalline rocks in Southern Bohemia. *Vestnik Ústředniho Ústavu Geologického, Praha*, **50**, 207–216.

Krásný, J. and Sharp, J.M. (2007) Hydrogeology of fractured rocks from particular fractures to regional approaches: State-of-the-art and future challenges. *In* Krásný, J. and Sharp, J.M. (eds.) *Groundwater in fractured rocks*, Selected papers from the Groundwater in Fractured Rocks International Conference, Prague, 2003. *International Association of Hydrogeologists, Selected Papers on Hydrogeology*, **9**, pp. 1–30. Taylor & Francis Group, London.

Laakso, M. (1966) The quality of water in rock wells [in Finnish with English abstract]. *Vesitalous*, **3**, 26–30.

Lahermo, P. (1970) Chemical geology of ground and surface waters in Finnish Lapland. *Bulletin de la Commission Géologique de Finlande*, **242**, 106 pp.

Lahermo, P. (1971) On the hydrogeology of the coastal region of southeastern Finland. *Geological Survey of Finland, Bulletin*, **252**, 44 pp.

Limpert, E., Stahel, W.A. and Abbt, M. (2001) Log-normal distributions across the sciences: keys and clues. *BioScience*, **51**, 341–352.

Logan, J. (1964) Estimating transmissibility from routine production tests of water wells. *Ground Water*, **2**, 35–37.

Maine Geological Survey (2007) Bedrock well data maps (scale 1:125,000). Maps showing well yield, well depth and estimated overburden thickness for drilled bedrock wells. http://www.maine.gov/doc/nrimc/mgs/pubs/online/bgwrm/bgwrm.htm.

Maine State Planning Office (2001) *Downeast salmon rivers water use management plan. Pleasant and Narraguagus Rivers, Mopang Stream*. Maine State Planning Office, July 2001, 88 pp

Mäkelä, J. (1993) Techniques for locating high-yield drilled wells in crystalline bedrock in Central Finland. *In* Banks, S. and Banks, D. (eds.) *Hydrogeology of Hard Rocks*, Memoirs of the XXIVth Congress of the International Association of Hydrogeologists, 28th June–2nd July 1993, Ås (Oslo), Norway, pp. 598–606.

Mäkelä, J. (1994) The groundwater databases of the Water and Environment District of Central Finland. *In* Suokko, T. and Soveri, J. (eds.) *Future Groundwater Resources at Risk*, Poster papers of the International Conference, Helsinki, Finland, 13–16 June 1994, *Publications of the Academy of Finland*, **4/94**, 181–189.

Maloszewski, P., Herrmann, A. and Zuber, A. (1999) Interpretation of tracer tests performed in fractured rock of the Lange Bramke basin, Germany. *Hydrogeology Journal*, **7**, 209–218.

Mather, J.D. and Sargent, F.P. (1986) Determination of the characteristics of crystalline rocks by field experiments: A review. *Philosophical Transactions of the Royal Society (London)*, **A319**, 139–156.

Misstear, B.D.R., Clark, L. and Banks, D. (2006) *Water wells and boreholes*. Wiley, Chichester, UK, 498 pp.

Mitzenmacher, M. (2004) A brief history of generative models for power law and lognormal distributions. *Internet Mathematics*, **1**, 226–251.

Moore, R.B., Schwarz, G.E., Clark, S.F., Walsh, G.J. and Degnan, J.R. (2002) Factors related to well yield in the fractured-bedrock aquifer of New Hampshire. *U.S. Geological Survey Professional Paper*, **1660**, 51 pp.

Morland, G. (1997) Petrology, lithology, bedrock structures, glaciation and sea level. Important factors for groundwater yield and composition of bedrock boreholes? *NGU rapport 1997.122* (two volumes), 401 pp.

Olofsson, B., Jacks, G., Knutsson, G. and Thunvik, R. (2001) Grundvatten i hårt berg: en analys av kunskapsläget. Chapter 4 in *Kunskapsläget på kärnavfallsområdet 2001* (Nuclear water, state of the art report 2001), *KASAM: Statens råd för kärnavfallsfrågor (Swedish National Council for Nuclear Waste) Report*, **SOU 2001:35**, pp. 113–189.

Rebouças, A.C. (1999) Selected case studies: northeastern Brazil. *In* Lloyd, J.W. (ed.) *Water resources of hard rock aquifers in arid and semi-arid zones*. UNESCO Studies and Reports in Hydrology, **58**, pp. 275–284.

Renard, P. and de Marsily, G. (1997) Calculating equivalent permeability: a review. *Advances in Water Research*, **20**, 253–278.

Renard, P., Le Loc'h, G., Ledoux, E., de Marsily, G. and Mackay, R. (2000) A fast algorithm for the estimation of the equivalent hydraulic conductivity of heterogeneous media. *Water Resources Research*, **36**, 3567–3580.

Rohr-Torp, E. (1994) Present uplift rates and groundwater potential in Norwegian hard rocks. *NGU Bulletin*, **426**, 47–52.

Rönkä, E. (1983) Drilled wells and groundwater in the Precambrian crystalline bedrock of Finland. *Publications of the Water Research Institute*, **52**, National Board of Waters, Helsinki, Finland, 57 pp.

Rönkä, E. (1993) Increased depth of drilled wells benefit or drawback?

In Banks, S. and Banks, D. (eds.) *Hydrogeology of Hard Rocks*, Memoirs of the XXIVth Congress of the International Association of Hydrogeologists, 28th June–2nd July 1993, Ås (Oslo), Norway, pp. 772–779.

Sander, P. (1997) Water-well siting in hard-rock areas: identifying promising targets using a probabilistic approach. *Hydrogeology Journal*, **5**, 32–43.

Sander, P. (2007) Lineaments in groundwater exploration: a review of applications and limitations. *Hydrogeology Journal*, **15**, 71–74.

Sigmond, E.M.O. (1992) *Bedrock map of Norway and adjacent ocean areas. Scale 1:3 million*. Norges geologiske undersøkelse, Trondheim.

SKB (2006) Granites of the TIB, Preliminary site description. Laxemar subarea—version 1.2. *SKB Report*, **R–06–10**.

Snow, D.T. (1969) Anisotropic permeability of fractured media. *Water Resources Research*, **5**, 1273–1289.

Stober, I. and Bucher, K. (2007) Hydraulic properties of the crystalline basement. *Hydrogeology Journal*, **15**, 213–224.

Struckmeier, W.F. (1993) Hydrogeological mapping in hard rock terrains. *In* Banks, S. and Banks, D. (eds.) *Hydrogeology of Hard Rocks*, Memoirs of the XXIVth Congress of the International Association of Hydrogeologists, 28th June–2nd July 1993, Ås (Oslo), Norway, pp. 1013–1020.

Theis, C.V. (1935) The relation between the lowering of the piezometric surface and the rate and duration of discharge of a well using ground-water storage. *Transactions of the American Geophysical Union*, **16**, 519–524.

Walsh, J.B. (1981) Effect of pore pressure and confining pressure on fracture permeability. *International Journal of Rock Mechanics and Mining Science & Geomechanics Abstracts,* **18**, 429–435.

Wladis, D. and Gustafson, G. (1999) Regional characterisation of hydraulic properties of rock using air-lift data. *Hydrogeology Journal*, **7**, 168–179.

Wright, E.P. (editor) (1989) The basement aquifer research project 1984–1989: final report to the Overseas Development Administration. *British Geological Survey Report No*. **WD/89/15**.

Zoback, M.L. (1992) First and second-order patterns of stress in the lithosphere: The World Stress Map Project. *Journal of Geophysical Research*, **97(B8)**, 11703–11728.

RESEARCH ARTICLE

Geochemistry and palaeogeographical setting of greenstone units on Frosta peninsula, Nord-Trøndelag, Central Norwegian Caledonides

Stephen J. Lippard[1,*] & David Roberts[2]

[1] *Institutt for geologi og bergteknikk, NTNU, 7491 Trondheim, Norway.*
[2] *Geological Survey of Norway, P.O.Box 6315 Sluppen, 7491 Trondheim, Norway.*
** stephen.lippard@ntnu.no*

Volcanic and high-level intrusive rocks of the Støren Nappe exposed on the west coast of Frosta peninsula occur in two, distinct, magmatic units; the bimodal *Fånes complex* and the metabasaltic *Granheim greenstone*. North of Småland, the former unit is stratigraphically overlain by a conglomerate (Helsingplassen conglomerate) comprising clasts of Fånes rocks. Felsite clasts in this conglomerate are indistinguishable petrographically and geochemically from felsites occurring in thick sheets in the Fånes complex. South of Småland, the pillowed Granheim greenstone is unconformably overlain by the Huva conglomerate, composed largely of clasts derived from the greenstone, and in turn overlain by limestones and calcareous phyllites (Risset limestone) of Katian (Late Caradocian) age. The Granheim-Huva-Risset succession can be followed westwards onto the island of Tautra.

Geochemically, the greenstones in the Fånes and Granheim units, although both showing broadly oceanic basalt compositions, are distinctly different. The greenstones of the Fånes complex have LREE-depleted, chondrite-normalised patterns, whereas the Granheim greenstones have relatively flat REE patterns and generally higher REE contents. Both are depleted in Ta, falling in the arc basalt field on the Th–Hf–Ta diagram, but have distinct MORB-normalised Ta/La ratios. This would imply that extrusion of the original basaltic flows is likely to have occurred in a subduction-related, arc environment. The felsites in the Fånes complex have highly evolved rhyolitic compositions and plot across the boundary between ocean-ridge and volcanic-arc granites on trace element discrimination diagrams. They have LREE-enriched, chondrite-normalised patterns with marked negative Eu anomalies that resemble the REE pattern in the Fagervika trondhjemite from the Bymarka ophiolite. By analogy with Fagervika, we suggest that the bimodal Fånes complex rocks were generated in a primitive island-arc setting on recently formed oceanic crust. Zircons from a felsite sheet have yielded a U–Pb age of 488 ± 5 Ma (see accompanying paper). This Tremadocian age for the Fånes complex is similar to ages reported from fragmented ophiolites and felsic rocks of primitive arc affinity in other parts of the Trondheim Region.

Lippard, S.J. and Roberts, D. (2010) Geochemistry and palaeogeographical setting of greenstone units on Frosta peninsula, Nord-Trøndelag, Central Norwegian Caledonides. *Norges geologiske undersøkelse Bulletin*, **450**, 48–59.

Introduction

In the Caledonides of central Norway, assemblages of mostly mafic, metavolcanic to high-level intrusive rocks occur widely in the Upper Allochthon in a series of nappes or thrust sheets known collectively as the Köli Nappes. Geochemical studies have shown that many of these magmatic units, traditionally called 'greenstones' in Scandinavia, are tholeiitic metabasalts, in places with associated, subordinate felsic rock types ranging from plagiogranite sheets and dykes to rhyodacite flows (Loeschke 1976, Halls et al. 1977, Lutro 1979, Grenne and Roberts 1980, Grenne and Lagerblad 1985, Roberts and Tucker 1998, Roberts and Stephens 2000, Roberts et al. 2002). Furthermore, some of the magmatic assemblages include sheeted mafic dykes, gabbros and even ultramafic cumulates, and are representative of fragmented and dismembered ophiolites (Gale and Roberts 1974, Grenne et al. 1980, Prestvik 1980, Furnes et al. 1985, 1988, Heim et al. 1987, Slagstad 1998, 2003, Roberts et al. 2002, Nilsson et al. 2005), some of which involve components of primitive arcs.

Initial deformation and metamorphism of these ophiolite fragments or immature arc rocks is generally tied to their obduction in Early Ordovician time prior to uplift, erosion and accumulation of Mid Arenig and younger volcanosedimentary successions in arc-related marginal basins (Roberts et al. 1984, 2002, Grenne and Lagerblad 1985). Application of U–Pb isotopic dating techniques, targeting zircons in felsic rocks, has greatly aided our understanding of the actual ages of these dismembered ophiolites or greenstone units. In the Trondheim Region of central Norway, the few, mafic to bimodal, magmatic assemblages so far dated fall in the age range from Late Cambrian (Furongian) to earliest Ordovician (Tremadocian), circa 495 to 480 Ma (Dunning 1987, Bjerkgård and Bjørlykke 1994, Roberts and Tucker 1998, Roberts et al. 2002).

Several other greenstone complexes in the Köli Nappes of this region have been studied geochemically, e.g., on Ytterøya, Inderøya and near Levanger and Steinkjer, but the results of these studies have yet to be published. Comparable magmatic units occur on the Frosta peninsula, in central Trondheimsfjord, part of which was the subject of an informal NGU report (Roberts 1982). In this contribution, we document the results of geological and geochemical studies of these rocks on Frosta. In a companion short paper, U–Pb zircon age data are presented from a felsic body within a greenstone complex, and from cobbles of felsite in a stratigraphically overlying conglomerate (Gromet and Roberts 2010).

Geological setting

The rocks of the Frosta peninsula comprise mostly middle greenschist-facies sedimentary successions of the Støren Nappe, one of several, oceanic, Köli Nappes in this part of the Norwegian Caledonides (Figure 1, inset map). The Støren Nappe is perhaps better known from the Hovin-Hølonda area southwest of Trondheim where the lower parts of the sedimentary succession contain a diverse fauna of Mid Arenig to Llanvirn age and largely Laurentian affinity (Bergström 1979, 1997, Bruton and Bockelie 1980, Ryan et al. 1980, Spjeldnæs 1985, Neuman and Bruton 1989). Higher up in the succession, faunas of Caradoc–Ashgill age are typically more cosmopolitan in character (Neuman et al. 1997), attesting to a diminished provinciality as the Iapetus Ocean contracted through Ordovician time.

In the Frosta area, poorly preserved body fossils—fragments of gastropods, stromatoporoids and corals—had been recorded from a limestone on Tautra (Spjeldnæs 1985), indicative of a Late Caradocian (Early Katian) age for that formation. More recently, pelagic, Early-Mid Katian conodonts have been recovered from the correlative Risset limestone on the mainland of the Frosta peninsula (Tolmacheva and Roberts 2007). Apart from these occurrences, trace fossil assemblages, notably the *Nereites* ichnocoenosis, have been recorded from different parts of the peninsula (Roberts 1969, 1984, Uchman et al. 2005). This particular ichnofacies is indicative of basin-plain and outer fan to fan-fringe sediments, and corroborates the interpretation of depositional environments made earlier for these dominantly turbiditic, siliciclastic rocks with interspersed submarine-channel and fan conglomerates (Roberts 1969, Pedersen 1981, Strømmen 1983). Sedimentological studies have indicated a bipolar provenance for the sediments, with volcanic arc and shelf material feeding into the elongate basin from a northwestern source (present-day coordinates) whereas largely continent–derived debris entered from the southeast (Pedersen 1981, Roberts et al. 1984).

Geology of the Småland area

Two different successions, each consisting of an oceanic igneous basement and a sedimentary cover sequence, occur, respectively, to the north and to the south of Småland on the west coast of Frosta peninsula (Figure 1). To the north of Småland, a bimodal sequence consisting mainly of mafic volcanites (greenstones) and shallow felsic intrusions (felsites) occurs in the Breivika area and extends inland and northwards to Fånesbukta (Figure 1). Directly northeast of Breivika, the rocks of this bimodal unit are in inferred tectonic contact with a thin wedge-shaped slice of higher grade, garnetiferous mica schists and minor amphibolite, quartzite and marble (Figure 1), but reappear just to the northeast and extend up to Fånes. For convenience of description we refer to this bimodal unit as the *Fånes complex*, with occasional reference to the mafic rocks as the Fånes greenstones. In the Breivika area, the bimodal Fånes rocks dip to the northeast but along strike they pass through the vertical to eventually dip eastwards southeast of Fånes. To the south and southeast, the Fånes

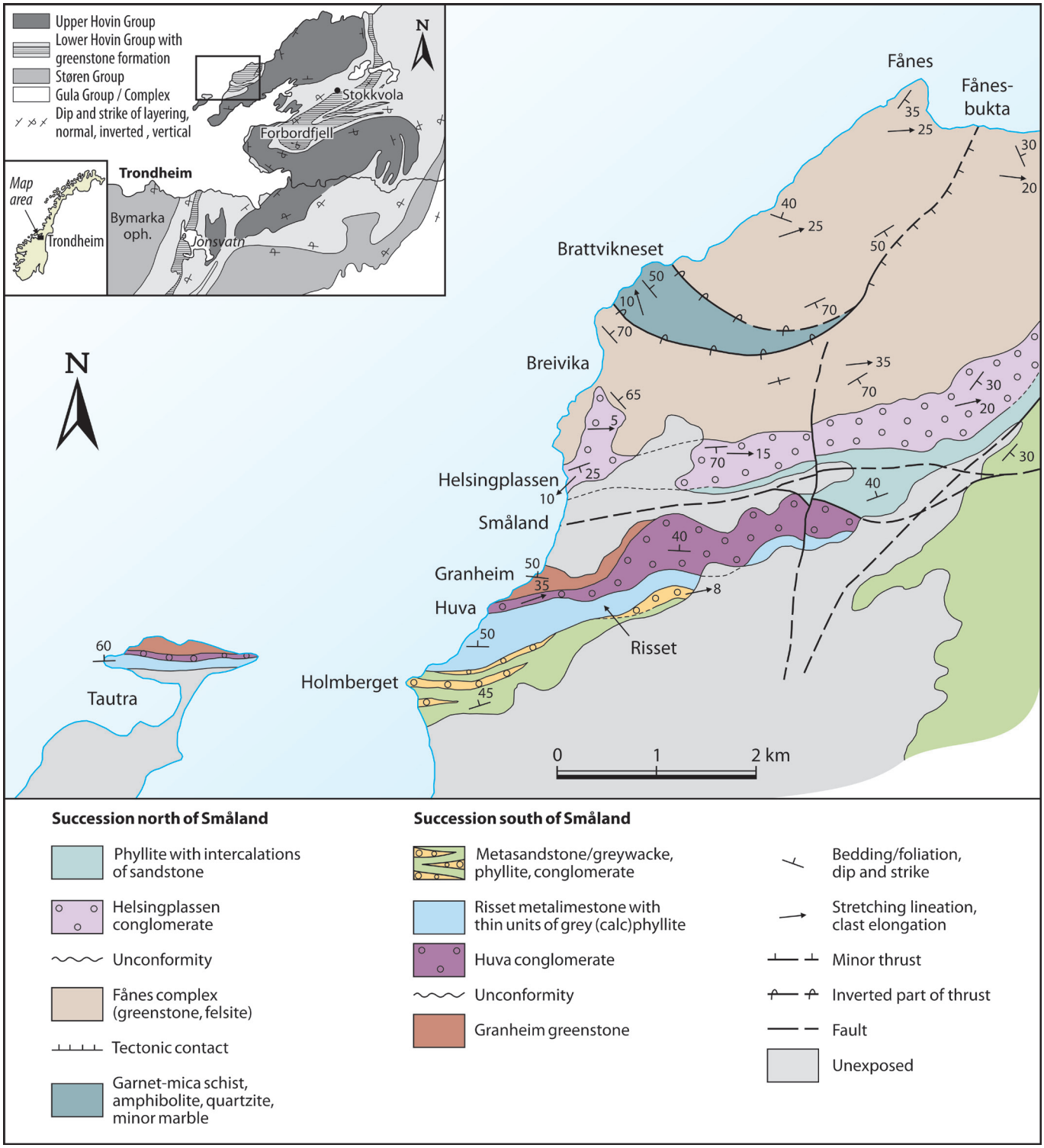

Figure 1. Simplified geological map of the southwestern part of Frosta peninsula and Tautra island.

greenstones are overlain unconformably by a polymict conglomerate containing abundant pebbles mainly of felsite and greenstone in a green-grey, silty phyllite matrix. This conglomerate is here named the *Helsingplassen conglomerate* from the locality on the coast where it is best exposed. The conglomerate is strongly deformed with highly elongate stretched pebbles up to 0.5 m in length, and with long axes trending ENE–WSW to NE–SW. Some of the clasts show an internal weak foliation at a high angle to the clast elongation, a fabric evidently acquired before sedimentation. Inland, the Helsingplassen conglomerate contains layers of green-grey sandstone with sporadic pebbles and is overlain by a thinly bedded succession of phyllite and metasandstone.

To the south of Småland, a c. 150–200 m-thick succession of

metabasaltic greenstones, including pillow lavas, crops out along the coast at Granheim, and a little farther south is in contact with a deformed conglomerate—the *Huva conglomerate* of Strømmen (1983)—containing pebbles mainly of greenstone with subordinate felsite. We refer to these metabasaltic rocks as the *Granheim greenstone*. Stretched pebbles in the Huva conglomerate are up to 20 cm in length and clast long-axis lineations trend ENE–WSW. The Granheim greenstone succession dips generally to the north at c. 50° such that the conglomerate lies structurally beneath. In its coastal exposure, the Huva conglomerate is no more than 20 m thick and displays a southward fining of clast material. To the south, it is in contact with a c. 250 m-thick sequence of both pure and impure metalimestones (the Risset limestone of Tolmacheva and Roberts 2007) with thin intercalations of black phyllite. The limestone formation passes structurally down section into either a polymict conglomerate or a metagreywacke and phyllite succession. The conglomerate contains clasts mainly of metaigneous rocks and limestone, with several large, subangular, limestone clasts up to 40 cm across. Other conglomerates are exposed on the coast at Holmberget (Figure 1). These turbiditic sandstones and submarine-fan conglomerates are generally assigned to the Upper Hovin Group (Vogt 1945), locally called the Ekne Group (Kiær 1932), whereas the Granheim, Huva and Risset formations are considered to be part of the Lower Hovin Group (Roberts 1985).

The structurally highest part of the succession south of Småland, comprising the massive and pillowed Granheim greenstone, the Huva conglomerate and the Risset limestone, is also exposed on the northern part of the island of Tautra to the west (Figure 1).

Stratigraphic way-up of the successions

In coastal parts of the map area between Holmberget and beyond Brattvikneset, both the Granheim and the Fånes magmatic units, and their sedimentary cover successions, dip to the north but appear to be structurally inverted. One of the aims of this paper is to show that the magmatic units and the clasts of such rocks in the adjacent conglomerates are petrographically and geochemically similar. In addition, pillow lava shapes both at Granheim (Figure 2) and on Tautra show that the volcanites young to the south and are thus stratigraphically and structurally inverted. This is contrary to Strømmen (1983) who interpreted the volcano-sedimentary succession between Småland and Holmberget as right way up and younging to the north, putting the Granheim greenstone at the stratigraphic top of the sequence. She based this interpretation on alleged sedimentary structures in the succession south of the Huva conglomerate, such as water-escape features and inferred channelling; however, re-examination suggests a tectonic rather than sedimentary origin for some of these structures. In this same part of the area, the abundant large clasts of limestone in the conglomerate structurally below the Risset limestone also points in favour of a structural inversion of the succession.

On Tautra, some of the shelly fossils have been reported to be in growth position (Spjeldnes 1983), suggesting that the succession youngs to the north, but again the evidence for this is not convincing. In our view, the compositional similarity between the magmatic rocks and the pebbles in the conglomerates is strong evidence that the latter are derived by erosion of the former, and that the conglomerates, at Huva and Helsingplassen, unconformably overlie the two magmatic complexes. This agrees with general relationships in other parts of the Trøndelag region where polymict or greenstone conglomerates (e.g., Venna, Stokkvola, Steinkjer and Lille Fundsjø conglomerates) directly overlie metabasaltic or bimodal magmatic successions as, for example, at Forbordfjell (Figure 1, inset), c. 10 km southeast of Frosta (Roberts 1975, Grenne and Roberts 1980).

Petrography of the igneous rocks

The greenstones are massive to foliated mafic rocks (in the latter case traditionally called greenschists) consisting largely of microcrystalline albitic plagioclase, stilpnomelane, actinolite, epidote and biotite with secondary quartz, carbonate, titanite and iron oxides. The felsites are also massive to foliated rocks and range from fine grained and commonly porphyritic to medium grained with granoblastic textures. The coarser grained rocks are characterised by myrmekite intergrowths of quartz and feldspar. Quartz occurs mostly in irregular masses comprising several grains with undulose extinction and serrated grain boundaries. Albite phenocrysts are commonly subhedral, generally occurring in clusters of grains, and variably altered (sericitised). Altered (chloritised) biotites are associated with the feldspars. The matrix is mostly granular quartz with epidote, generally in clusters of small grains. Titanite and secondary iron oxides occur in irregular patches and as veins. The pebbles in the Helsingplassen conglomerate show the same variety of textures as the in situ felsites, but are generally slightly more altered and veined, and with secondary quartz and calcite.

Geochemistry

Analytical procedures

Major and trace elements of the greenstone and felsite samples were measured by XRF on fused glass beads and pressed powder pellets, respectively, at the Geological Survey of Norway, Trondheim, using common international standards for calibration. Six greenstone samples and three greenstone pebbles were analysed by Instrumental Neutron Activation for rare earth elements (REE) and the elements Hf, Ta, Th and U at the Department of Physico-Chemical Geology, University of Leuven, Bel-

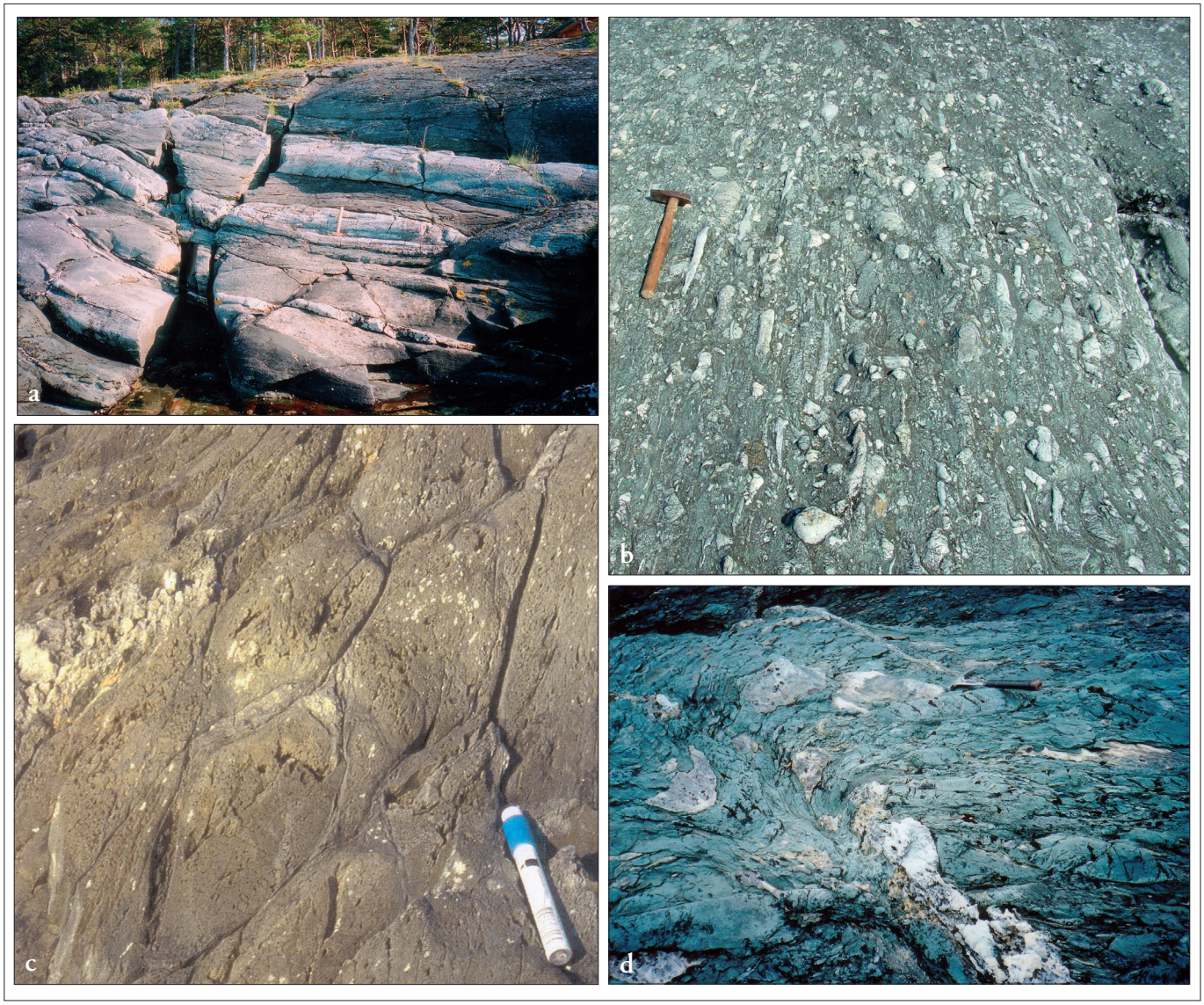

Figure 2. Field photographs. (a) Fånes complex. Concordant felsite layers (light coloured) in greenstone. The hammer is 35 cm long. Coastal exposure, Breivika. (b) Helsingplassen conglomerate with abundant elongate light-coloured felsite clasts. The darker clasts are mostly greenstone with minor gabbro. The hammer is 40 cm long. Coastal exposure at Helsingplassen. (c) Pillow lavas from the Granheim greenstones just north of the contact with the Huva conglomerate. The lavas dip steeply to the north (left), but the pillow shapes, with cuspate bases and rounded tops, show younging to the south (right). The marker pen is 15 cm long. (d) Huva conglomerate. Elongate greenstone clasts, some with transverse fractures. The light areas are folded quartz-calcite veins. The hammer is 30 cm long. Coastal exposure at Huva.

gium (analyst Jan Hertogen). REE data plus Hf, Ta, Th and U analyses were also acquired for the eight samples of felsic rocks, by laser ablation ICP–MS analysis at the Geological Survey of Norway; and at the same time three additional samples of greenstone were analysed for the same elements for comparison with the other analyses.

Major and trace element geochemistry

Greenstones

In a preliminary, unpublished geochemical study of 31 greenstones from the area depicted in Figure 1, Roberts (1982) referred to these mafic volcanic rocks collectively as the 'Frosta greenstones'. Eleven of these samples were from the Granheim greenstone and 5 of pebbles taken from the Huva conglomerate. The remaining 15 samples were taken north of Småland from the Fånes complex. The full analytical data for these 31 samples are available as an Excel file, upon request. Strømmen (1983) also reported 9 major and trace element analyses from the greenstones south of Småland and 3 analyses of greenstone clasts from the Huva conglomerate.

The mafic volcanic rocks are mostly metabasalts, possibly extending into the field of more evolved basaltic andesites, and show a range of SiO_2 contents from 45.92 to 54.35%. Both Strømmen and Roberts concluded that the 'Frosta greenstones' are predominantly tholeiitic ocean-floor basalts, based on trace element discrimination diagrams, with one or two samples showing trends toward island-arc and within-plate composi-

Table 1. Major and trace element analyses of greenstones and felsites. Greenstones: FR1 and FR10 from the Fånes complex, FR26 from the Granheim greenstone. Felsites: F5–F7 in situ; F8–F12 clasts from the Helsingplassen conglomerate.

Sample no	FR1	FR10	FR26	F5	F6	F7	F8	F9	F10	F11	F12
Easting	589650	588050	584050	5845500	584510	584510	584250	584250	584250	584250	584250
Northing	7056000	7057100	7052350	7054150	7053950	7053950	7053600	7053600	7053600	7053600	7053600
SiO_2	48.74	44.1	47.5	75.03	78.87	77.79	76.81	76.35	77.16	77.05	78.57
Al_2O_3	15.1	14.8	13.7	13.36	12.22	12.04	11.53	11.65	10.92	10.81	11.96
Fe_2O_3	13.3	13.1	12.7	2.4	1.26	1.73	2.14	1.27	1.72	1.68	0.76
TiO_2	1.87	1.4	1.81	0.34	0.15	0.19	0.2	0.15	0.15	0.14	0.15
MgO	6.23	5.21	6.99	0.47	0.19	0.12	0.12	0.09	0.24	0.22	<0.01
CaO	8.58	11.4	9.13	1.37	0.38	1.33	3.46	2.85	3.27	3.17	1.39
Na_2O	3.88	3.58	3.5	5.96	6.38	5.97	4.52	5.46	4.64	4.72	6.01
K_2O	0.08	0.08	0.11	0.24	0.09	0.05	0.08	0.07	0.06	0.06	0.06
MnO	0.12	0.17	0.18	0.04	0.02	0.02	0.02	0.02	0.03	0.03	<0.01
P_2O_5	0.15	0.12	0.19	0.06	0.02	0.02	0.03	0.02	0.02	0.03	0.02
LOI	2.22	4.17	2.72	0.49	0.35	0.33	0.62	1.24	1.23	1.22	0.32
Total	100.27	98.13	98.53	99.76	99.93	99.59	99.53	99.17	99.44	99.13	99.24
Y	41	23	28	186	141	152	161	146	126	126	258
Zr	103	56	79	50	20	59	55	58	44	42	37
Nb	1.4	0.8	2.7	4.3	3	7.1	4.6	4	3.9	3.8	4.6
La	5.6	2.5	5.4	16	14	18	11	21	14	13	15
Ce	16	8.1	15	36	33	50	32	55	39	35	45
Pr	2.5	1.4	2.2	4.3	3.1	5.9	4.1	5.7	4.3	3.8	4.6
Nd	15	8.9	12	20	13	27	20	26	19	17	20
Sm	4.6	3.3	4.1	5.3	2.9	7.5	6.2	6.8	5.5	4.7	5
Eu	1.8	1.2	1.6	0.9	0.5	1	1.1	1.1	0.9	0.8	0.9
Gd	5.3	3.7	4.6	5.2	2.7	7.3	6.5	6.6	5.2	4.6	4.4
Tb	0.9	0.8	0.9	0.9	0.5	1.3	1.2	1.2	1	0.9	0.8
Dy	6.3	4.8	5.6	6.5	3.1	9.2	8	8	6.5	6.1	5.2
Ho	1.5	0.9	1.1	1.6	0.8	2.1	1.9	2	1.5	1.5	1.3
Er	4.1	2.7	3.2	5	2.1	6.3	5.8	5.6	4.5	4.5	4.1
Tm	0.7	0.4	0.5	0.8	0.4	1	0.9	0.9	0.8	0.8	0.7
Yb	4	2.7	2.9	5.5	2.4	6.7	6.1	5.7	5.1	5.2	4.4
Lu	0.56	0.4	0.43	0.86	0.38	0.98	0.87	0.81	0.72	0.67	0.65
Hf	2.5	1.9	2.5	5.3	4.3	4.9	4.7	4.4	3.7	3.8	6.4
Ta	<0.1	<0.1	0.2	0.3	0.3	0.4	0.3	0.4	0.3	0.3	0.4
Tb	0.3	0.3	0.5	3.7	1.8	2.8	2.5	3	2.3	2.1	3.4
U	<0.3	<0.3	0.3	1.3	1	1.4	1.2	1.4	1.1	1.1	1.6

Coordinates apply to UTM Zone 32, WGS84.

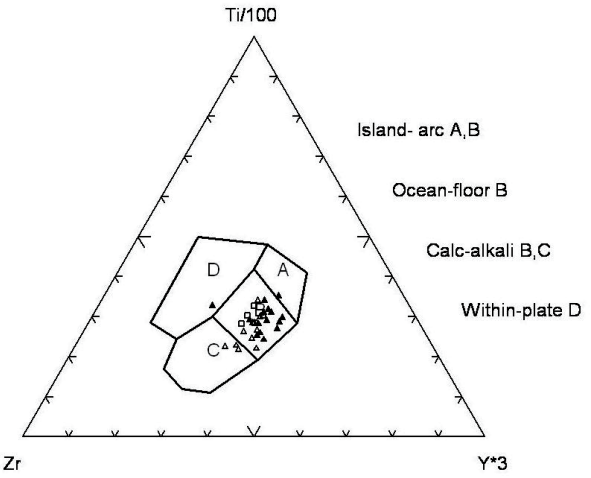

Figure 3. Ti-Zr-Y plot (Pearce and Cann 1973). Fånes greenstones: filled triangles; Granheim greenstones: open triangles; clasts in the Huva conglomerate: open squares.

tions (Figure 3), and Roberts (1982) compared them to the geochemically similar middle member of the Forbordfjell greenstones (Grenne and Roberts 1980). It was also noted that the greenstone pebbles in the Huva conglomerate are compositionally similar to the structurally overlying (Granheim) greenstone. In our present study, we have also reanalysed three of the original greenstones sampled by Roberts (1982), FR1, FR10 and FR26, with the addition of rare earth element analyses (Table 1).

Felsites

New analyses of 3 felsite samples from the Fånes complex and 5 samples of clasts extracted from the Helsingplassen conglomerate are incorporated in this study (Table 2). The felsites have high SiO_2 contents (the 3 in situ samples, F5–F7, include those with the highest (78.87%) and lowest (75.03%) values), relatively low Al_2O_3 and Fe_2O_3 and very low MgO contents. Variable CaO is partly due to secondary calcite veining, especially notable in the pebbles from the conglomerate (F8–F12). Geochemically, the felsites have typical trondhjemitic compositions, plotting in the Ab corner of the normative Ab–An–Or triangular plot (Barker 1979). Normative 'Q' is about 40% and normative 'Ab' about 50%. On an alkali-silica volcanic rock classification diagram they plot at the high SiO_2 end of the rhyolite field (Le Bas et al. 1986). However, it is possible that the silica and alkali contents have been altered by low-grade metamorphism and metasomatism. On stable trace-element, tectonic environment, discrimination diagrams they plot across the boundary between the ocean ridge granite (ORG) and volcanic arc granite (VAG) fields (Figure 4).

Table 2. Rare earth elements and Hf, Ta, Th and U contents (ppm) of greenstones from the Fånes complex (FR3, FR8, FR 13), the Granheim greenstones (FR16, FR20, FR21) and clasts from the Huva conglomerate (PEB2, PEB4, PEB5).

Sample	FR-3	FR-8	FR-13	FR-16	FR-20	FR21	FR/PEB-2	FR/PEB-4	FR/PEB-5
Easting	589250	588250	586250	584300	584150	584150	584000	584000	584000
Northing	7056050	7056200	7054700	7052600	7052550	7052550	7052350	7052350	7052350
La	4.8	2.24	2.8	4.5	6.2	5.9	6.9	7.5	7.7
Ce	15.8	7.6	8.7	13.3	18.2	16.7	18.7	20.3	19.8
Nd	14.3	8.8	8.5	10.6	13.6	12.8	15.5	15.8	14.6
Sm	4.71	3.28	3.05	3.32	3.96	3.88	4.66	4.5	4.49
Eu	1.65	1.32	1.25	1.13	1.38	1.24	1.71	1.65	1.85
Gd						4.7	5.8		
Tb	1.18	0.88	0.84	0.75	1.04	0.87	1.05	1	1.02
Yb	4.82	3.36	3.2	3.02	4	3.59	3.46	3.19	3.1
Lu	0.81	0.58	0.43	0.52	0.55	0.63	0.56	0.51	0.42
Hf	3.27	2	1.96	2.84	3.41	3.36	2.95	0.3	0.25
Ta	0.15	0.04	0.06	0.21	0.24	0.22	0.25	0.3	0.25
Th	0.6	0.39	<0.2	0.6	0.87	0.75	0.39	0.76	0.57
U	0.17	<0.15	<0.15	0.21	0.2	0.2	0.34	0.39	0.22

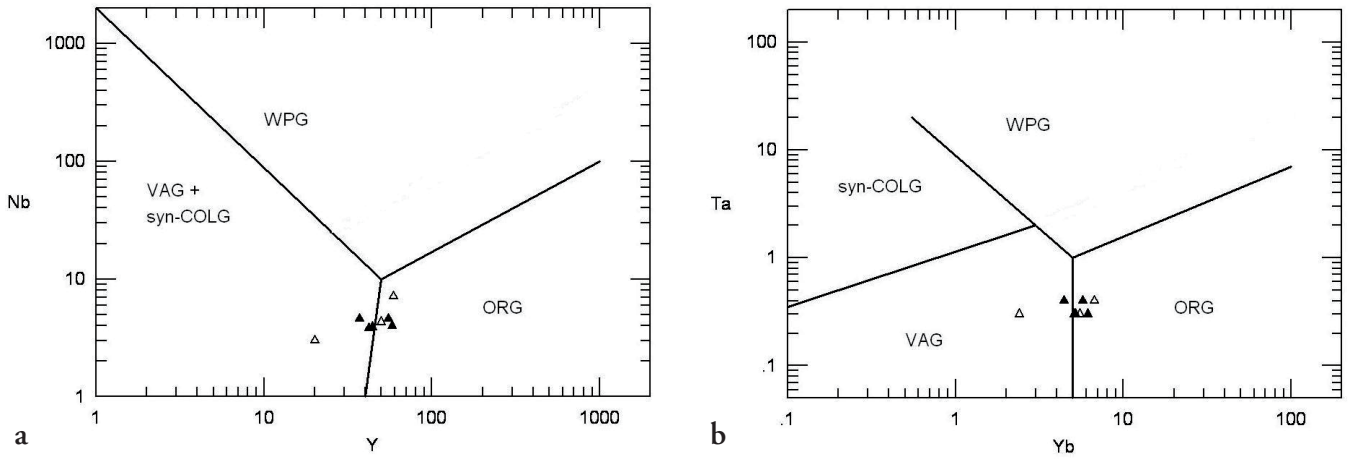

Figure 4. (a) Nb–Y and (b) Ta–Yb tectonic environment discrimination diagrams for granitic rocks (Pearce et al. 1984). Open symbols – in situ felsites, closed symbols – conglomerate clasts. ORG, Ocean ridge granite, VAG, volcanic arc granite, WPG, within-plate granite, syn-COLG, syn-collision granite.

Rare earth element geochemistry

Previously unpublished REE and Hf, Ta, Th and U analyses of six samples of greenstones (3 from the Fånes and 3 from the Granheim) and three samples of greenstone pebbles from the Huva conglomerate are shown in Table 2. On chondrite-normalised plots the greenstones have flat to light rare earth (LREE) depleted patterns (Figure 5). The Fånes complex greenstones, some of which are interbedded with the felsites, have mainly LREE-depleted patterns, whereas the Granheim greenstones have flat patterns, as do the pebbles from the overlying Huva conglomerate. According to Sun and McDonough (1989), depleted and flat REE patterns correspond broadly to N-type and E-type MORBs, respectively.

Rare earth element and Hf, Ta, Th and U analyses of the 8 felsites (3 in situ samples from the Fånes complex and 5 pebbles from the Helsingplassen conglomerate) are shown in Table 1. They have similar chondrite-normalised REE patterns with enrichment in the LREEs and marked negative Eu anomalies (Figure 6). The heavy rare earth elements (HREE) show a flat pattern. Compared to the Fånes greenstones they are enriched in the REEs, except for Eu, most markedly in the LREEs and less so in the HREEs. One of the in situ felsite samples (F6) has markedly lower contents of the intermediate and heavy REEs than the others, although the general pattern is similar; the reason for this disparity, however, is not clear.

Th, Hf and Ta analytical data

Both the Fånes and the Granheim greenstones have moderate (Granheim) to large (Fånes), negative Ta anomalies which point towards a subduction-related arc setting (Pearce 1982).

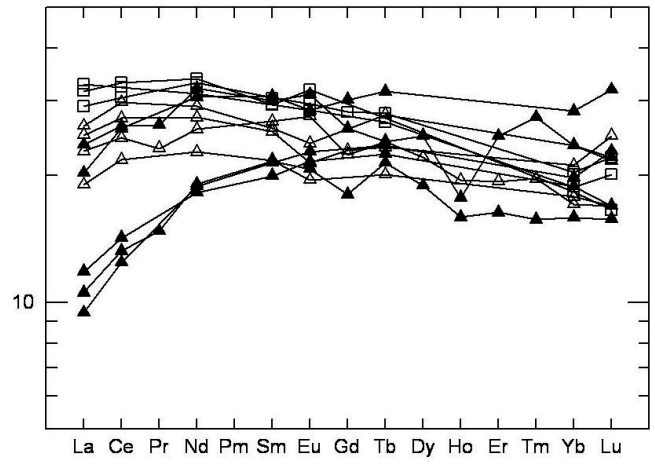

Figure 5. Chondrite-normalised REE plot of the analysed greenstone samples (normalisation values after Sun and McDonough 1989). Fånes greenstones: filled triangles; Granheim greenstones: open triangles; clasts in the Huva conglomerate: open squares.

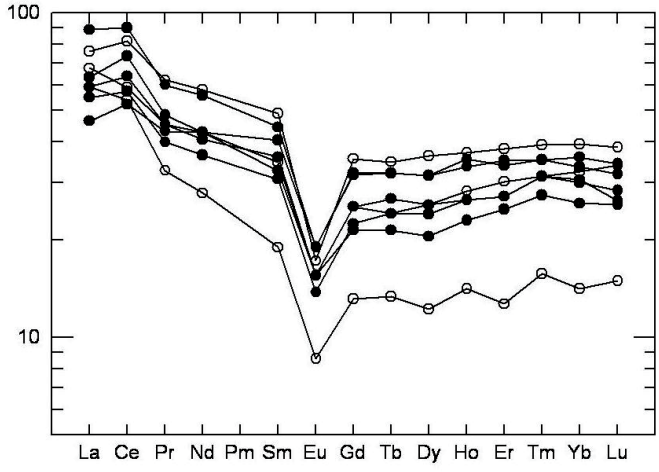

Figure 6. Chondrite-normalised REE plot of the analysed felsites (normalisation values after Sun and McDonough 1989). In situ felsites (open symbols) and clasts from the Helsingplassen conglomerate (closed symbols).

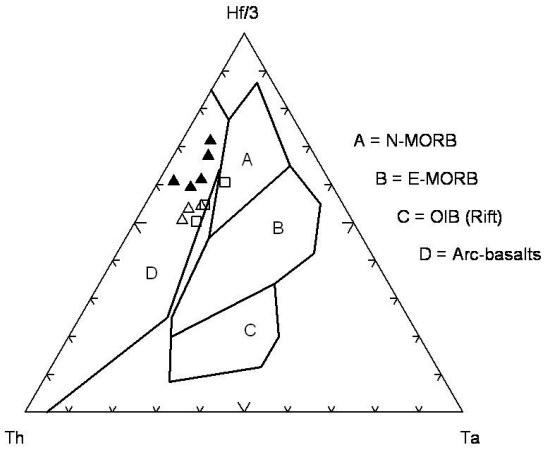

Figure 7. Th–Hf–Ta plot (Wood 1980). Fånes greenstones: filled triangles; Granheim greenstones: open triangles; clasts in the Huva conglomerate: open squares

Furthermore, the Fånes greenstones have MORB-normalised Ta/La ratios of <0.6 (range 0.34–0.59), whereas such ratios for the Granheim greenstones are >0.7 (range 0.70–0.88). On the Th–Hf–Ta plot of Wood (1980), the two greenstones plot separately, but both are located in the field of arc-related basalts (Figure 7). There is, thus, good reason, in this particular case, to dismiss the interpretation of Sun and McDonough (1989) which is based solely on REE patterns.

Discussion

Presentation of the geochemical data has pointed to a measure of uncertainty or ambiguity in interpreting the extrusive setting of these mafic volcanites. As noted above, from REE patterns alone, LREE depletion in the greenstones of the Fånes complex would traditionally favour an N-MORB origin (Sun and McDonough 1989), whereas the flat pattern of the Granheim greenstones might signify their generation as E-type MORB lavas. The felsite component of the Fånes complex, on the other hand, points to a transitional ocean floor to island arc affinity. On a Ti–Zr–Y plot (Figure 3) (Pearce and Cann 1973), both greenstones fall in the ocean floor field, yet in the Th–Hf–Ta diagram of Wood (1980) (Figure 6) they are clearly located in the field for island-arc tholeiites. As the Fånes complex is bimodal, with the felsites indicating arc involvement, then a subduction-related, primitive arc setting appears to be more likely than a non-arc scenario, moreso as the greenstones show large, negative Ta anomalies.

In comparing our geochemical data with those of other extrusive magmatic complexes in the central Trøndelag region, it is natural to look first at the Forbordfjell greenstone formation just 15 km to the southeast of Frosta (Figure 1, inset map), which has been divided into 3 members (Grenne and Roberts 1980). Trace element discrimination diagrams and chrondrite-normalised REE plots show that the middle member consists of LREE-depleted, ocean floor tholeiitic basalts, whereas the upper and lower members show flat to slightly LREE-enriched patterns and are more akin to within-plate basalts. The middle member thus shows similarities in the REE pattern to our Fånes greenstone. The Forbordfjell metabasalts have not yet been dated, but an Early to Mid Ordovician age has been inferred (Roberts 1975).

The Jonsvatn greenstones, southeast of Trondheim (Figure 1, inset), have similar compositions with both LREE-depleted ocean floor and slightly LREE-enriched 'transitional within-plate' greenstone types (Grenne and Roberts 1980). In the Trondheim area, the mafic extrusive component of the Bymarka ophiolite fragment (Slagstad 1998) comprises greenstones with mainly ocean-floor basalt affinities, as do the Løkken and Resfjell ophiolites farther to the southwest (Grenne 1986, 1989, Heim et al. 1987).

The Bymarka ophiolite fragment (Slagstad 1998) contains three distinct types of felsic rocks (Slagstad 2003). Geochemically, the Fånes felsites most resemble the Fagervika trondhjemite, inasmuch as they have similar REE patterns (Figure 8), although the latter are slightly more enriched in the LREEs. The Fagervika trondhjemite forms a large, late, cross-cutting body, interpreted by Slagstad (2003) as having been generated in an island-arc setting on recently formed oceanic crust. It is noteworthy that these rocks, like the Fånes felsites, plot on the boundary between volcanic arc and ocean floor granites on trace-element discrimination diagrams. A metarhyolite from the upper volcanic member of the Løkken ophiolite (Grenne 1989) also has a similar rare earth pattern to the Fånes felsites and is interpreted as having formed in a transitional ocean floor to island-arc environment (Grenne 1989).

The geochronology reported in Gromet and Roberts (2010) has shown that one of the felsite sheets in the Fånes complex

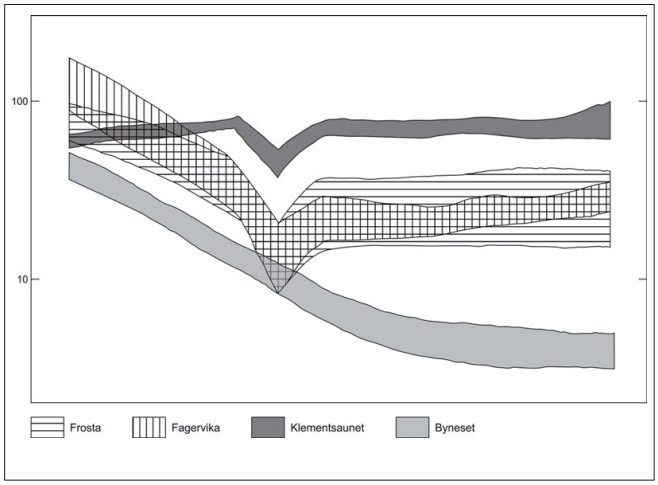

Figure 8. Comparison of the chrondrite-normalised REE patterns of the felsites from Frosta (this paper) with the Fagervika, Klementsaunet and Byneset felsic rock types from Bymarka (Slagstad 2003).

yielded a U–Pb zircon age of 488 ± 5 Ma, interpreted as the age of crystallisation. This age is indistinguishable from an age of 482 ± 5 Ma for a rhyodacite in the Bymarka ophiolite (Roberts et al. 2002). Zircons from the Fagervika trondhjemite yielded a less precise U–Pb age of c. 481 Ma. The bimodal volcanism in the Fånes complex, and at least the dated part of the Bymarka ophiolite, would then be of Tremadocian age. The age of the Granheim greenstone remains unknown. Whilst we can speculate that it may be broadly similar in age to the Fånes complex, it cannot be ruled out that it may be slightly younger, and form part of the Lower Hovin Group, as is the case for the Jonsvatn greenstone formation east of Trondheim (Grenne and Roberts 1980, Solli et al. 2003). The volcano-sedimentary succession of the Lower Hovin Group is generally regarded as having accumulated in a back-arc, marginal basin setting (Bruton and Bockelie 1980, Roberts et al. 1984).

Following the eruption of the Fånes and Granheim volcanic assemblages, a period, or periods, of uplift and erosion led to the deposition of the Helsingplassen and Huva conglomerates. Although the timing and duration of this hiatus is unknown, it is not unreasonable to suggest that, in the case of the Helsingplassen conglomerate at least, it may correspond to the Early Arenig (Floian) *Trondheim event*, during which time several of the fragmented ophiolites and arc rocks in Norway were obducted and variably metamorphosed (Roberts 2003). The pre-depositional foliation recorded in some of the clasts may conceivably relate to this event. In the case of the Huva conglomerate, which lacks a lower age constraint, another possibility for the hiatus is the younger *Ekne disturbance* (Vogt 1936), of Early Caradoc (Sandbian) age. This suggestion may be supported by the fact that the Risset limestone, which appears not far above the Huva conglomerate, is of Late Ordovician, Katian age (Tolmacheva and Roberts 2007). Alternatively, accepting just one tectonothermal and major uplift (Trondheim) event, this may conceivably imply that parts of the Middle Ordovician sedimentary record could be missing in this particular area of the Støren Nappe.

Conclusions

A partial revision of the geology of part of the coastal area of western Frosta peninsula around Småland has demonstrated the presence of two, distinctive, volcanic units, one consisting of a bimodal assemblage of greenstones and felsites (the Fånes complex) and another comprising just greenstones (the Granheim greenstone), both of which are overlain by conglomerates – the Helsingplassen and Huva conglomerates, respectively – consisting largely of clasts derived from the underlying volcanic units. The volcanite assemblages and their sedimentary cover successions, both to the north and to the south of Småland, dip to the north, but are shown to be inverted based on the compositional and geochemical similarity between the volcanites and the clasts in the conglomerates, and also from the way-up of pillow structures in the Granheim greenstone. Greenstone clasts in the Huva conglomerate closely resemble the Granheim greenstones in their overall geochemical signature.

The Fånes and Granheim greenstones are geochemically distinct, although they plot in broadly the same fields in the Ti–Zr–Y and Th–Hf–Ta discrimination diagrams, which show features intermediate between ocean-floor and primitive island-arc basalts. The Fånes greenstones are LREE depleted, whereas the Granheim greenstones have comparatively flat, chondrite-normalised REE patterns. Both greenstones show large, negative Ta anomalies, indicative of arc involvement during their generation, but their MORB-normalised Ta/La ratios are sufficiently different to confirm their gross geochemical dissimilarities. Overall, the geochemistry of these tholeiitic metabasalts is thus suggestive of extrusion in a supra-subduction zone, arc setting. The felsites in the Fånes complex and the felsite clasts in the Helsingplassen conglomerate are petrographically and geochemically indistinguishable. They have highly evolved rhyolitic compositions and geochemically they are most closely related to oceanic granites with arc-type geochemical signatures. In terms of extrusive setting, this would be more or less identical to that envisaged for the Fånes greenstones. Interestingly, the felsites have similar, chondrite-normalised, REE patterns (LREE enrichments and marked negative Eu anomalies) to that of the Fagervika trondhjemite from the Bymarka ophiolite – a trondhjemite which has been interpreted as having intruded in a primitive island-arc setting on recently formed oceanic crust. In a companion paper, zircons from a felsite sheet in the Fånes complex have been U–Pb-dated at 488 ± 5 Ma, interpreted as the age of crystallisation. This Late Furongian to Tremadocian age is similar to U–Pb ages reported from felsic rocks in the Bymarka and related, fragmented ophiolites in the Støren Nappe in the vicinity of Trondheim.

Acknowledgements
We are grateful to Professor Jan Hertogen, University of Leuven, Belgium, for providing INAA analyses of rare earth elements of six samples of greenstones and of three separate greenstone clasts. Valuable comments and suggestions from the two reviewers, professors Kurt Hollocher and Calvin Barnes, were extremely helpful in leading to improvements in the final manuscript. Dr. Hollocher is also thanked for his subsequent e-mail comments and discussion on the ambiguities surrounding certain aspects of the interpretation of magmatic setting based on REE data and element ratios.

References

Barker, F. (1979) Trondhjemite: definition, environment and hypothesis of origin. *In* Barker F. (ed.) *Trondhjemites, Dacites and Related Rocks*, Elsevier, Amsterdam, pp. 1–12.

Bergström, S.M. (1979) Whiterockian (Ordovician) conodonts from the Hølonda Limestone of the Trondheim Region, Norwegian

Caledonides. *Norsk Geologisk Tidsskrift,* **59**, 295–307.

Bergström, S.M. (1997) Conodonts of Laurentian faunal affinities from the middle Ordovician Svartsaetra limestone in the Trondheim Region, Central Norwegian Caledonides. *Norges geologiske undersøkelse Bulletin,* **432**, 59–69.

Bjerkgård, T. and Bjørlykke, A. (1994) The geology of the Folldal area, southern Trondheim Region Caledonides, Norway. *Norges geologiske undersøkelse Bulletin*, **426**, 53–75.

Bruton, D.L. and Bockelie, J.F. (1980) Geology and paleontology of the Hølonda area, western Norway—A fragment of North America? *In* Wones, D.R. (ed.). *The Caledonides in the USA*. Blacksburg, Virginia, Virginia Polytechnic Institute and State University, pp. 41–47.

Dunning, G.R. (1987) U–Pb zircon ages of Caledonian ophiolites and arc sequences: implications for tectonic setting. (Abstract) *Terra Cognita*, **7**, pp. 179.

Furnes, H., Ryan, P.D., Grenne, T., Roberts, D., Sturt, B.A. and Prestvik, T. (1985) Geological and geochemical classification of the ophiolite fragments in the Scandinavian Caledonides. *In* Gee, D.G. and Sturt, B.A. (eds.) *The Caledonide orogen—Scandinavia and related areas*, John Wiley & Sons, Chichester, pp. 657–670.

Furnes, H., Pedersen, R.B. and Stillman, C.J. (1988) The Leka ophiolite complex, central Norwegian Caledonides: field characteristics and geotectonic significance. *Journal of the Geological Society of London*, **145**, 401–412.

Gale, G.H. and Roberts. D. (1974) Trace element geochemistry of Norwegian Lower Palaeozoic basic volcanics and its tectonic implications. *Earth and Planetary Science Letters*, **22**, 380–390.

Grenne, T. (1986) Ophiolite-hosted Cu-Zn deposits at Løkken and Høydal, Trondheim Nappe Complex, Upper Allochthon. *Sveriges Geologiska Undersökning*, **60**, 55–65.

Grenne, T. (1989) Magmatic evolution of the Løkken SSZ Ophiolite, Norwegian Caledonides: relationships between anomalous lavas and high-level intrusions. *Geological Journal*, **24**, 251–274.

Grenne, T. and Roberts, D. (1980) Geochemistry and volcanic setting of the Ordovician Forbordfjell and Jonsvatn greenstones, Trondheim Region, central Norwegian Caledonides. *Contributions to Mineralogy and Petrology*, **74**, 374–386.

Grenne, T. and Lagerblad, B. (1985) The Fundsjø group, central Norway–a Lower Palaeozoic island arc sequence: geochemistry and regional implications. *In* Gee, D.G. and Sturt, B.A. (eds.) *The Caledonide orogen—Scandinavia and related areas*, John Wiley & Sons, Chichester, pp. 745–760.

Grenne, T., Grammeltvedt, G. and Vokes, F.M. (1980) Cyprus-type sulphide deposits in the western Trondheim district, central Norwegian Caledonides. *In* Panayioutou, A. (ed.) *Ophiolites*. Proceedings of the International Ophiolite Symposium, Cyprus, 1979. *Geological Survey of Cyprus, Nicosia*, pp. 727–743.

Gromet, L.P. and Roberts, D. (2010) Early Ordovician ages of zircons from felsic rocks and a conglomerate clast, Frosta peninsula, Central Norwegian Caledonides. *Norges geologiske undersøkelse Bulletin*, **450**, 60-64.

Halls, C., Reinsbakken, A., Ferriday, I., Haugen, A. and Rankin, A. (1977) Geological setting of the Skorovas orebody within the allochthonous metavolcanic stratigraphy of the Gjersvik Nappe, central Norway. *Institute of Mining and Metallurgy, Special Paper*, 128–151.

Heim, M., Grenne, T. and Prestvik, T. (1987) The Resfjell ophiolite fragment, central Norwegian Caledonides. *Norges geologiske undersøkelse Bulletin*, **409**, 49–72.

Kiær, J. 1932 The Hovin Group in the Trondheim area. Stratigraphical researches on the fossiliferous horizons in Meldalen, Hølandet and Gauldalen. *Det Norske Videnskabs-Akademiet i Oslo, Skrifter I, Mat.-nat. Kl. 1932*, **4**, 1.

Le Bas, M.J., LeMaitre, R.W., Strekeisen, A. and Zanettin, B. (1986) A chemical classification of volcanic rocks based on the total alkali silica diagram. *Journal of Petrology*, **27**, 745–750.

Loeschke, J. (1976) Petrochemistry of eugeosynclinal magmatic rocks of the area around Trondheim (central Norwegian Caledonides). *Neues Jahrbuch für Mineralogie, Abhandlungen*, **128**, 1–44.

Lutro, O. (1979) The geology of the Gjersvik area, Nord-Trøndelag, Central Norway. *Norges geologiske undersøkelse*, **354**, 553–100.

Nakamura, N. (1974) Determination of REE, Ba, Fe, Mg, Na and K in carbonaceous and ordinary chondrite. *Geochimica et Cosmochimica Acta*, **38**, 757–775.

Neuman, R.B. and Bruton, D.L. (1989) Brachiopods and trilobites from the Ordovician Lower Hovin Group (Arenig/Llanvirn), Hølonda area, Trondheim Region, Norway: new and revised taxa and palaeogeographic interpretations. *Norges geologiske undersøkelse Bulletin*, **414**, 49–89.

Neuman, R.B., Bruton, D.L. and Pojeta, J.Jr. (1997) Fossils from the Ordovician 'Upper Hovin Group' (Caradoc-Ashgill), Trondheim Region, Norway. *Norges geologiske undersøkelse Bulletin*, **432**, 25–58.

Nilsson, L.P., Roberts, D. and Ramsay, D.M. (2005) The Raudfjellet ophiolite fragment, Central Norwegian Caledonides: principal lithological and structural features. *Norges geologiske undersøkelse Bulletin*, **445**, 101–117.

Pearce, J.A. (1982) Trace element characteristics of lavas from destructive plate boundaries. *In* Thorpe, R.S. (ed.) *Orogenic Andesites and Related Rocks*, John Wiley, Chichester, pp. 525–548.

Pearce, J.A., Harris, B.W. and Tindle, A.G. (1984) Trace element discrimination diagrams for the tectonic interpretation of granitic rocks. *Journal of Petrology*, **25**, 956–983.

Pearce, J.A. and Cann, J.R. (1973) Tectonic setting of basic volcanic rocks determined using trace element analyses. *Earth and Planetary Science Letters*, **19**, 290–300.

Pedersen, P.Å. (1981) *Resedimenterte konglomerater og turbiditter på overgangen mellom under/øvre Hovingruppe (Llandeilo-Caradoc) i Åsenområdet, Nord-Trøndelag*. Unpublished Cand. real. thesis, University of Bergen, 134 pp.

Prestvik, T. (1980) The Caledonian ophiolite complex of Leka, north-central Norway. *In* Panayioutou, A. (ed.) *Ophiolites*. Proceedings of the International Ophiolite Symposium, Cyprus, 1979.

Geological Survey of Cyprus, Nicosia, pp. 555–566.

Roberts, D. (1969) Trace fossils from the Hovin Groups, Nord-Trøndelag, and their bathymetric significance. *Norges geologiske undersøkelse*, **258**, 228–236.

Roberts, D. (1975) The Stokkvola conglomerate–a revised stratigraphical position. *Norsk Geologisk Tidsskrift*, **55**, 361–371.

Roberts, D. (1982) En foreløpig rapport om geokjemien av Frostagrønnsteinene. *Unnumbered Norges geologiske undersøkelse Report, January 1982*, 4 pp. + figures and tables.

Roberts, D. (1984) *Nereites* from the Ordovician rocks of the eastern Trondheimsfjord area, Central Norwegian Caledonides. *Norges geologiske undersøkelse Bulletin*, **396**, 43–45.

Roberts, D. (1985) Frosta, berggrunnsgeologisk kart 1622–2 – 1:50000, foreløpig utgave. *Norges geologiske undersøkelse*.

Roberts, D. (2003) The Scandinavian Caledonides: event chronology, palaeogeographic settings and likely modern analogues. *Tectonophysics*, **365**, 283–299.

Roberts, D. and Tucker, R.D. (1998) Late Cambrian U–Pb zircon age of a metatrondhjemite from Ytterøya, Trondheimsfjorden, Central Norwegian Caledonides. *Norsk Geologisk Tidsskrift*, **78**, 253–258.

Roberts, D. and Stephens, M.B. (2000) Caledonian orogenic belt. *In* Lundqvist, T. and Autio, S. (eds.) *Description to the Bedrock Map of Central Fennoscandia (Mid-Norden)*, Geological Survey of Finland Special Paper, **28**, pp. 79–104.

Roberts, D., Grenne, T. and Ryan, P.D. (1984) Ordovician marginal basin development in the central Norwegian Caledonides. *In* Kokelaar, B.P. and Howells, M.F. (eds.) *Marginal Basin geology*, Geological Society of London, Special Publication, **16**, pp. 233–244.

Roberts, D., Walker, N., Slagstad, T., Solli, A. and Krill, A. (2002) U–Pb zircon ages from the Bymarka ophiolite, near Trondheim, Central Norwegian Caledonides, and regional implications. *Norsk Geologisk Tidsskrift*, **82**, 19–30.

Ryan, P.D., Williams, D.M. and Skevington, D. (1980) A revised interpretation of the Ordovician stratigraphy of Sør-Trøndelag, and its implications for the evolution of the Scandinavian Caledonides. *In* Wones, D.R. (ed.) *The Caledonides in the USA*, Virginia Polytechnic Geological Sciences Memoir, **2**, pp. 99–105.

Slagstad, T. (1998) *High-K_2O plagiogranite and greenstones in ophiolitic rocks of Bymarka, Trondheim*. Diploma thesis, Norwegian University of Science and Technology, Trondheim, 98 pp.

Slagstad, T. (2003) Geochemistry of trondhjemites and mafic rocks in the Bymarka ophiolite, Trondheim, Norway: petrogenesis and tectonic implications. *Norwegian Journal of Geology*, **83**, 167–185.

Solli, A., Grenne, T., Slagstad, T. and Roberts, D. (2003) Berggrunnskart Trondheim 1621 IV, M 1:50 000, foreløpig utgave. *Norges geologiske undersøkelse*.

Spjeldnæs, N. (1985) Biostratigraphy of the Scandinavian Caledonides. *In* Gee, D.G. and Sturt, B.A. (eds.). *The Caledonide orogen—Scandinavia and related areas*, John Wiley & Sons, Chichester, pp. 317–329.

Strømmen, S.K. (1983) *Marine avsetninger i under og øvre Hovingruppe (?øvre ordovicium) på Frosta og Tautra i Nord-Trøndelag*. Unpublished Cand. real. thesis, University of Bergen, 306 pp.

Sun, S-S. and McDonough, W.F. (1989) Chemical and isotopic systematic of oceanic basalts: implications for mantle composition and processes. *In* Saunders, A.D. and Norry, M.J. (eds.) *Magmatism in the ocean basins*, Geological Society of London, Special Publications, **42**, pp. 313–345.

Tolmacheva, T.J. and Roberts, D. (2007) New data on Upper Ordovician conodonts from the Trondheim region, Central Norwegian Caledonides. *Norges geologiske undersøkelse Bulletin*, **447**, 5–15.

Uchman, A., Hanken, N.M. and Binns, R. (2005) Ordovician bathyal trace fossils from metasiliciclastics in Central Norway and their sedimentological and palaeogeographical implications. *Ichnos*, **12**, 105–133.

Vogt, T. (1936) Orogenesis in the region of Paleozoic folding of Scandinavia and Spitsbergen, *Report of the 16th International Geological Congress, Washington*, 953.

Vogt, T. (1945) The geology of part of the Hølonda-Horg district, a type area in the Trondheim region. *Norsk Geologisk Tidsskrift*, **25**, 449–528.

Wood, D.A. (1980) The application of a Th–Hf–Ta diagram to problems of tectonomagmatic classification and to establishing the nature of crustal contamination of basaltic lavas of the British Tertiary volcanic province. *Earth and Planetary Sciences Letters*, **50**, 11–30.

Early Ordovician ages of zircons from felsic rocks and a conglomerate clast, Frosta peninsula, Central Norwegian Caledonides

L. Peter Gromet[1,*] and David Roberts[2]

[1] *Department of Geological Sciences, Brown University, Providence, RI 02912, USA.*
[2]*Geological Survey of Norway, Post Box 6315 Sluppen, 7491 Trondheim, Norway.*
[*]*Peter_Gromet@brown.edu*

Zircons extracted from a felsic sheet in the bimodal, magmatic, Fånes complex of the Støren Nappe on Frosta peninsula yielded a U–Pb age of 488 ± 5 Ma, interpreted as the age of crystallisation. A large clast of geochemically similar felsite in an overlying polymict conglomerate provided a U–Pb zircon age of 482 ± 3 Ma. The presented crystallisation ages are thus mutually indistinguishable and indicate that the conglomerate was sourced, at least in part, from the Fånes complex. The age results constrain the accumulation of the Fånes complex to a Late Cambrian (Furongian) to earliest Ordovician (Tremadocian) time span, similar to the ages of other felsic extrusive or intrusive rocks in fragmented ophiolites or suprajacent, primitive, island-arc trondhjemites in the Trondheim Region.

Introduction

In a companion paper in this Bulletin volume, Lippard and Roberts (2010) present the results of a geochemical study of two volcanic rock complexes occurring in the Støren Nappe on the Frosta peninsula, situated roughly 25 km northeast of Trondheim. They also include analyses of clasts of felsic and mafic volcanic rocks occurring in two, separate, conglomerate formations in this same area. During the fieldwork, extra samples were taken from a felsite sheet interlayered with metabasaltic greenstones, and also from a large clast of felsite in one of the overlying conglomerates, with the aim of retrieving zircons for U–Pb dating.

A sufficient number of zircon grains were obtained from these samples and duly analysed, and in this short contribution we present the results and interpretation of the data.

General geology

The geological setting of the rocks exposed in the Småland area of the Frosta peninsula has been described in some detail by Lippard and Roberts (2010). Accordingly, we present only a summary here, together with a map (Figure 1) showing where the samples were taken.

The volcanosedimentary succession on Frosta peninsula forms a part of a Cambro-Ordovician assemblage assigned to the Støren Nappe, which is one of several thrust sheets under the collective name Köli Nappes. In terms of Caledonide tectonostratigraphy, the Köli Nappes represent the more exotic, oceanic terranes that derived from outboard of the Baltoscandian margin of the palaeocontinent Baltica during the main Caledonian, *Scandian* orogeny, and form the bulk of the Upper Allochthon (Roberts and Gee 1985, Stephens and Gee 1989). The

Gromet, L.P. and Roberts, D. (2010) Early Ordovician ages of zircons from felsic rocks and a conglomerate clast, Frosta peninsula, Central Norwegian Caledonides. *Norges geologiske undersøkelse Bulletin*, **450**, 60–64.

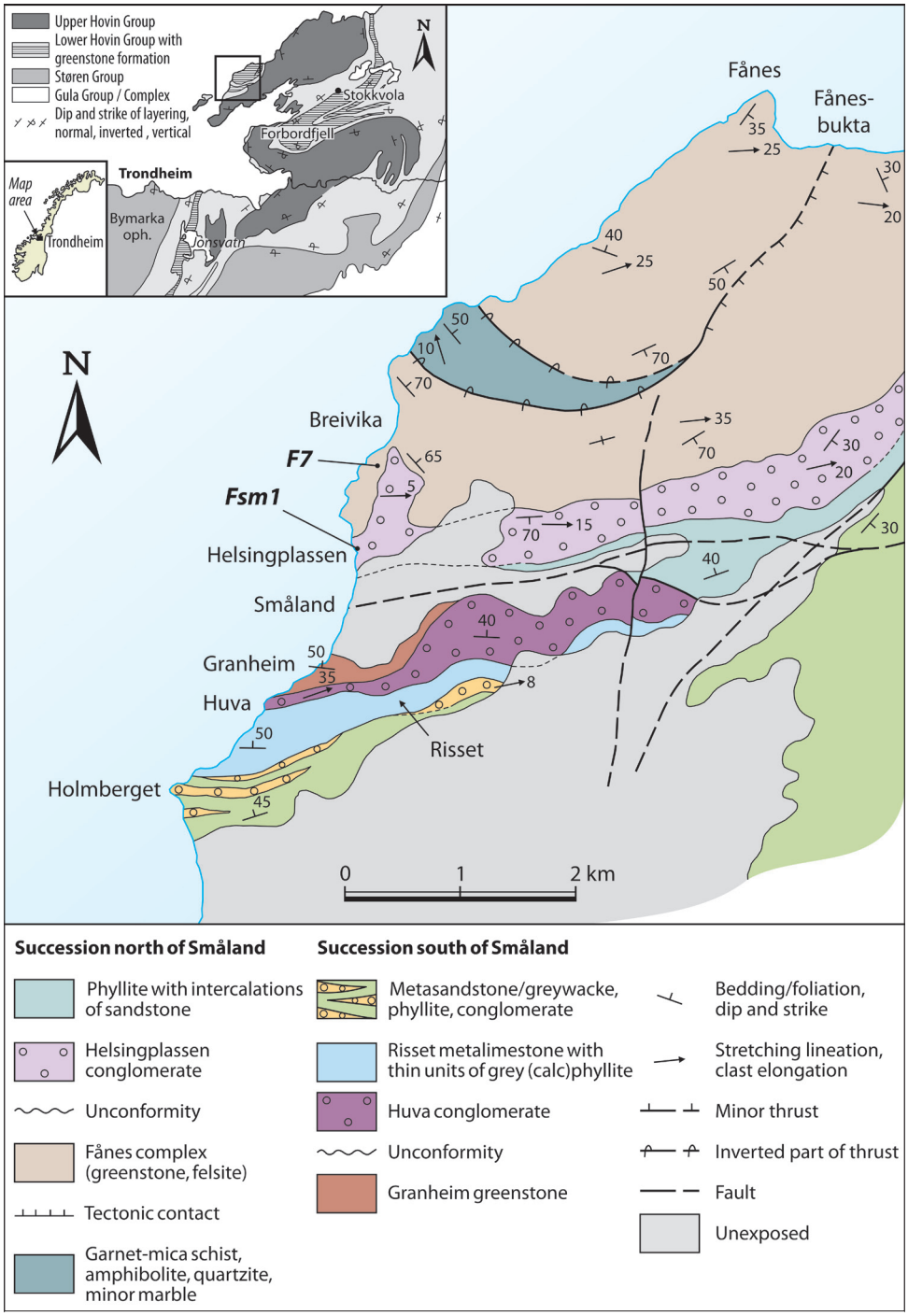

Figure 1. Simplified geological map of southwestern Frosta peninsula showing the locations of the samples F7 and Fsm1. Locality F7 is a roadside outcrop at 584730 7054350 on 1:50,000 map-sheet Leksvik 1622 III. Locality Fsm1 is a wave-washed shore outcrop at 584600 7053650, also on the map-sheet Leksvik. Coordinates apply to UTM Zone 32, WGS84.

Köli rocks also incorporate most of the fragmented ophiolites and island arcs that have been described from the Norwegian Caledonides (e.g., Gale and Roberts 1974, Furnes et al. 1985, Dunning and Pedersen 1988; other references are cited in the companion paper).

In the Småland area (Figure 1), two different successions each consisting mainly of oceanic extrusive rocks overlain by a sedimentary cover sequence have been mapped and described by Lippard and Roberts (2010). North of Småland there is a bimodal succession of mainly mafic volcanites (traditionally termed greenstones) and shallow felsic intrusions (termed felsites) which together constitute the *Fånes complex*. This is overlain unconformably by the polymict *Helsingplassen conglomerate* (Figure 1), the clasts of which consist mainly of greenstones and felsites derived from the subjacent Fånes complex. South of Småland, a formation of metabasaltic greenstones, including pillow lavas, is termed the *Granheim greenstone*. This is structurally inverted and is stratigraphically overlain by the *Huva conglomerate*, consisting mostly of greenstone pebbles with subordinate felsite, which is in turn overlain by a metalimestone, conglomerates, and interbedded phyllites and turbiditic greywackes. Conodonts in the metalimestone provide an

Early to Mid Katian (Late Caradocian) age for this formation (Tolmacheva and Roberts 2007).

The Granheim and Fånes greenstones are geochemically distinct, the former showing flat REE patterns whereas the Fånes mafic rocks are depleted in LREE. Whilst an initial interpretation would suggest their extrusion as E-type (Granheim) and N-type (Fånes) MORB lavas, other geochemical criteria point to generation in a subduction-related, primitive-arc setting. The felsites also show an arc-type geochemical signature. Clasts of felsite in the Helsingplassen conglomerate are petrographically and geochemically indistinguishable from the felsite sheets in the Fånes complex.

Although several of the ophiolitic and magmatic arc assemblages in the Central Norwegian Caledonides have been dated, with zircon ages ranging from 497 ± 2 to 480 ± 4 Ma (see Figure 7 in Roberts et al. 2002), no isotopic dating has hitherto been reported from the Frosta region. Moreover, the volcanic successions on Frosta are constrained biostratigraphically only to be older than Late Caradocian. The data reported here thus help to fill a gap in our overall knowledge of timing of Early Palaeozoic magmatism in this part of the Caledonide orogen.

Geochronology

The rocks sampled for this study are a felsite sheet from the Fånes complex (sample no. F7) and a large clast of geochemically similar felsite from the Helsingplassen conglomerate (sample no. Fsm1) (Figure 1; grid coordinates are given in the figure caption). Zircon concentrates for both samples were prepared at NGU, and zircon grains were hand picked from these materials at Brown University for U–Pb isotopic analysis. The F7 felsite yielded relatively few zircons, and they are characteristically small stubby prisms and prism fragments (<100 µm in longest dimension), exhibited some cloudiness, and contained some inclusions and cracks. Six fractions were prepared for analysis, each consisting of 10 to 12 grains. The Fsm1 felsite clast yielded zircons with similar qualities but of slightly larger size, from which four fractions were prepared.

The fractions were processed through HF dissolution and chemical separation, largely following analytical procedures given by Krogh (1973). Pb and U were analysed on a Finnigan MAT 261 mass spectrometer, using either combined Faraday-SEM multicollection or peak hopping into the SEM, according to signal intensity. Results are reported in Table 1 and plotted on a concordia diagram in Figure 2.

All zircon fractions analysed have low U contents and therefore developed relatively low amounts of radiogenic Pb since their crystallisation. Three of the six fractions of F7 (fractions z2, z3, and z6) show very low $^{206}Pb/^{204}Pb$ ratios (<500) even after correction for blank and fractionation, leading to larger errors in their calculated ages, especially the $^{207}Pb/^{235}U$ ages. One additional fraction from F7 (z1) has large errors due to low signal

Table 1. Zircon analyses from samples F7 and Fsm1.

			$^{206}Pb/^{204}Pb$		$^{206}Pb/^{238}U$	$^{207}Pb/^{235}U$	ρ (rho)	$^{206}Pb/^{238}U$	$^{207}Pb/^{235}U$	$^{207}Pb/^{206}Pb$
Sample	U (ppm)	Pb (ppm)	measured[1]	corrected	err abs[2]	err abs[2]	err corr[3]	age (Ma)	age (Ma)	age (Ma)
F7 zir 1	10.541	0.856	299.9	1027	0.07926 ± 202	0.5876 ± 348	0.502	492 ± 13	469 ± 28	361 ± 116
F7 zir 2	13.222	1.0924	231.9	385.8	0.08081 ± 157	0.6193 ± 289	0.496	501 ± 10	489 ± 23	436 ± 91
F7 zir 3	25.668	2.0432	330.2	490.3	0.07750 ± 98	0.5930 ± 173	0.506	481 ± 6	473 ± 14	432 ± 56
F7 zir 4	26.311	2.123	661.9	877.5	0.07883 ± 47	0.6158 ± 97	0.457	489 ± 3	487 ± 8	478 ± 31
F7 zir 5	13.334	1.068	437.9	745.8	0.07784 ± 83	0.6130 ± 142	0.530	483 ± 5	486 ± 11	496 ± 43
F7 zir 6	12.245	0.997	195.2	301.1	0.07925 ± 167	0.6097 ± 312	0.494	492 ± 10	483 ± 25	444 ± 99
Fsm1 zir 1	31.819	2.4775	1450	4217	0.07736 ± 40	0.6114 ± 66	0.549	480 ± 3	484 ± 5	504 ± 20
Fsm1 zir 2	28.553	2.2421	749.0	1179	0.07754 ± 45	0.6108 ± 72	0.561	481 ± 3	484 ± 6	497 ± 22
Fsm1 zir 3	43.760	3.4642	1445	2733	0.07799 ± 37	0.6156 ± 50	0.628	484 ± 2	487 ± 4	501 ± 14
Fsm1 zir 4	23.779	1.8631	699.9	1180	0.07758 ± 77	0.6009 ± 102	0.634	482 ± 5	477 ± 8	459 ± 29

All zircon fractions were dissolved in the presence of a mixed ^{205}Pb–^{235}U spike calibrated against NBS and NBL metal standards. All Pb/U ratios are corrected for total blanks of 10 ± 5 pg Pb, 2 ± 1 pg U, mass fractionation of 0.08 ± 0.06%/amu, and initial Pb (age-appropriate values from Stacey and Kramers 1975). Pb/U ratio and age errors are reported at 2σ level. Concentrations are approximate because they are based on estimated sample weights (too small to measure).

[1] Uncorrected for fractionation and blank.

[2] err abs refers to 2σ absolute errors in last decimal places.

[3] Error correlation (rho) of ^{206}Pb–^{238}U and ^{207}Pb–^{235}U ratios.

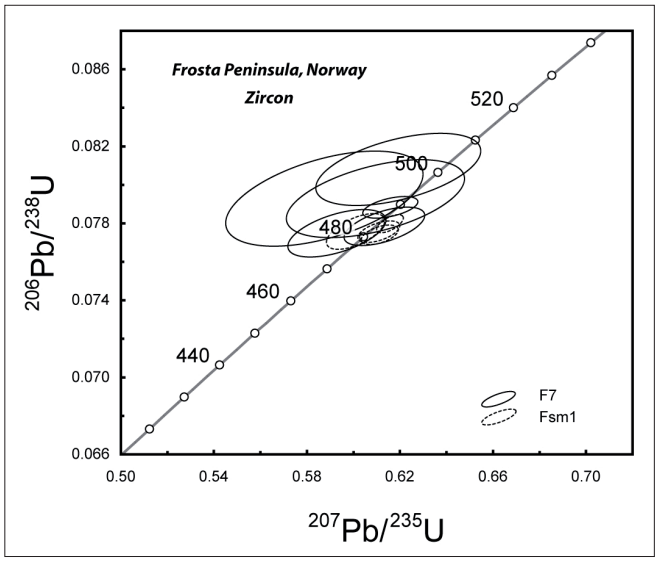

Figure 2. Concordia diagram for the zircon fractions from samples F7 and Fsm1.

intensity during mass spectrometer analysis. The four fractions from Fsm1 all yielded larger corrected $^{206}Pb/^{204}Pb$ ratios (>1000) and low uncertainties in their calculated ages.

On the concordia diagram, error ellipses for all analyses cluster between 480 and 500 Ma and overlie the concordia curve, and are therefore considered concordant. The larger errors for 4 of the 6 fractions from the F7 felsite provide little additional constraint beyond that provided by the two more precise and overlapping ages from fractions z4 and z5 in this sample, but they serve to indicate the absence of both inheritance and discordance. Inheritance is not expected in these primitive, oceanic volcanic rocks, and discordance due to radiation damage is not anticipated given the low U contents of the zircon. Considering only the more precise z4 and z5 fractions from F7 along with the four fractions from the Fsm1 felsite clast, the $^{206}Pb/^{238}U$ ages cluster tightly between 480 and 490 Ma.

Given the relatively low $^{206}Pb/^{204}Pb$ ratios and the sensitivity of $^{207}Pb/^{235}U$ ages to the common Pb correction, and the concordant nature of the ages, the most appropriate estimate of error for these ages is considered to be that based on the $^{206}Pb/^{238}U$ ages. The weighted average of z4 and z5 of sample F7 is 487 ± 9 Ma (95% c.l.), with an MSWD of 4.2, which provides an identical but less precise age than that given by the weighted average of all 6 fractions: 488 ± 5 Ma (95% c.l.) with an MSWD of 3.5. The 488 ± 5 Ma age based on all 6 analysed fractions is accepted as the best estimate of the age of crystallisation of sample F7. The weighted average of all 4 fractions of sample Fsm1 is 482 ± 3 Ma (95% c.l.) with an MSWD of 1.7.

Based on these considerations, the crystallisation ages of the two samples are at the limits of resolvability. The felsite clast in Fsm1 may be marginally younger than the felsite in the stratigraphically subjacent volcanic rocks, but the ages of these two samples cannot be confidently distinguished.

Discussion

The U–Pb zircon ages reported here point to a likely Tremadocian or latest Furongian age for the bimodal Fånes complex. In the Köli Nappes of the Trondheim Region, several felsic rocks in ophiolites or primitive island-arc intrusions invading oceanic metabasalts have provided U–Pb zircon dates ranging from Late Cambrian (Furongian) to Early Ordovician (Tremadocian) age (see summary in Roberts et al. 2002). The age of the arc-type, Fånes felsite thus falls within this restricted time slice.

The mutually indistinguishable ages of the felsite of the Fånes complex and the felsic clast in the overlying Helsingplassen conglomerate, in conjunction with their geochemical similarities, argue strongly that the provenance of the conglomerate included the felsic rocks of the Fånes complex. There is good evidence from elsewhere in the Trondheim Region that the ophiolites and primitive, magmatic arc rocks were obducted and weakly metamorphosed in Early Arenig (Floian) time—termed the *Trondheim event*—just prior to rapid uplift and erosion which led to deposition of the Mid/Late Arenig (Dapingian) to Late Caradoc (Katian), Hovin and Horg groups (Roberts 2003, Lippard and Roberts, 2010). The actual age of the Helsingplassen conglomerate, containing the clasts of felsite, is unknown, but based on our knowledge of the geology and biostratigraphy of the Støren Nappe it is inferred to be of Late Arenig-Llanvirn (Dapingian to Darriwilian) age.

Acknowledgements
We thank the reviewers, professors Calvin Barnes and Kurt Hollocher, for their helpful comments and suggestions on the manuscript. Professor Stephen Lippard assisted in the collection of sample F7.

References

Dunning, G.R. and Pedersen, R.B. (1988) U/Pb ages of ophiolites and arc-related plutons of the Norwegian Caledonides: implications for the development of Iapetus. *Contributions to Mineralogy and Petrology*, **98**, 13–23.

Furnes, H., Ryan, P.D., Grenne, T., Roberts, D., Sturt, B.A. and Prestvik, T. (1985) Geological and geochemical classification of the ophiolite fragments in the Scandinavian Caledonides. *In* Gee, D.G. and Sturt, B.A. (eds.) *The Caledonide orogen —Scandinavia and related areas*, John Wiley & Sons, Chichester, pp. 657–670.

Gale, G.H. and Roberts, D. (1974) Trace element geochemistry of Norwegian Lower Palaeozoic basic volcanics and its tectonic implications. *Earth and Planetary Science Letters*, **22**, 380–390.

Krogh, T.E. (1973) A low-contamination method for hydrothermal decomposition of zircon and extraction of U and Pb for isotopic age determinations. *Geochimica et Cosmochimica Acta*, **37**, 485–495.

Lippard, S.L. and Roberts, D. (2010) Geochemistry and palaeogeographical setting of greenstone units on Frosta peninsula, Nord-Trøndelag, Central Norwegian Caledonides. *Norges geologiske undersøkelse Bulletin*, **450**, 48-59.

Roberts, D. (2003) The Scandian Caledonides: event chronology, palaeogeographic settings and likely modern analogues. *Tectonophysics*, **365**, 283–299.

Roberts, D. and Gee, D.G. (1985) An introduction to the structure of the Scandinavian Caledonides. *In* Gee, D.G. and Sturt, B.A. (eds.) *The Caledonide orogen—Scandinavia and related areas*, John Wiley & Sons, Chichester, pp. 55–68.

Roberts, D., Walker, N., Slagstad, T., Solli, A. and Krill, A. (2002) U–Pb zircon ages from the Bymarka ophiolite, near Trondheim, Central Norwegian Caledonides, and regional implications. *Norsk Geologisk Tidsskrift*, **82**, 19–30.

Stacey, J.S. and Kramers, J.D. (1975) Approximation of terrestrial lead isotope evolution by a two stage model. *Earth and Planetary Science Letters*, **26**, 207–221.

Stephens, M.B. and Gee, D.G. (1989) Terranes and polyphase accretionary history in the Scandinavian Caledonides. *Geological Society of America Special Paper*, **230**, 17–30.

Tolmacheva, T.J. and Roberts, D. (2007) New data on Upper Ordovician conodonts from the Trondheim region, Central Norwegian Caledonides. *Norges geologiske undersøkelse Bulletin*, **447**, 5–15.